MANCHESTER 1824
The University of Manchester

ATLAS EXPERIMENT

ATLAS Trigger-Level Analysis (TLA)

Phys. Rev. D 112, 092015 (2025)

Tobias Fitschen on behalf of the analysis team

24 February 2026

Liverpool Particle Physics Seminar

European Research Council
Established by the European Commission

https://doi.org/10.1103/15p2-bkg8

PHYSICAL REVIEW D **112,** 092015 (2025)

Search for electroweak-scale dijet resonances using trigger-level analysis with the ATLAS detector in 132 fb^{-1} of pp collisions at $\sqrt{s} = 13$ TeV

G. Aad *et al.*[*]
(ATLAS Collaboration)

(Received 3 September 2025; accepted 14 October 2025; published 24 November 2025)

arxiv:2509.01219 aux material HepData

Abundant evidence for dark matter (DM) from astro physics and cosmology

Rotational curves

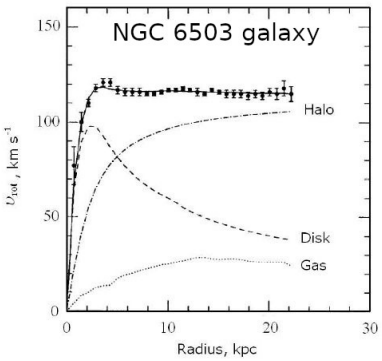

arxiv:0812.4005

Colliding galaxy clusters

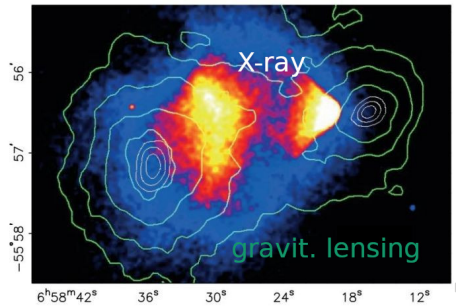

adapted: NASA

bullet cluster

CMB power spectrum

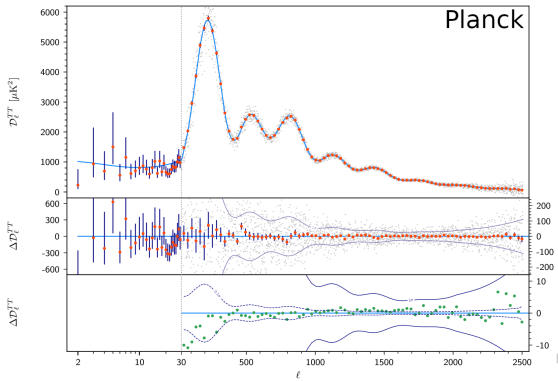

arxiv:1907.12875

So far DM evades detection as a particle

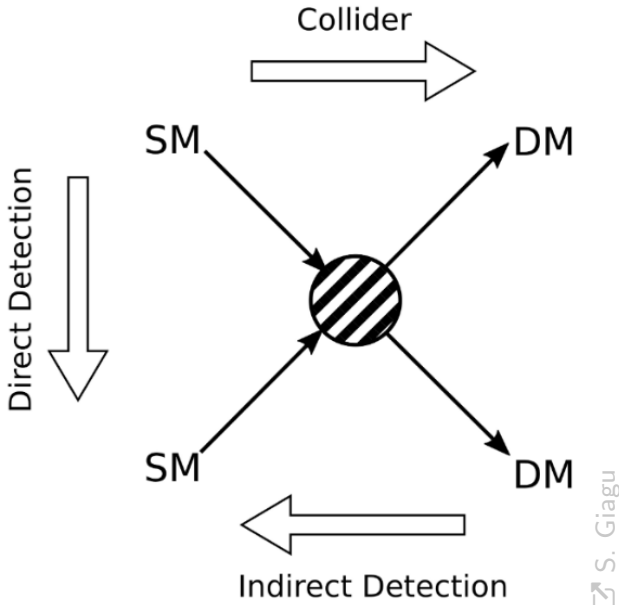

S. Giagu

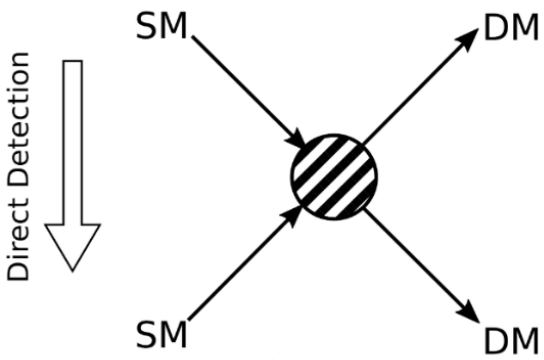

Direct detection

- Earth travels through galaxy's DM halo
- DM may rarely interact with atoms in large volumes of regular matter
- Goal: Measure signal of such interactions

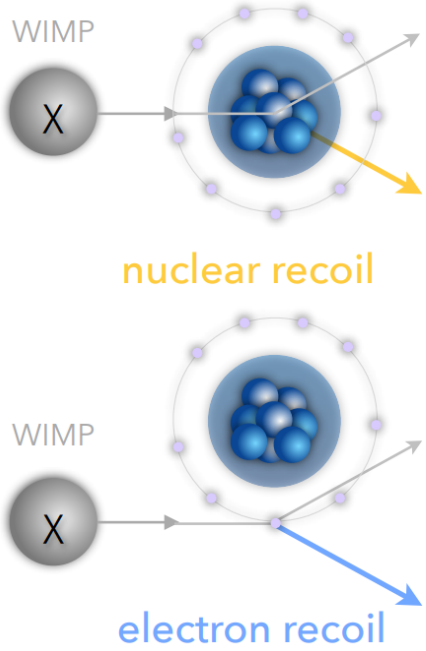

adapted: G. Fiorillo

Darkside 20k

G. Fiorillo

50 tonnes of liquid Argon

NEWS-G

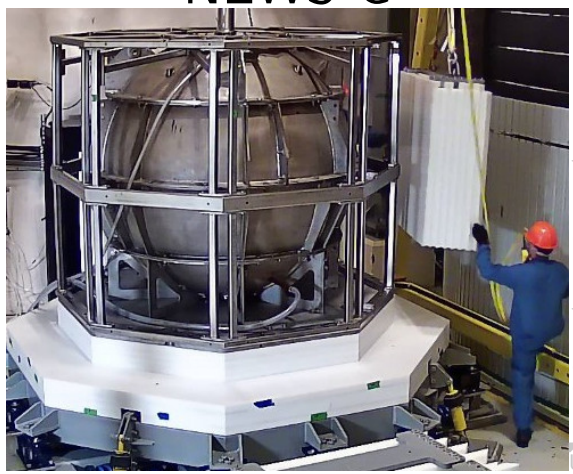

snolab.ca/experiment/news-g

$\varnothing$ =135 cm copper sphere

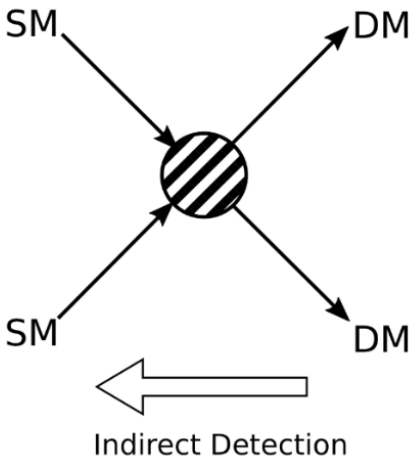

Indirect detection

- DM may annihilate in regions with large abundance
  - Within galactic nuclei or stars
- Products (photons, neutrinos) may reach earth to be detected

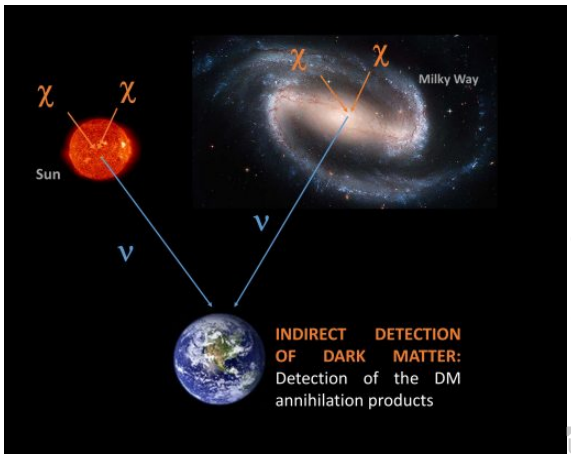

antares.in2p3.fr

ICE CUBE

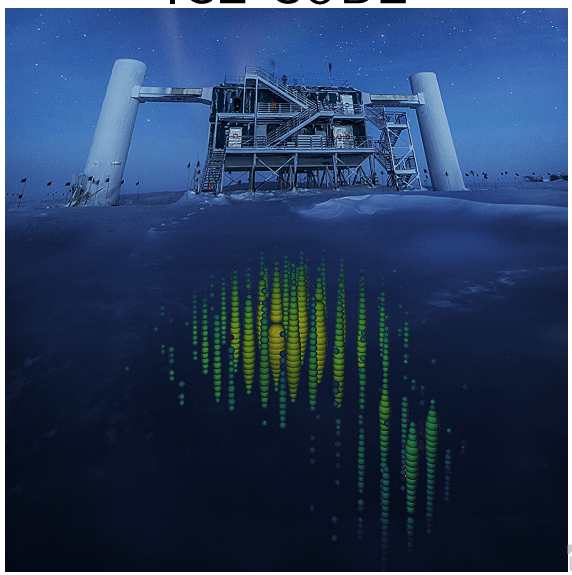
phys.org

neutrino observatory

FERMI satellite


wikimedia commons

gamma ray telescope

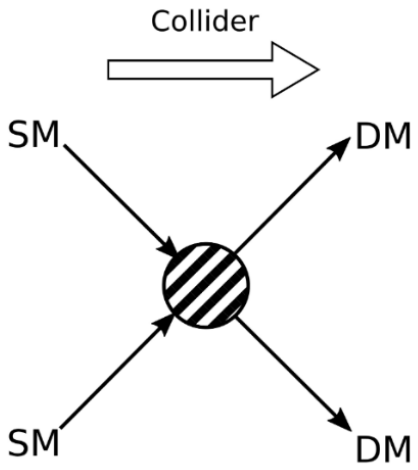

Collider searches

- SM may interact with DM via mediator
- DM production: large missing energy (MET)
  - Together with SM product: X+MET
- SM→BSM mediator→SM
  - Di-X resonance search
  - This talk: Dij-jet resonance search

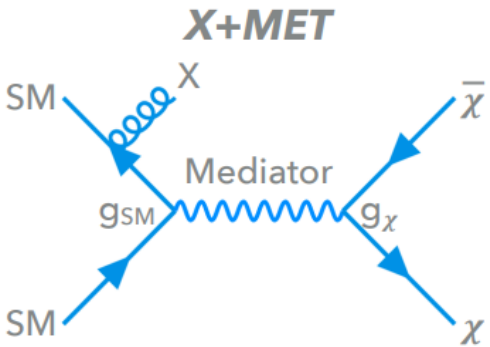

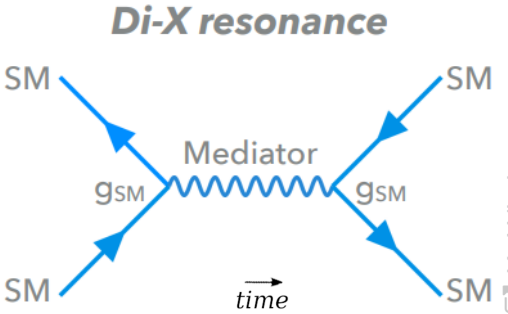

K. Whalen

Large Hadron Collider (LHC)

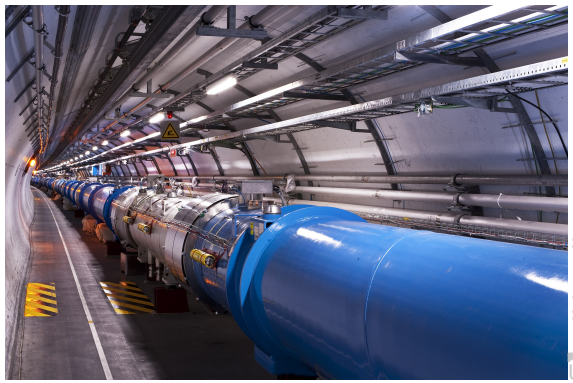

wikimedia commons

$\sqrt{s} = 14$ TeV pp collider

ATLAS Experiment

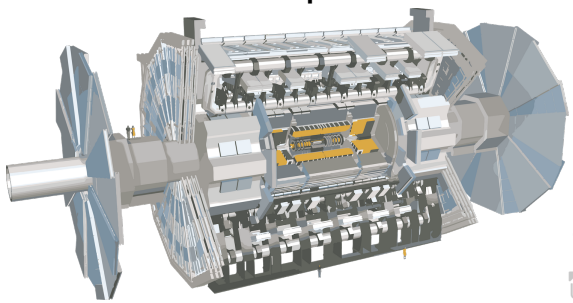

atlas.cern

Particle detector at the LHC

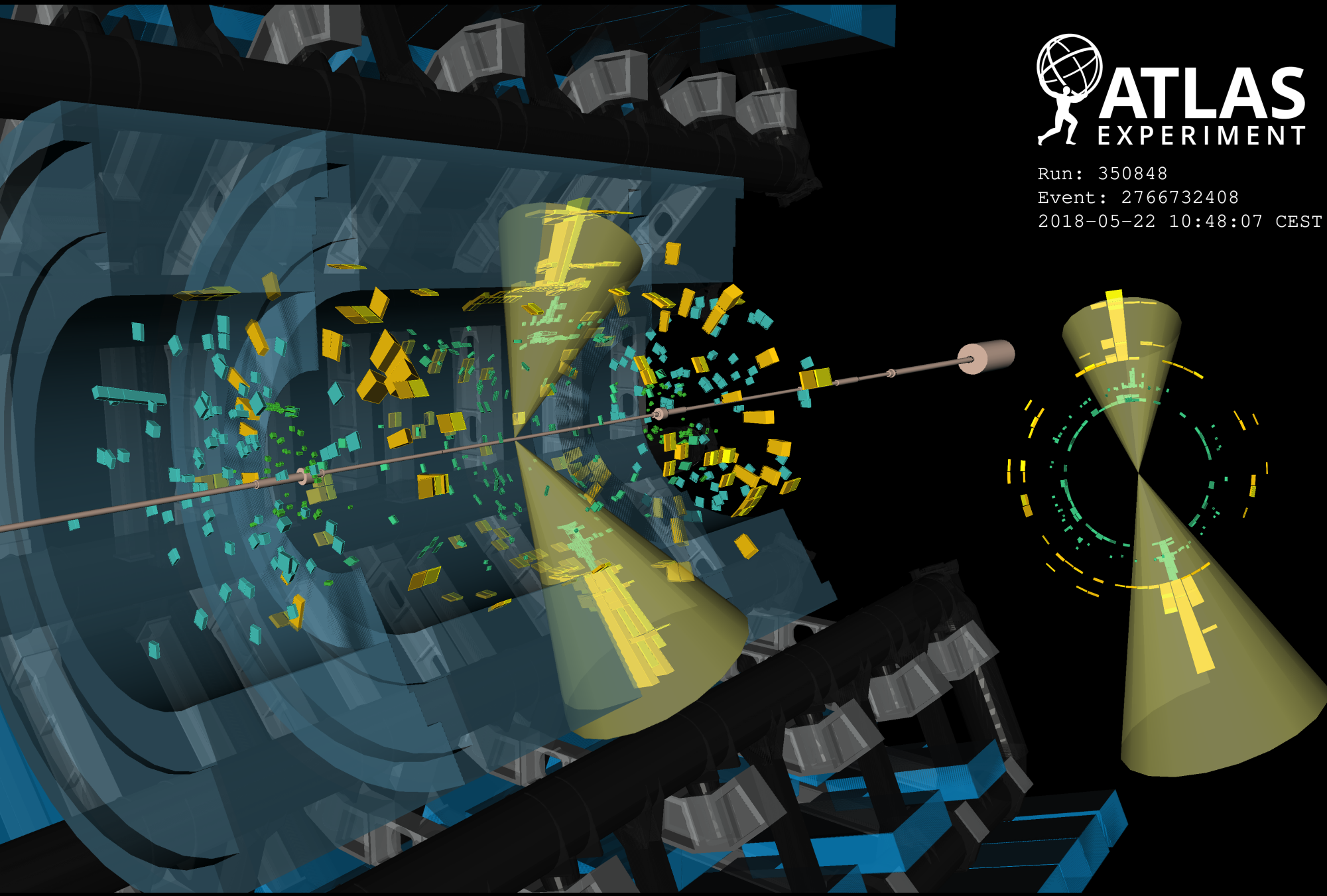
ATLAS
EXPERIMENT
Run: 350848
Event: 2766732408
2018-05-22 10:48:07 CEST

Scattering Theory: Dijet Events at Leading Order

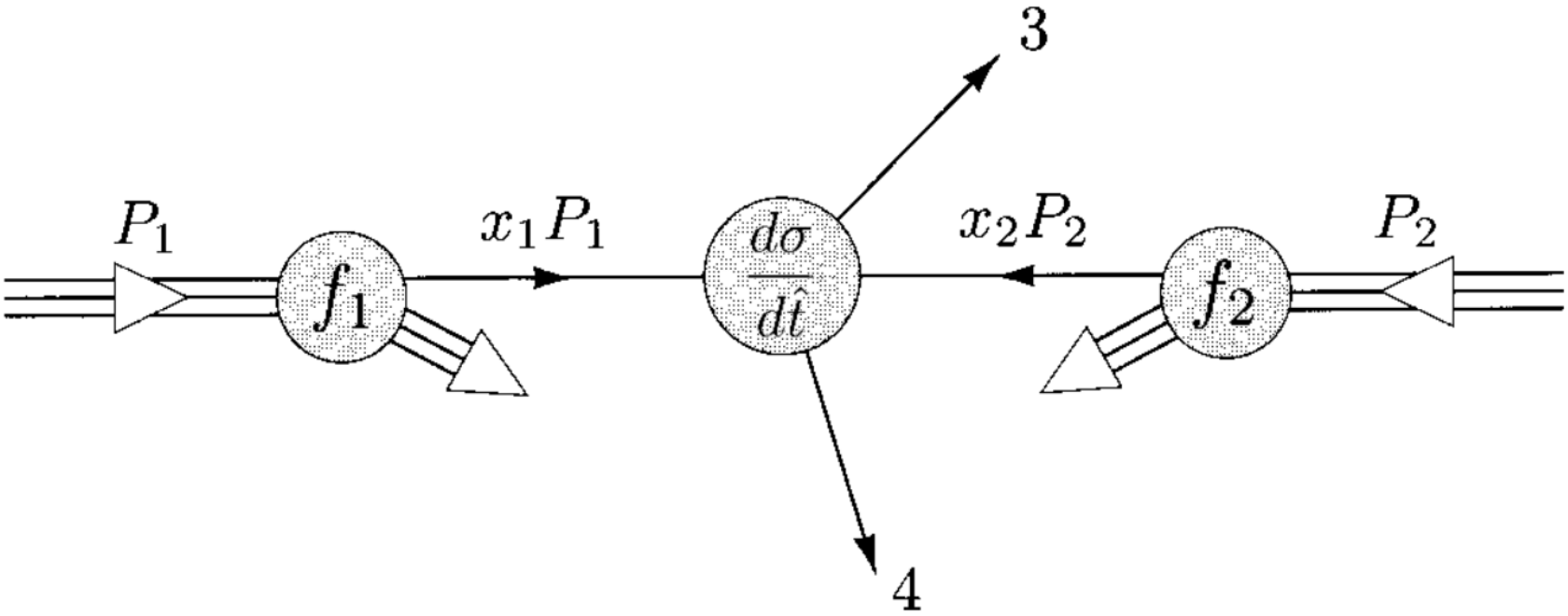

adapted from: Peskin & Schroeder

The total cross-section can be divided in 2 parts:

$$\frac{\mathrm{d}^4\sigma}{\mathrm{d}y_3\mathrm{d}y_4\mathrm{d}^2p_\mathrm{T}} = \underbrace{x_1 f_1(x_1) x_2 f_2(x_2)}_{\text{proton PDFs}} \frac{1}{\pi} \underbrace{\frac{\mathrm{d}\hat{\sigma}}{\mathrm{d}\hat{t}}(1+2\to 3+4)}_{\text{partonic cross section}}$$

Balanced transverse momenta $p_\mathrm{T}^3 = p_\mathrm{T}^4 \equiv p_\mathrm{T}$

But rapidities may differ: $y_3 \neq y_4$ due to boost along beam axis ($x_1 \neq x_2$)

Parton Distribution Functions (PDF)

PDF: Probability to find parton with momentum fraction x in proton

$\rightarrow$ dominates the shape of mass spectrum:

$$\frac{\mathrm{d}\sigma}{\mathrm{d}M^2} \propto \underbrace{x_1 f_1(x_1) x_2 f_2(x_2)}_{\text{proton PDFs}}$$

Dijet mass (parton level): $M = \sqrt{\hat{s}} = \sqrt{x_1 x_2}\sqrt{s}$

$\sqrt{\hat{s}}$: Parton CM energy (unknown)

$\sqrt{s} = 13$ TeV: LHC CM energy (Run 2)

High M $\rightarrow$ high x_1, x_2 $\rightarrow$ low $x_1 f(x_1), x_2 f(x_2)$

$\rightarrow$ strongly suppressed by PDFs

$\rightarrow$ Steeply falling spectrum

Proton PDFs at NLO

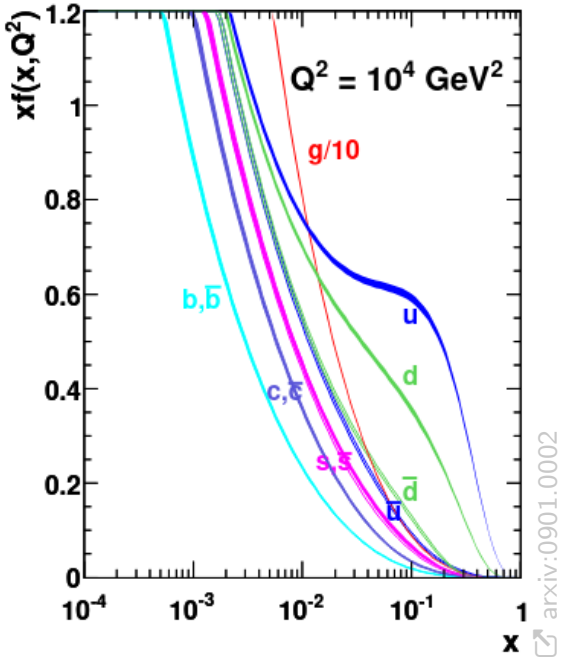

Long history of dijet "bump hunts" at hadron colliders

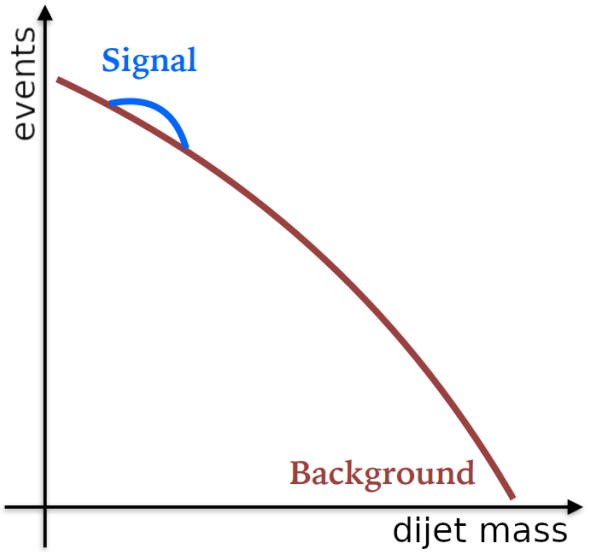

Expt.	Acc.	Year	$\sqrt{s}$ [TeV]	$\int L dt$ [pb^{-1}]	m_{jj} range [TeV]	Ref.
UA1	$Sp\bar{p}S$	1986	0.63	0.26	0.07 - 0.3	1
UA1	$Sp\bar{p}S$	1988	0.63	0.49	0.11 - 0.3	2
CDF	Tevatron	1990	1.8	0.026	0.06 - 0.5	3
UA2	$Sp\bar{p}S$	1990	0.63	4.7	0.05 - 0.3	4
CDF	Tevatron	1993	1.8	4.2	0.14 - 1.0	5
UA2	$Sp\bar{p}S$	1993	0.63	11	0.05 - 0.3	6
CDF	Tevatron	1995	1.8	19	0.15 - 0.9	7
CDF	Tevatron	1997	1.8	106	0.18 - 1.0	8
D0	Tevatron	2004	1.8	109	0.18 - 1.2	9
CDF	Tevatron	2009	1.96	1130	0.18 - 1.3	10
ATLAS	LHC	2010	7	0.32	0.20 - 1.7	11
CMS	LHC	2010	7	2.9	0.22 - 2.1	12
ATLAS	LHC	2011	7	36	0.50 - 2.8	13
CMS	LHC	2011	7	1000	0.84 - 3.7	14
ATLAS	LHC	2011	7	1000	0.72 - 4.1	15
ATLAS	LHC	2012	7	1000	0.8 - 4.0	16
ATLAS	LHC	2012	7	4800	1.0 - 8.0	16
CMS	LHC	2013	8	4000	1.0 - 4.8	17
CMS	LHC	2015	8	19700	1.2 - 6.5	18
ATLAS	LHC	2015	8	20300	0.8 - 4.5	19
CMS	LHC	2016	13	2400	1.5 - 0.7	20
ATLAS	LHC	2016	13	3600	1.5 - 6.5	21
CMS	LHC	2017	13	12900	1.5 - 7.5	22
ATLAS	LHC	2017	13	37000	1.5 - 3.5	23
CMS	LHC	2018	13	36000	1.6 - 8.1	24
ATLAS	LHC	2020	13	139000	1.5 - 5.0	25
CMS	LHC	2020	13	77800	1.8 - 8.0	26

As $\sqrt{s}$ increased...

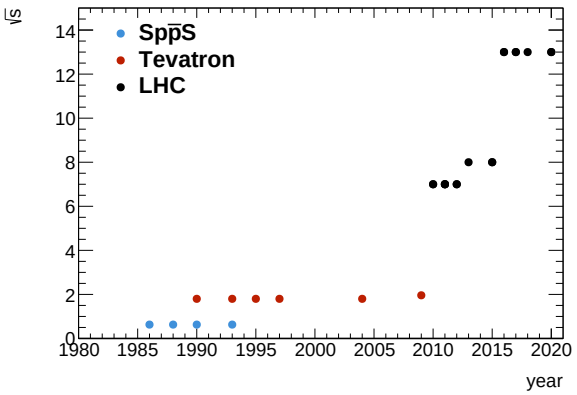

so did the luminosity...

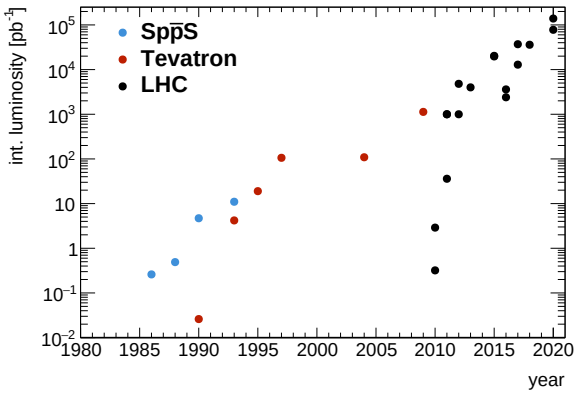

...and the dijet mass reach

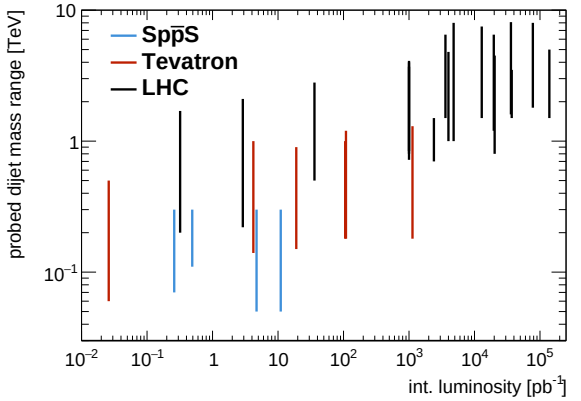

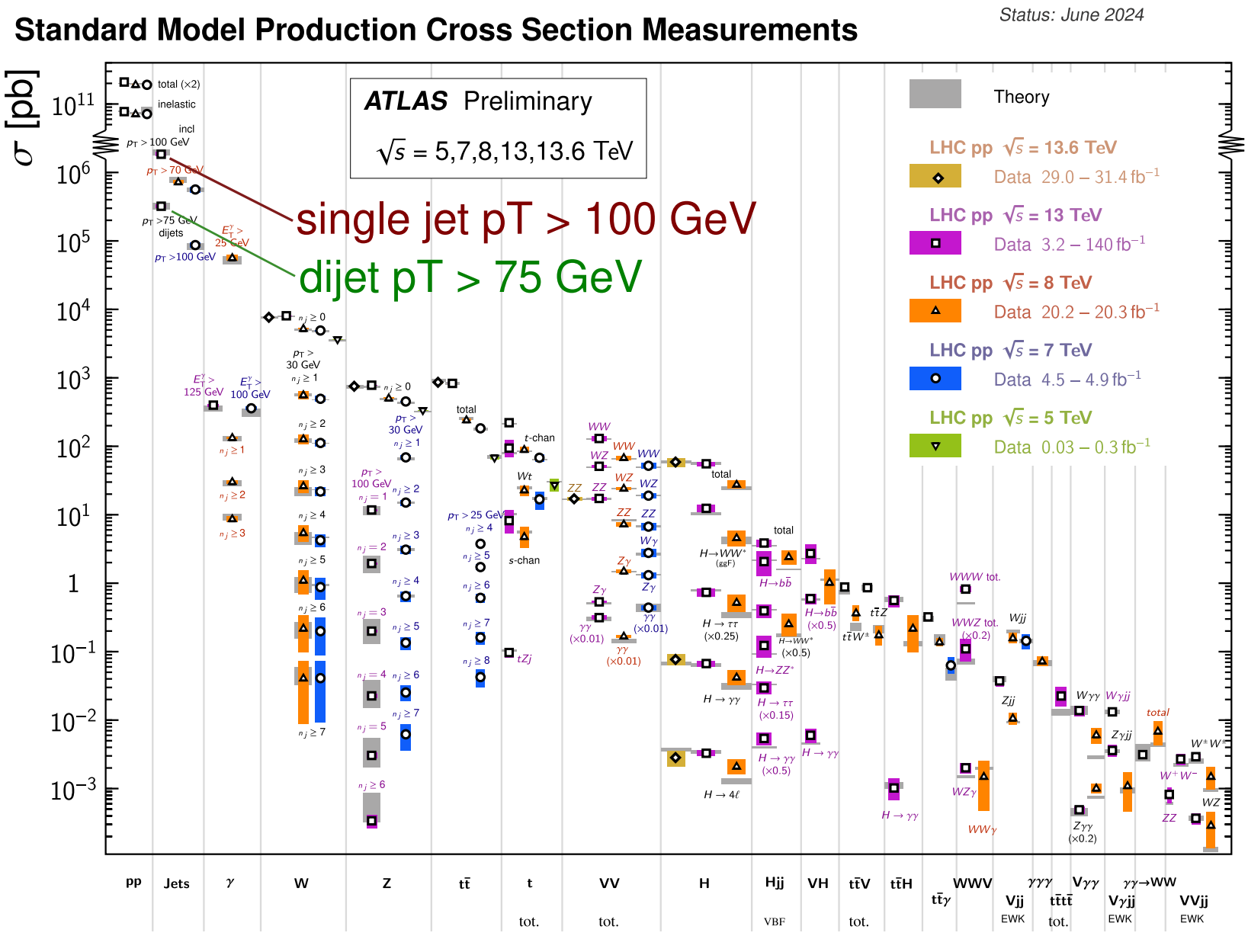
Standard Model Production Cross Section Measurements
Status: June 2024
ATLAS Preliminary
√s = 5,7,8,13,13.6 TeV
Theory
LHC pp √s = 13.6 TeV
Data 29.0 – 31.4 fb⁻¹
LHC pp √s = 13 TeV
Data 3.2 – 140 fb⁻¹
LHC pp √s = 8 TeV
Data 20.2 – 20.3 fb⁻¹
LHC pp √s = 7 TeV
Data 4.5 – 4.9 fb⁻¹
LHC pp √s = 5 TeV
Data 0.03 – 0.3 fb⁻¹
σ [pb]
single jet pT > 100 GeV
dijet pT > 75 GeV
pp
Jets
γ
W
Z
tt̄
t
VV
H
Hjj
VH
tt̄V
tt̄H
WWV
γγγ
Vγγ
γγ→WW
tt̄γ
Vjj
EWK
tt̄tt̄
tot.
Vγjj
EWK
VVjj
EWK
VBF
ATLAS Summary Plot

The ATLAS Trigger System

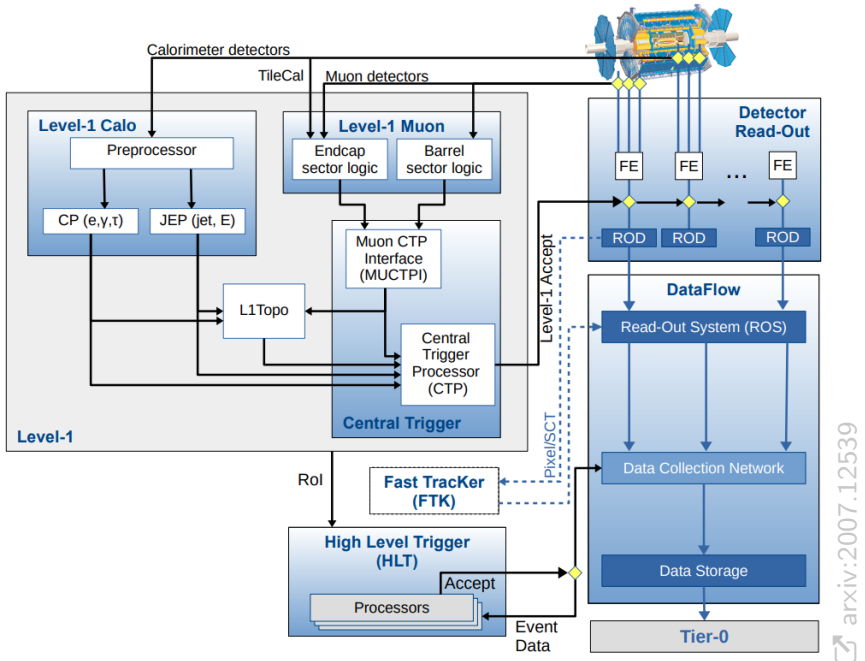

The ATLAS trigger system retains only a small fraction of the collisions

- Raw input: 30 MHz
- L1 hardware trigger: 100 kHz
- HLT software trigger: 1 kHz

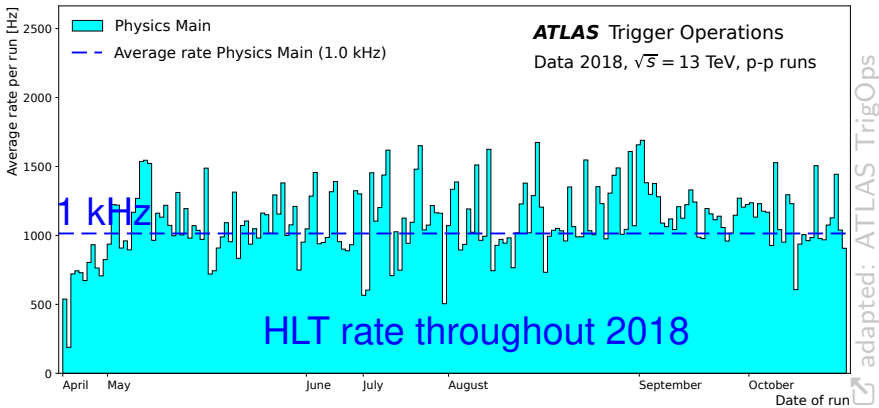

Predicted L1 rate vs p_T threshold

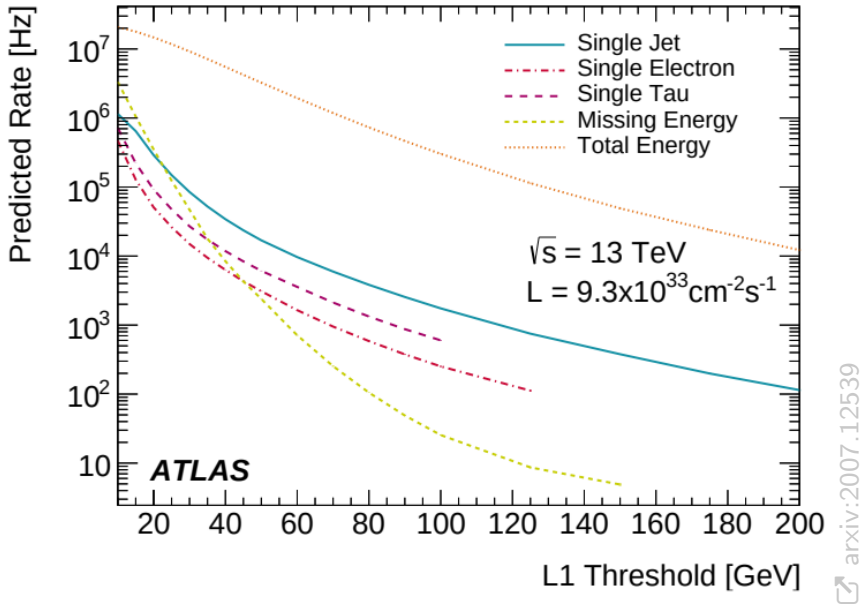

Many search targets lie at high p_T

- Simple strategy: Pick a threshold and discard everything below
- Employed (better) strategy: Prescaling
  - Divide into multiple p_T thresholds with different "prescale factors" P
  - Retains only every Pth event passing that threshold
  - Lower thresholds have larger prescale factors

Prescaling

L1 jet trigger efficiencies

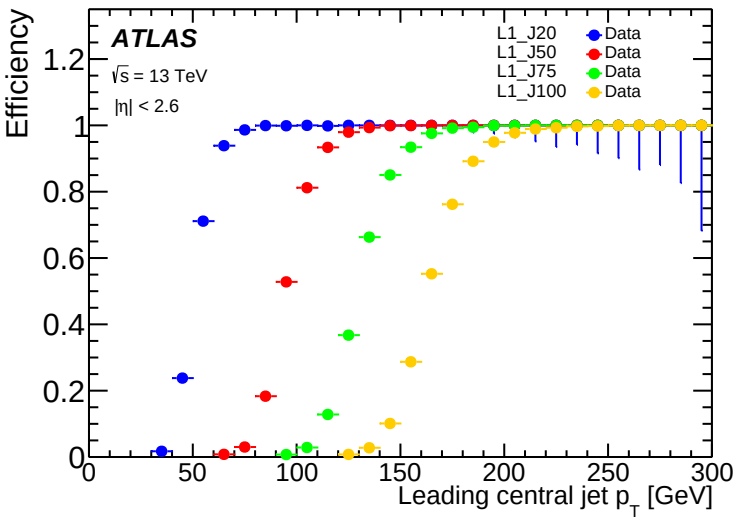

arxiv:1611.09661

HLT jet trigger efficiencies

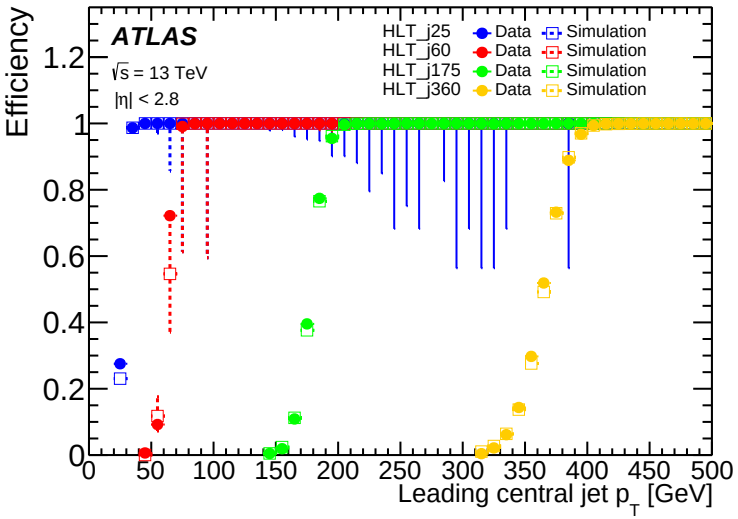

arxiv:1611.09661

- Multiple jet triggers at L1 and HLT
- With different p_T thresholds x:

  L1_Jx and HLT_jx

Resulting jet p_T after HLT

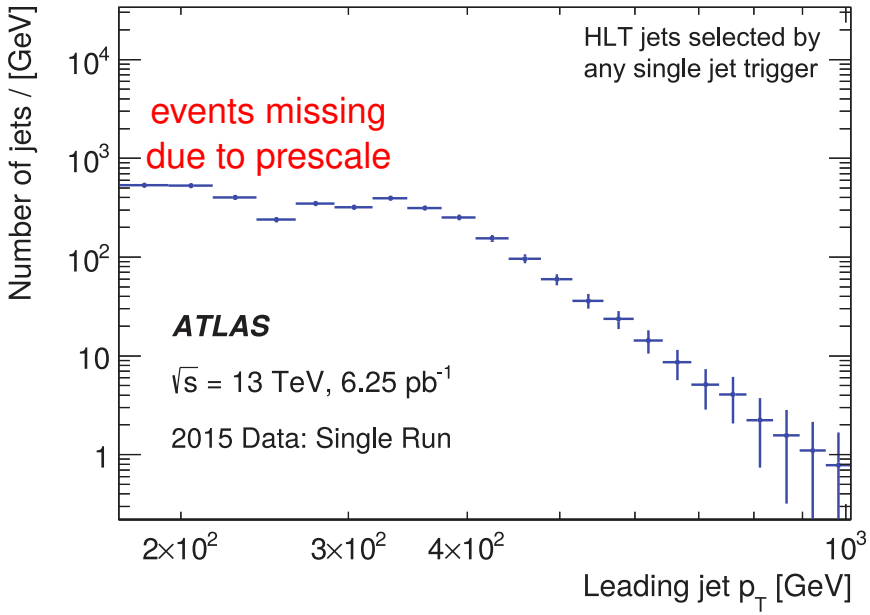

adapted: arxiv:1611.09661

Tapers out towards low p_T

Trigger-Level Analysis

The 1 kHz HLT rate limit is dictated by the
Readout bandwidth = rate × event size

Stream	Average event size
Physics Main	1 MB
Trigger-Level Analysis	6.5 kB
Calibration	1.3 kB to 1 MB
B-Physics, Light States	1 MB

adapted: arxiv:2007.12539

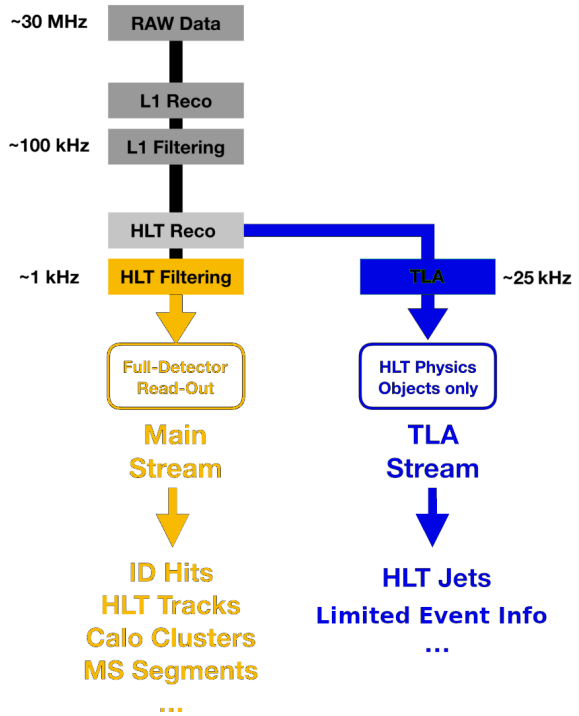

adapted from: M. Montella

Solution: Create dedicated jet trigger stream:
TLA running in parallel to Main

Greatly reduced event size ($\ll 1\%$ of Main)
allows for much higher rate than Main
And all of it is jets!

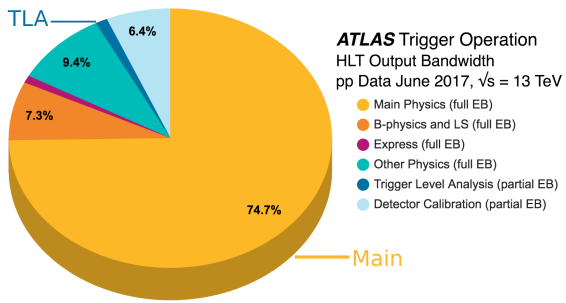

TrigOps

HLT bandwidth

Only the jet four-momenta and very limited event info are retained

Lowest unprescaled HLT jet trigger: $p_T \gtrsim 400$ GeV

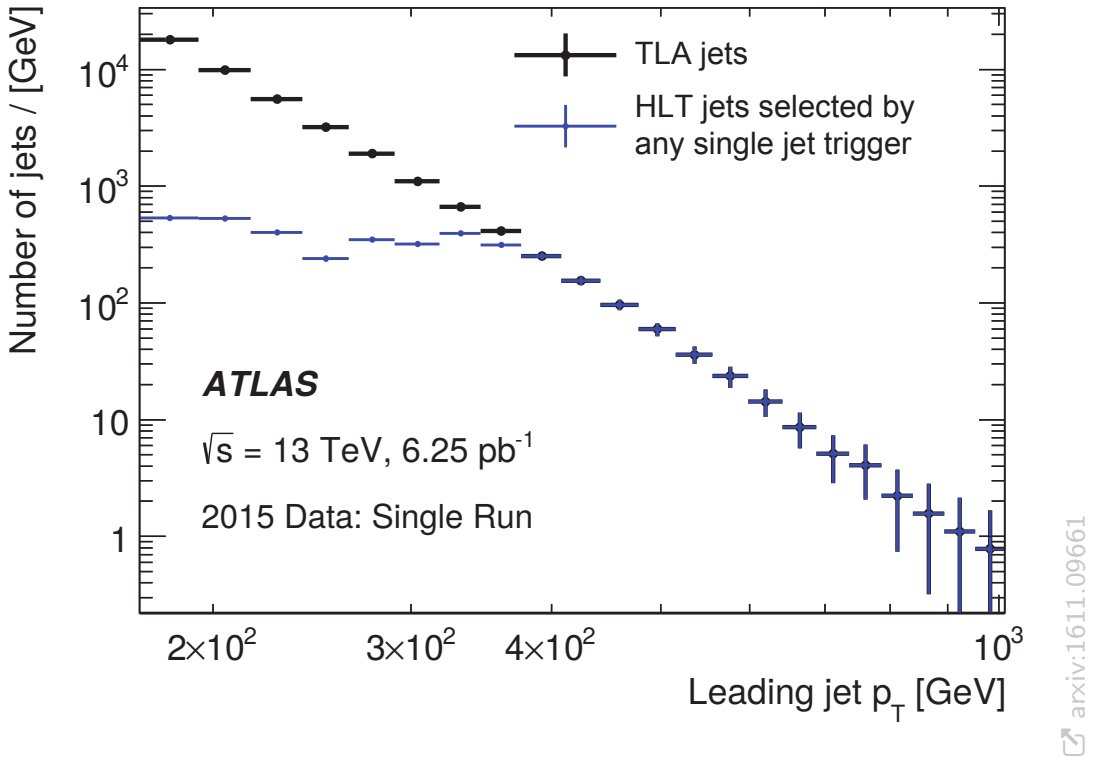

Which corresponds to a dijet mass of:

$$M = 4p_T^2 \cosh^2 y^* = 900 \text{ GeV}$$

for $p_T = 400$ GeV, $y^* = 0.6$

For anything below that TLA outperforms Main

Run 2 TLA Dataset

There are two TLA datsets seeded by different L1 jet triggers:

- J100: 132 fb^{-1}
  - No prescale, active throughout all of Run 2
- J50 (and J50Topo): 15 fb^{-1}
  - Prescaled, active at end of fills

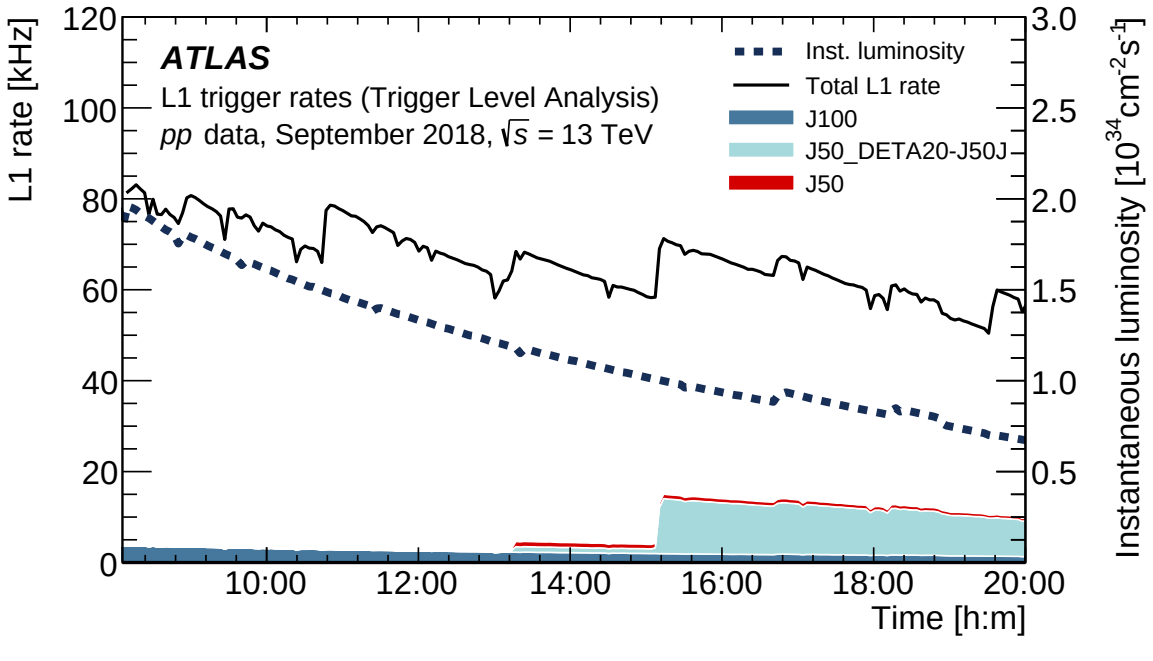

Decreasing luminosity at end of fill allows to enable higher rate triggers

L1Topo

- FPGA processors
- Allow kinematic cuts on combinations of objects

  jets, taus, muons, missing E_{T}

J50_DETA20-J50J (J50Topo):

→ Two L1 jets with:

$p_{\mathrm{T}}^{0} > 50$ GeV & $p_{\mathrm{T}}^{1} > 15$ GeV

and rapidity separation

$|y^{*}| = \frac{|y^{1} - y^{0}|}{2} < 1$

→ Similar to our analysis-level event selection

→ Especially suited for dijet

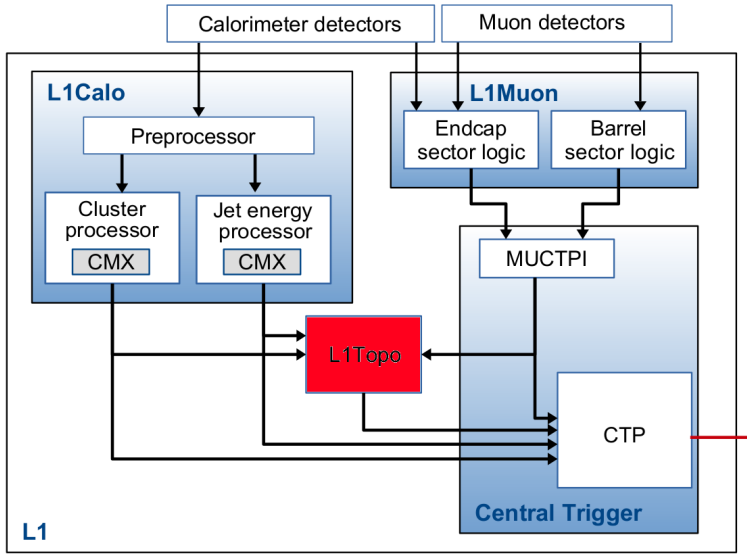

adapted: arxiv:2509.01219

L1Topo module

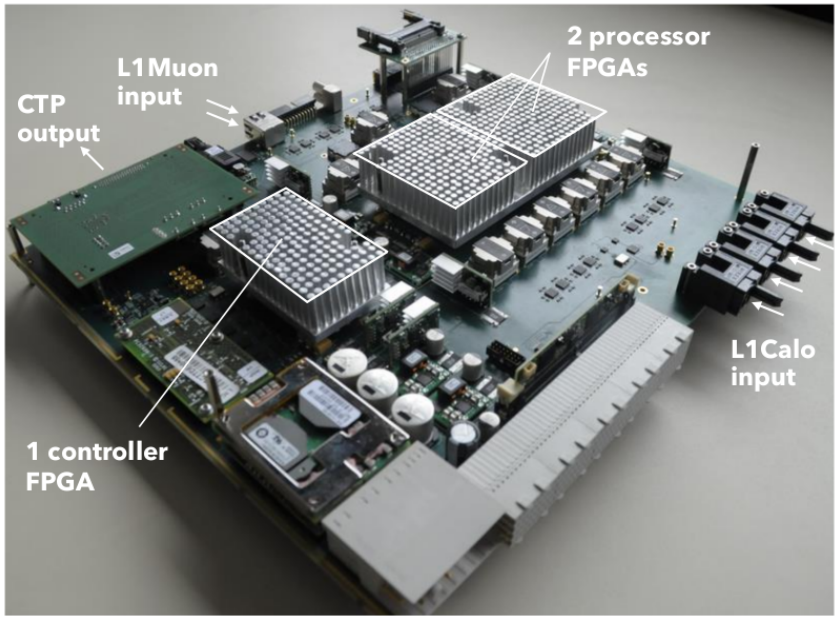

arxiv:2509.01219

Scattering Theory: Dijet Events at Leading Order

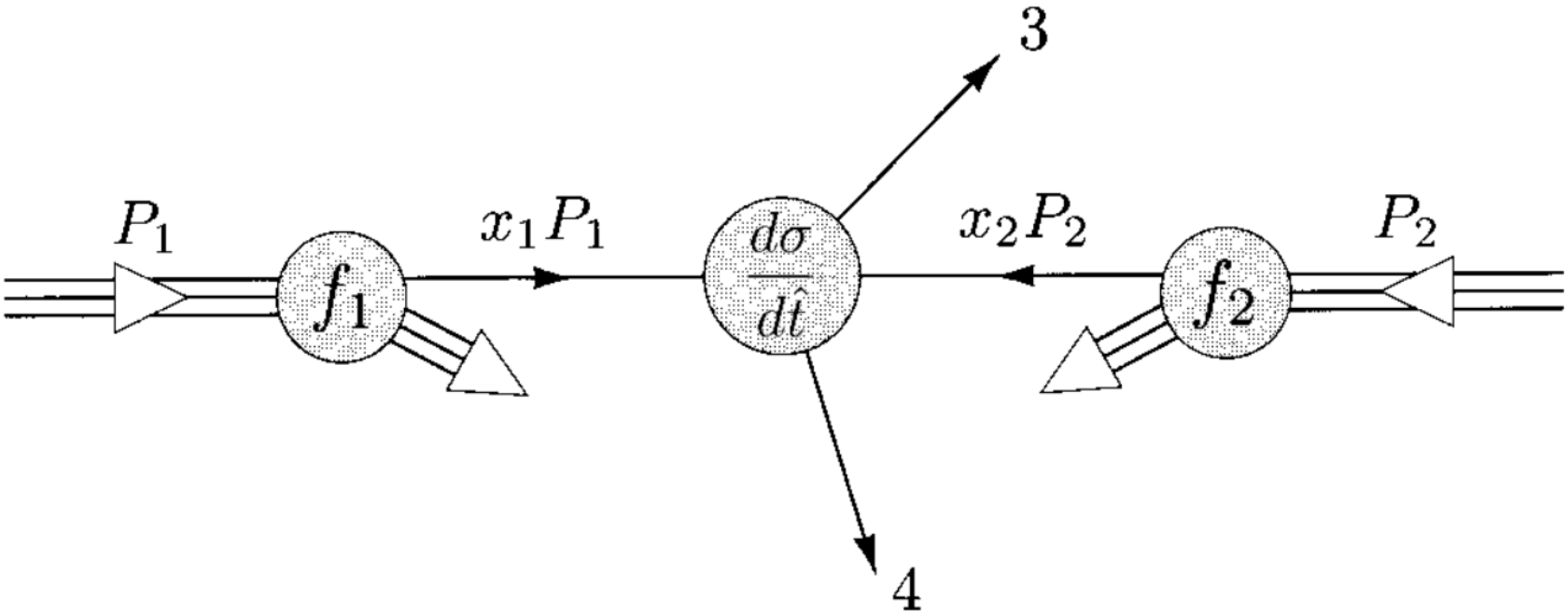

adapted from: Peskin & Schroeder

The total cross-section can be divided in 2 parts:

$$\frac{\mathrm{d}^4\sigma}{\mathrm{d}y_3\mathrm{d}y_4\mathrm{d}^2p_\mathrm{T}} = \underbrace{x_1 f_1(x_1) x_2 f_2(x_2)}_{\text{proton PDFs}} \frac{1}{\pi} \underbrace{\frac{\mathrm{d}\hat{\sigma}}{\mathrm{d}\hat{t}}(1+2\to 3+4)}_{\text{partonic cross section}}$$

Balanced transverse momenta $p_\mathrm{T}^3 = p_\mathrm{T}^4 \equiv p_\mathrm{T}$

But rapidities may differ: $y_3 \neq y_4$ due to boost along beam axis ($x_1 \neq x_2$)

Partonic Cross Section

cross-section of hard process

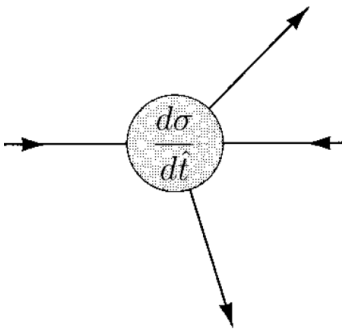

Each of the 4 partons can be any type of quark or gluon

Many subprocesses:

$gg \to gg$

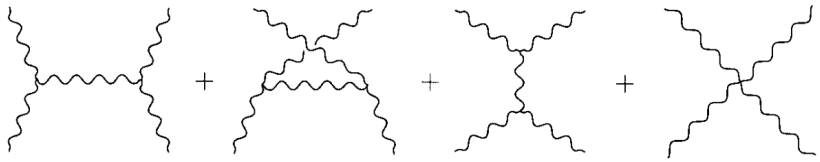

$q\bar{q} \to gg$

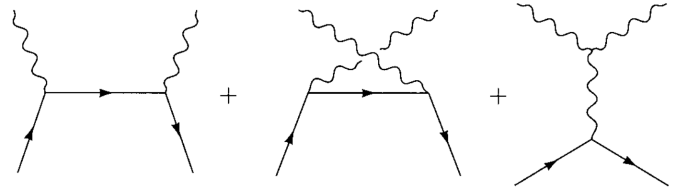

$q\bar{q} \to q\bar{q}$

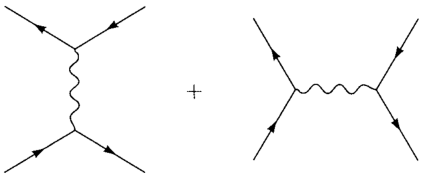

...

Subprocess	$\frac{\hat{s}^2}{\pi\alpha_s^2}\frac{d\hat{\sigma}}{d\hat{t}}(ij \to kl)$
$q_1q_2 \to q_1q_2$	$\frac{4}{9}\frac{\hat{s}^2+\hat{u}^2}{\hat{t}^2}$
$q_1\bar{q}_2 \to q_1\bar{q}_2$	$\frac{4}{9}\frac{\hat{s}^2+\hat{u}^2}{\hat{t}^2}$
$qq \to qq$	$\frac{4}{9}\left(\frac{\hat{s}^2+\hat{u}^2}{\hat{t}^2}+\frac{\hat{s}^2+\hat{t}^2}{\hat{u}^2}\right)-\frac{8}{27}\frac{\hat{s}^2}{\hat{u}\hat{t}}$
$q_1\bar{q}_1 \to q_2\bar{q}_2$	$\frac{4}{9}\frac{\hat{t}^2+\hat{u}^2}{\hat{s}^2}$
$q\bar{q} \to q\bar{q}$	$\frac{4}{9}\left(\frac{\hat{s}^2+\hat{u}^2}{\hat{t}^2}+\frac{\hat{s}^2+\hat{t}^2}{\hat{u}^2}\right)-\frac{8}{27}\frac{\hat{u}^2}{\hat{s}\hat{t}}$
$q\bar{q} \to gg$	$\frac{32}{27}\frac{\hat{t}^2+\hat{u}^2}{\hat{t}\hat{u}}-\frac{8}{3}\frac{\hat{t}^2+\hat{u}^2}{\hat{s}^2}$
$gg \to q\bar{q}$	$\frac{1}{6}\frac{\hat{t}^2+\hat{u}^2}{\hat{t}\hat{u}}-\frac{3}{8}\frac{\hat{t}^2+\hat{u}^2}{\hat{s}^2}$
$gq \to gq$	$-\frac{4}{9}\frac{\hat{s}^2+\hat{u}^2}{\hat{s}\hat{u}}+\frac{\hat{u}^2+\hat{s}^2}{\hat{t}^2}$
$gg \to gg$	$\frac{9}{2}\left(3-\frac{\hat{t}\hat{u}}{\hat{s}^2}-\frac{\hat{s}\hat{u}}{\hat{t}^2}-\frac{\hat{s}\hat{t}}{\hat{u}^2}\right)$

$\hat{s}$, $\hat{t}$, $\hat{u}$: Mandelstam variables

adapted from: arxiv:1110.5302

The t-Channel Pole

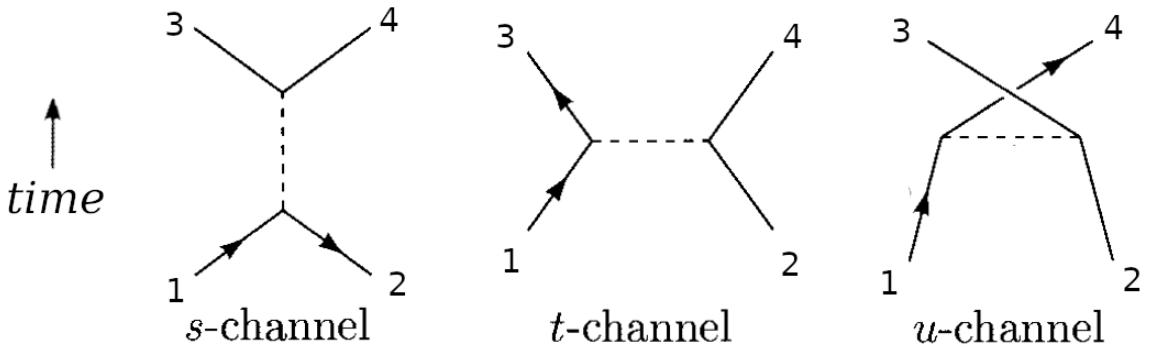

$$\hat{s} = (p_1 + p_2)^2 = (p_3 + p_4)^2$$
$$\hat{t} = (p_1 - p_3)^2 = (p_4 + p_2)^2$$
$$\hat{u} = (p_1 - p_4)^2 = (p_3 + p_2)^2$$

Determine the θ^* dependence for each subprocess:

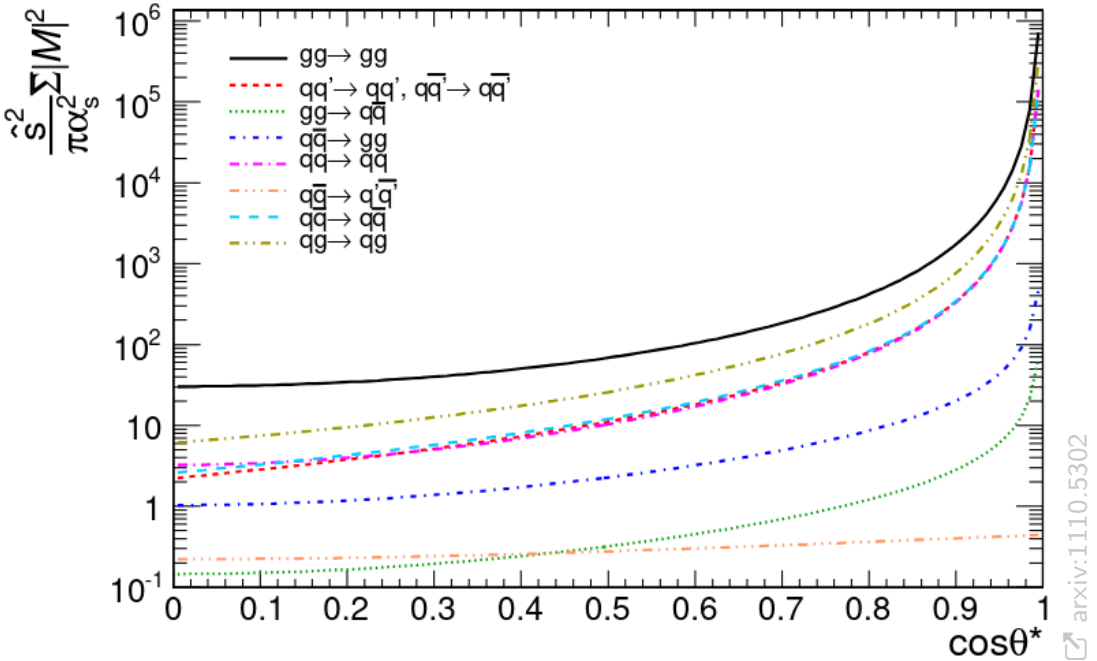

Most behave like Rutherford scattering: $\propto \frac{1}{(1-\cos\theta^*)^2}$

With scattering angle θ^* in the CM*

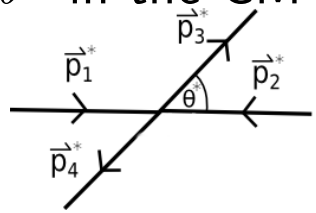

For massless partons:

$$\hat{s} = M^2 = \frac{4p_T^2}{\sin\theta^*}$$
$$\hat{t} = -\frac{\hat{s}}{2}(1 - \cos\theta^*)$$
$$\hat{u} = -\frac{\hat{s}}{2}(1 + \cos\theta^*)$$

Optimal Angular Cut

BSM signals with resonant decays have very different $\cos\theta^*$ dependence:

relations from: arxiv:1110.5302

BSM model	$\frac{d\hat{\sigma}}{d\cos\theta^*}$
E_6 diquark, color octet scalars	constant
excited quarks	$\propto 1 + \cos\theta^*$
W', Z', axigluon, coloron	$\propto 1 + \cos^2\theta^*$
RS graviton $gg \to G \to q\bar{q}$	$\propto 1 - \cos^4\theta^*$
RS graviton $gg \to G \to gg$	$\propto 1 + 6\cos^2\theta^* + \cos^4\theta^*$
RS graviton $q\bar{q} \to G \to q\bar{q}$	$\propto 1 - 3\cos^2\theta^* + 4\cos^4\theta^*$
QCD dijet	$1/(1-\cos\theta^*)^2$

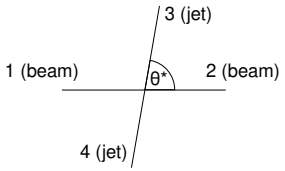

signal: close to orthogonal

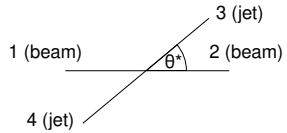

background (QCD): collinear

Allows to derive optimal $|\cos\theta^*|_{\max}$ cut for best $S/\sqrt{B}$:

$$S \propto \int_{-\cos\theta^*_{\max}}^{+\cos\theta^*_{\max}} \text{const}\ d\cos\theta^* = 2\cos\theta^*_{\max}$$

$$B \propto \int_{-\cos\theta^*_{\max}}^{+\cos\theta^*_{\max}} \frac{1}{(1-\cos\theta^*)^2}\ d\cos\theta^* = \frac{2\cos\theta^*_{\max}}{1-\cos^2\theta^*_{\max}}$$

$$\Rightarrow \frac{S}{\sqrt{B}} = \frac{2\cos\theta^*_{\max}}{\sqrt{\frac{2\cos\theta^*_{\max}}{1-\cos^2\theta^*_{\max}}}} \to \text{maximum at } \cos\theta^*_{\max} = \frac{1}{\sqrt{3}}$$

$$\cos\theta^* = \tanh y^* \Rightarrow \text{best } y^* \text{ cut: } \tanh^{-1}\frac{1}{\sqrt{3}} \approx 0.66$$

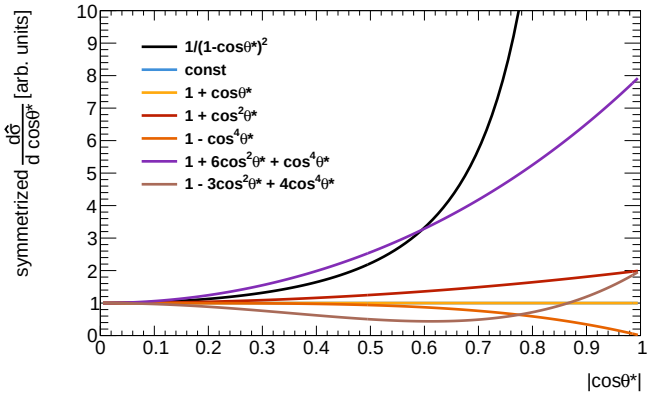

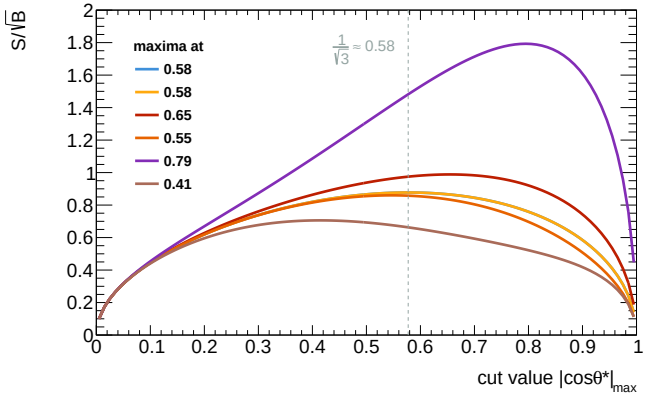

Event Selection

TLA Run 2 TLA dataset has:

- $>$ 60 billion events in J100
- $>$ 40 billion in J50 (overlaps with J100)
- For comparison: All of Physics Main in Run1 & 2 combined:

  $\approx$ 25 billion events (source)

cutflow	J50 dataset	J100 dataset
initial	40 763 638 635	62 285 765 243
$\lvert\eta^{0,1}\rvert < 2.4$, veto $1.0 < \lvert\eta^{0,1}\rvert < 1.6$	17 640 375 792	27 460 791 144
$p_{\mathrm{T}}^{0,1} > 85$ GeV	7 261 455 769	15 827 611 199
$\lvert y^{*}\rvert < 0.6$	3 964 040 080	8 348 429 622
trigger: J50(Topo) or J100	2 666 093 601	5 549 390 857
J50: $m_{jj} > 344$ GeV	351 223 259	–
J100: $m_{jj} > 481$ GeV	–	765 234 799

HepData:161624

After Event selection: $>$ 0.3 & $>$ 0.7 billion events

Event Selection

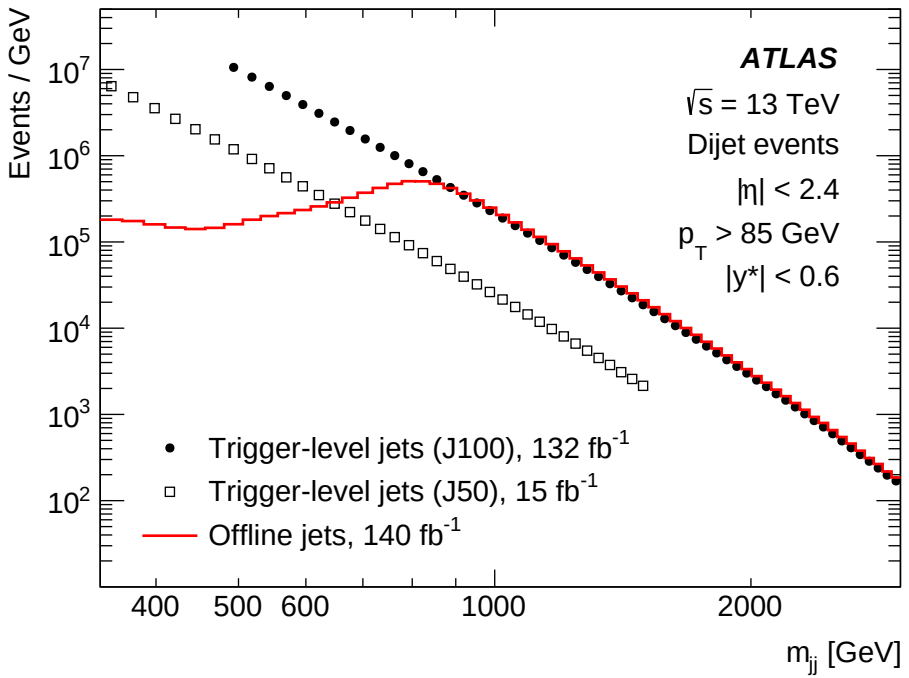

- Advantage over offline (physics main) dataset at $m_{jj} \ll 1$ TeV

Getting the jet energy right demands calibration

The ATLAS calorimeter

- Non-compensating:
  - Different response to EM and hadronic signals
- Sampling:
  - Not all material is active

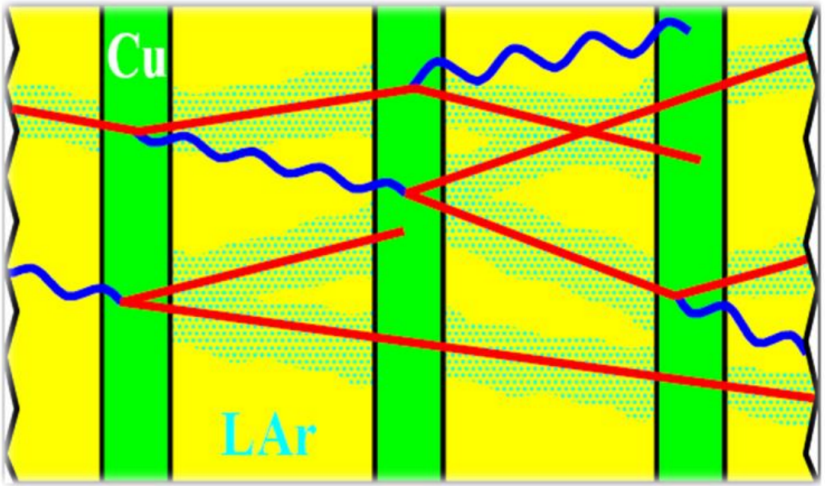

P. Loch

Additional effects from collisions

Underlying event

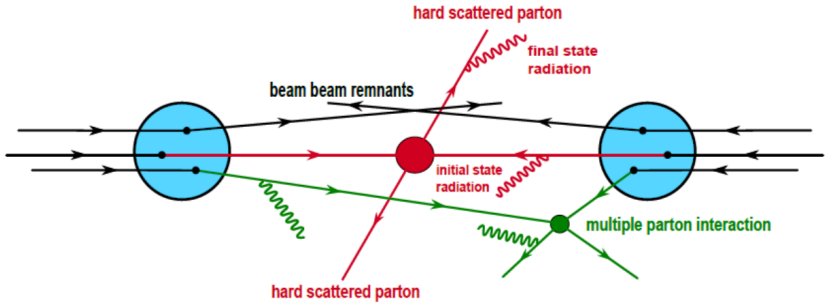

O. Kepka

Pileup

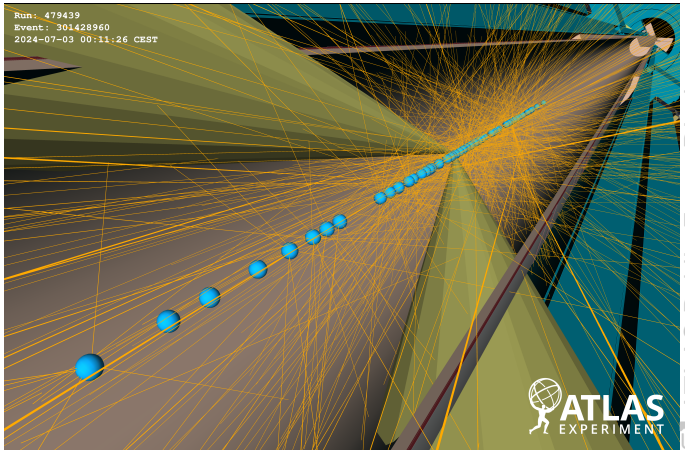

ATLAS Public Event Display

(dijet event at $\mu = 65$)

... and many more effects ...

Jet Calibration

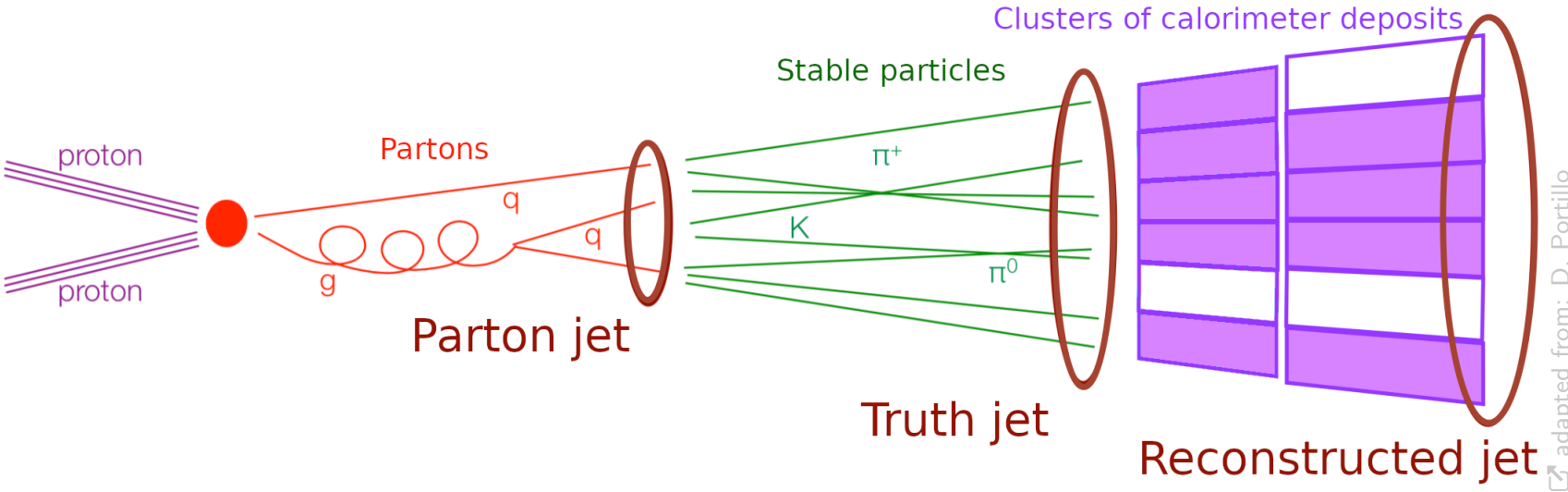

- ΔR-match isolated reco to truth jets in MC
- Response $\frac{p_{\mathrm{T}}^{\mathrm{reco}}}{p_{\mathrm{T}}^{\mathrm{truth}}}$
- Gaussian fit determined mode of distribution
- Resolution: Width of response distribution

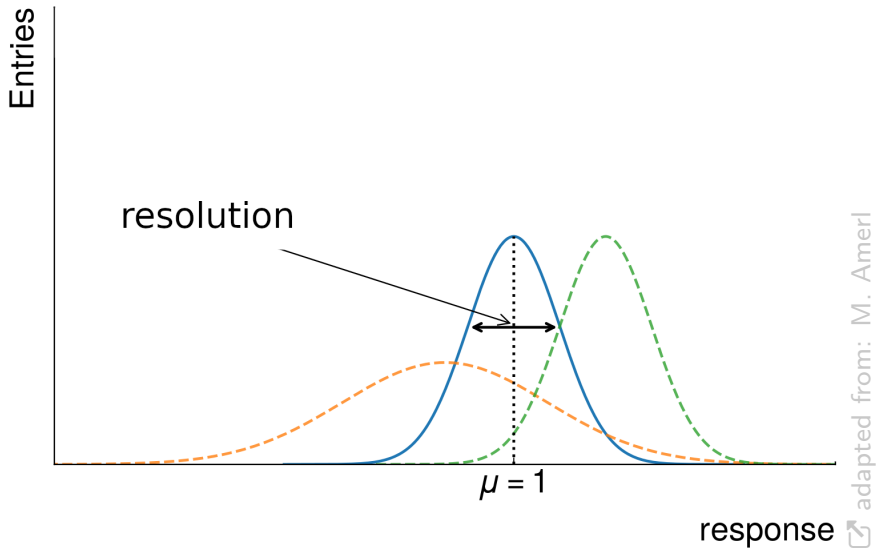

→ Calibration factor: Inverse of response binned in e.g. p_{T}, η etc

Jet Calibration

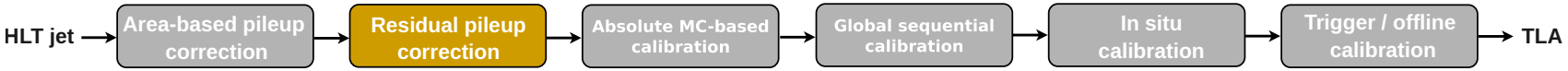

Residual pileup correction

- After area-based correction residual pileup dependencies remain
- Offline: Corrected for two pileup-estimators:
  - N_{PV}: Number of primary vertices
  - μ: Average number of interactions per bunch crossing

μ throughout Run 2

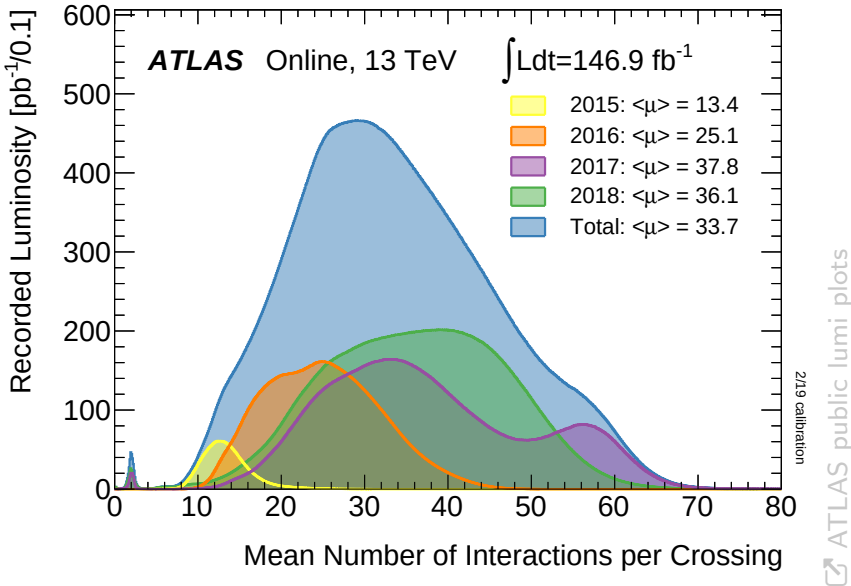

$$p_{\mathrm{T}}^{\mathrm{res}} = p_{\mathrm{T}}^{\mathrm{area}} - \alpha \frac{\partial p_{\mathrm{T}}}{\partial N_{\mathrm{PV}}}(N_{\mathrm{PV}} - 1) - \beta \frac{\partial p_{\mathrm{T}}}{\partial \mu}\mu$$

- TLA: Good closure achieved with regards to μ term
- NPV term not possible for trigger jets due to lack of tracking in TLA

Jet Calibration

HLT jet → Area-based pileup correction → **Residual pileup correction** → Absolute MC-based calibration → Global sequential calibration → In situ calibration → Trigger / offline calibration → TLA

Trigger-Level

μ dependence

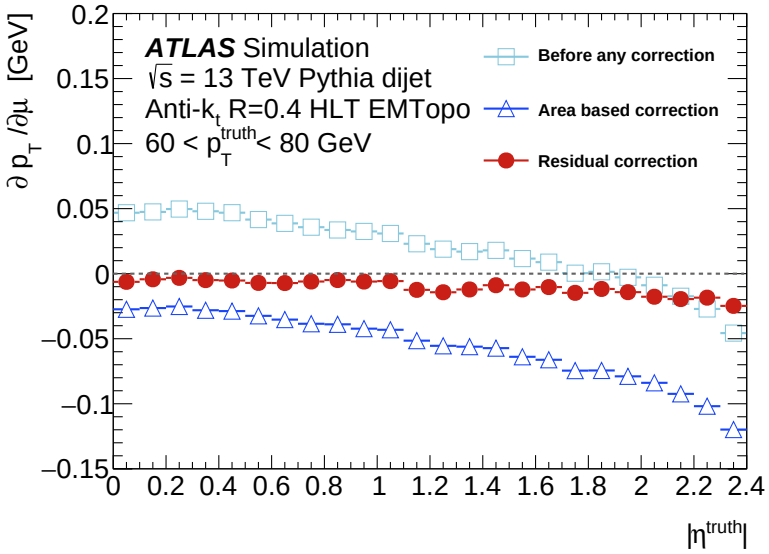

Phys. Rev. D 112, 092015

N_{PV} dependence

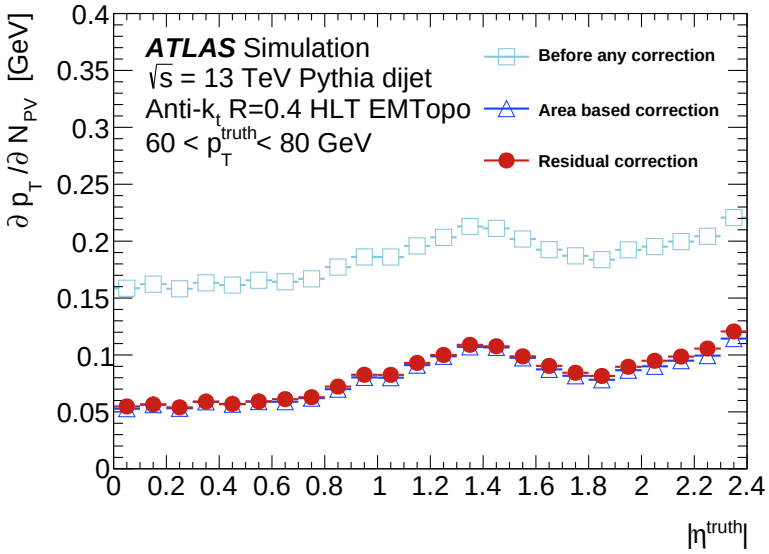

Phys. Rev. D 112, 092015

Offline

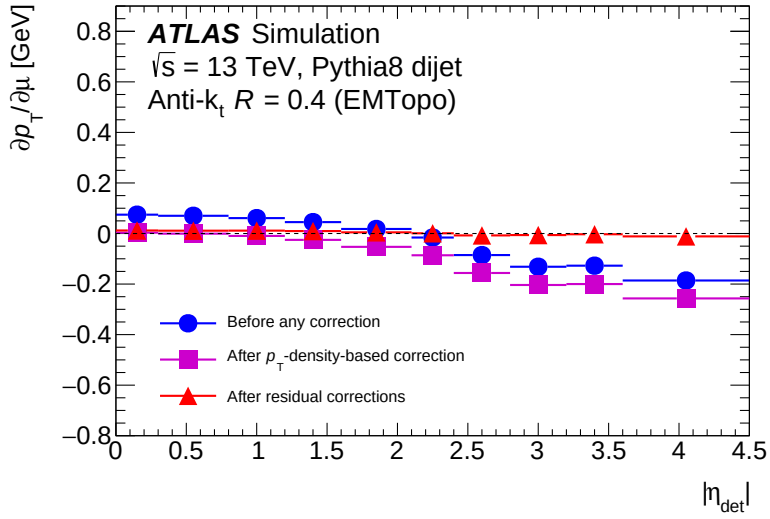

JETM-2018-05

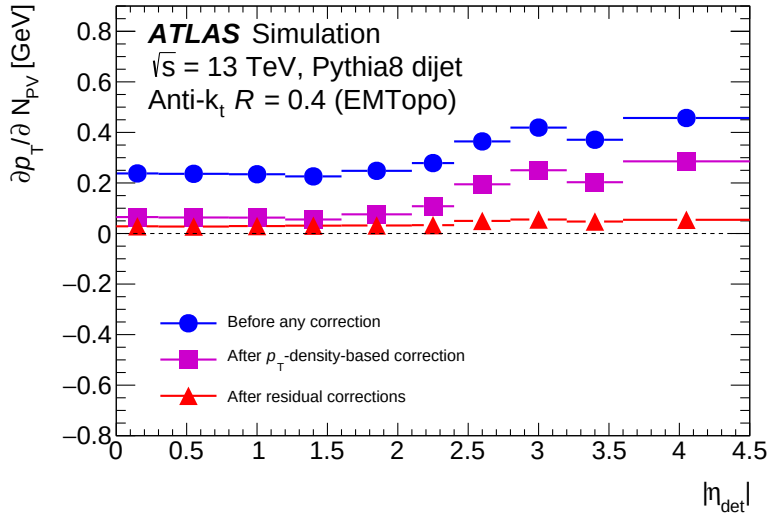

JETM-2018-05

Jet Calibration

HLT jet → Area-based pileup correction → Residual pileup correction → **Absolute MC-based calibration** → Global sequential calibration → In situ calibration → Trigger / offline calibration → TLA

Absolute MC-based calibration

- Performs bulk of response calibration
- Corrects according to response measured in MC
- Small angular correction to η
- Response binned in E, η fitted with functional form:

$$\mathcal{F}_{\mathrm{JES}}(E^{\mathrm{truth}}) \sum_{i=0}^{N_{\mathrm{max}}} a_i (\ln E^{\mathrm{truth}})^i$$

- Calibration factors from numerical inversion
- Excellent closure of E across η

Trigger-Level

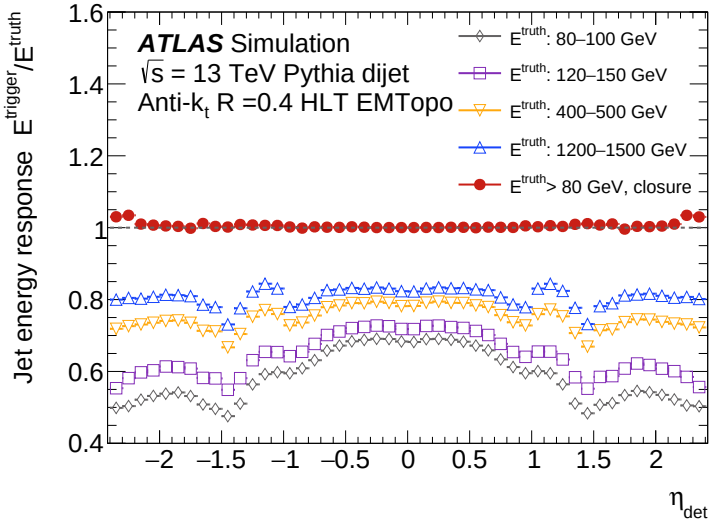

Offline

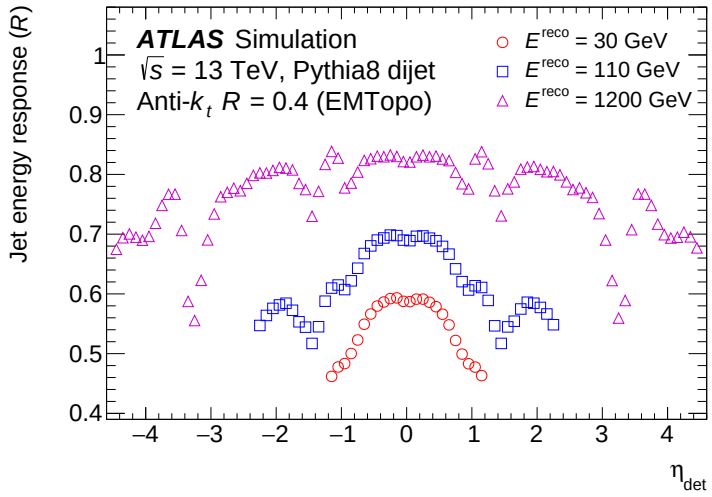

Phys. Rev. D 112, 092015

JETM-2018-05

Jet Calibration

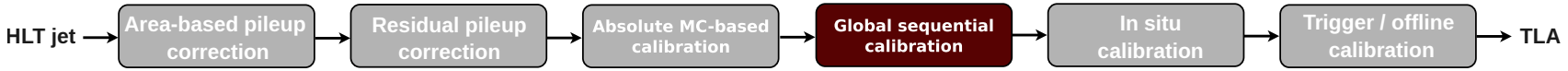

Global sequential calibration

- Improves resolution
- While leaving response unchanged
- Idea: Different populations of jets have higher/lower response
- Correcting them individually towards the mean improves overall resolution
- Only 2 out of the 5 GSC variables are available in TLA
- But they are the main contributors
- Missing: Track- and muon-based variables: n_{trk}, w_{trk}, n_{segments}
- Still: Considerable improvement in resolution from TLA GSC

Trigger-Level

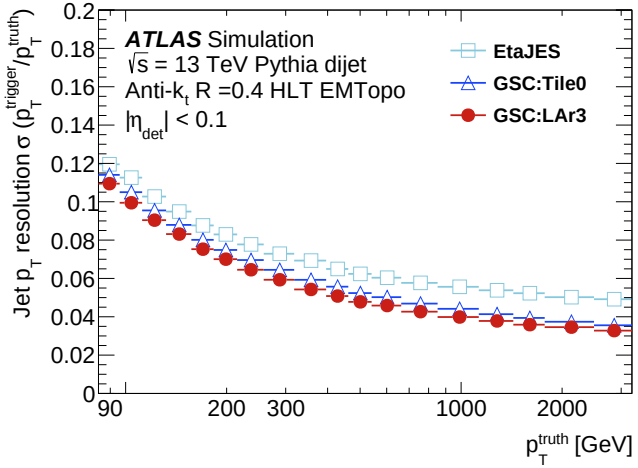

Phys. Rev. D 112, 092015

Offline

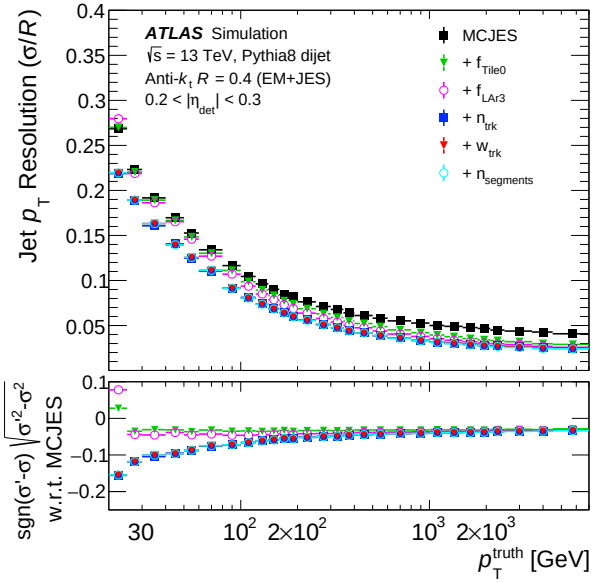

JETM-2018-05

Jet Calibration

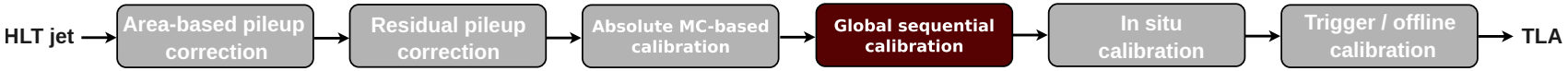

- Quark- and gluon-initiated jets differ in response
- Lack of tracking in TLA does not allow for q/g-sensitive GSC steps: n_{trk} (number of tracks), w_{trk} (track-width)
- Rederived flavour-composition and -response uncertainty

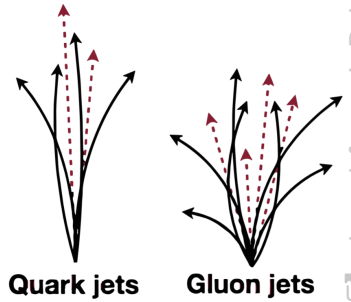

adapted from: J. Babbar

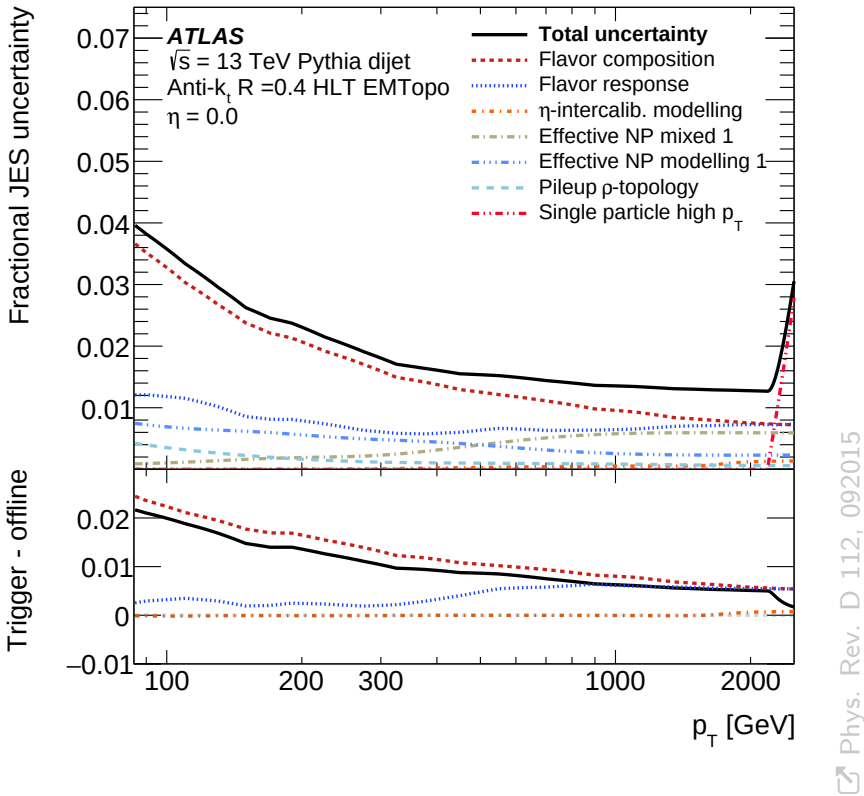

Phys. Rev. D 112, 092015

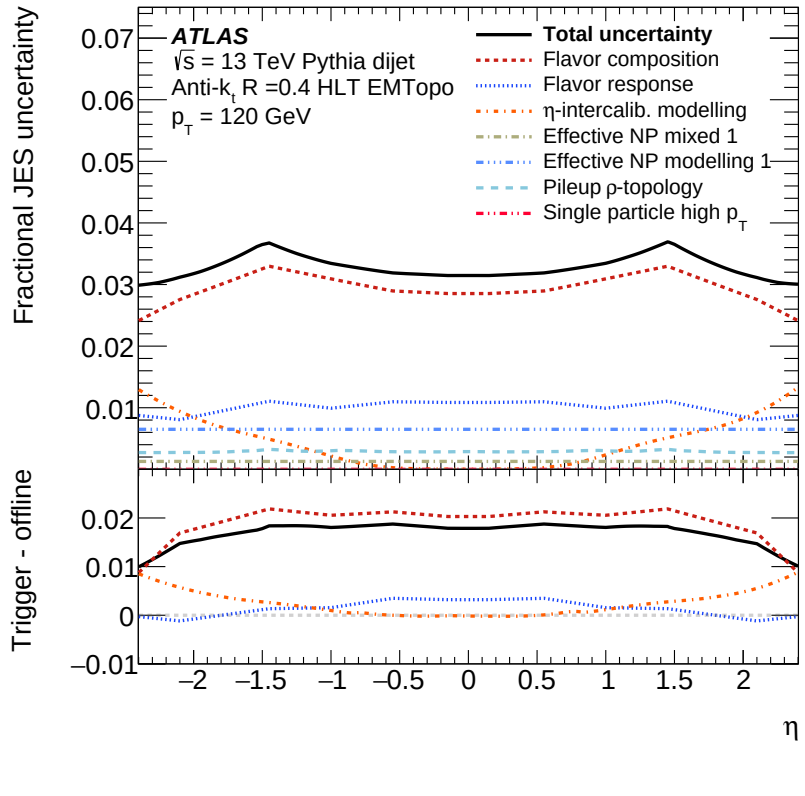

Phys. Rev. D 112, 092015

Jet Calibration

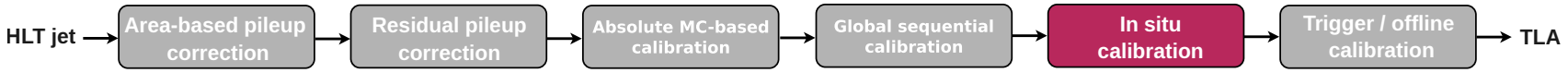

- All previous steps are applied to MC and data
- In situ: only applied to data
- Corrects for residual differences in data/MC

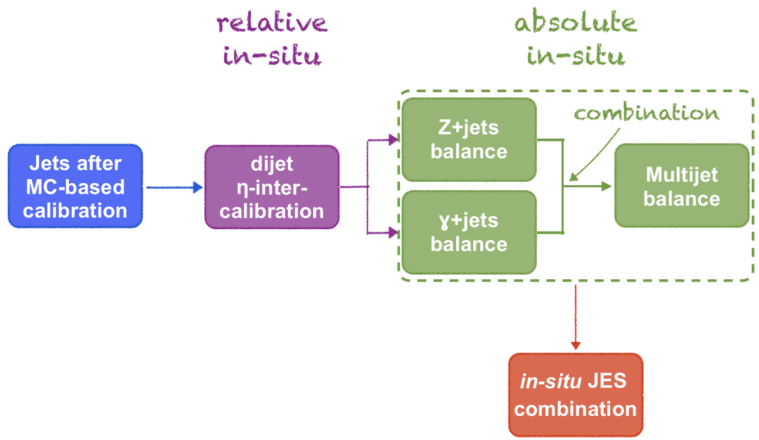

Relative *in-situ* JES: correct jets with $|\eta| > 0.8$ to the same energy scale as $|\eta| < 0.8$
Absolute *in-situ* JES: correct jets with $|\eta| < 0.8$ to a precise reference object

C. Delitzsch

Relative in situ calibration

- Use well measured central jets

  to constrain forward jet momenta

Absolute in situ calibration

- Use balance of jets agains well measured objects

  (photons, multiple jets)

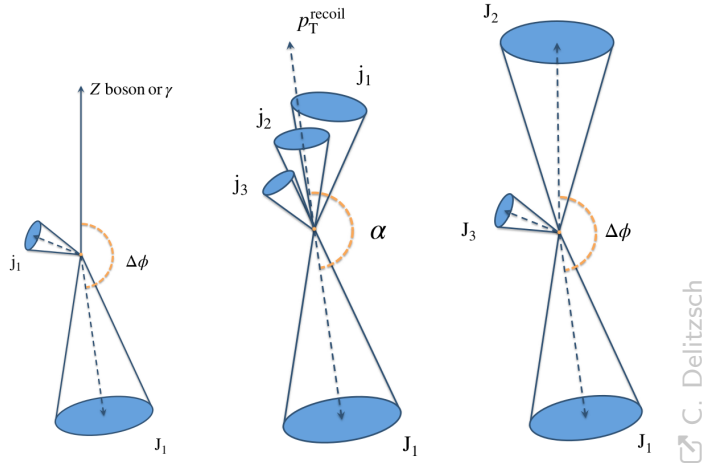

C. Delitzsch

→ Factors derived for offline jets also used for trigger jets

Jet Calibration

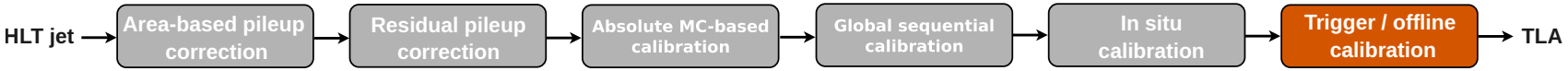

Trigger/offline jet correction brings trigger jets to offline scale

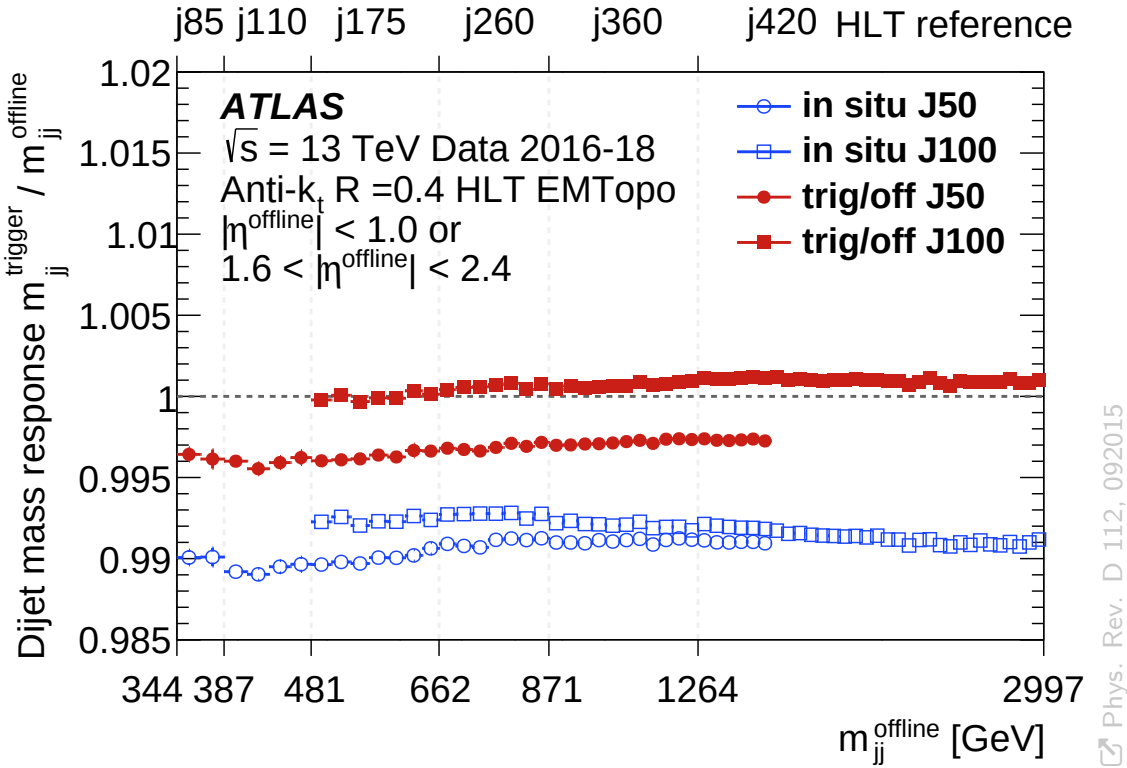

- Allows use of most uncertainties derived for offline jets
- Derived independently for each year (2016, 2017, 2018) and dataset (J50, J100) to compensate for different pileup conditions
- Excellent closure within 5 per-mille both in m_{jj} and in p_T

Data-driven background estimate

- With dijet m_{jj} functional form
- Observed m_{jj} spectrum consistent with bkg-only hypothesis
- Bump-Hunter identifies most significant excess at 650 GeV
  - Global BH p-value: 0.27

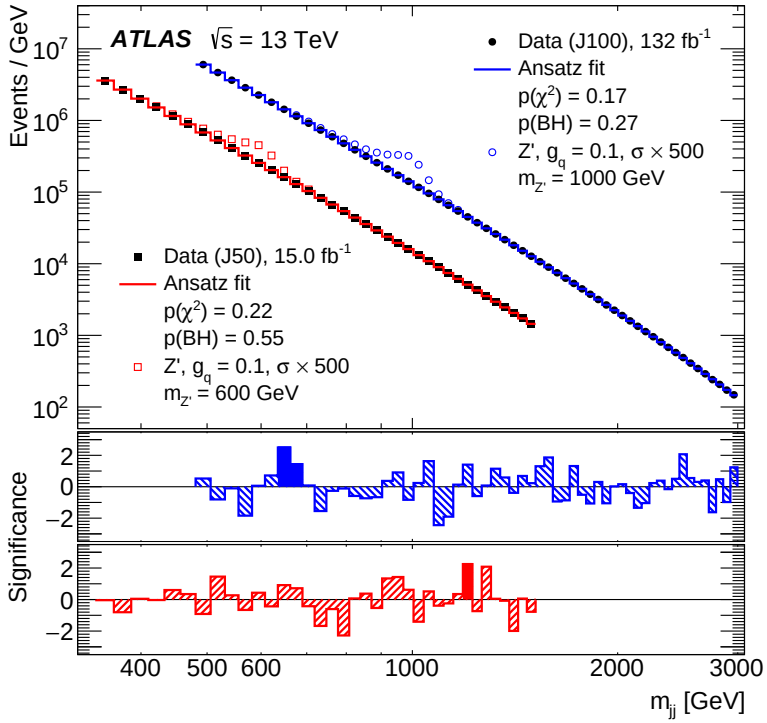

$$f(x) = \underbrace{p_1(1-x)^{p_2} x^{\sum_{i=3}^{N} p_i \log^{(i-3)}(x)}}_{\text{dijet function}} \underbrace{\left(1 + \sum_{j=1}^{n_{\text{syst}}} \theta_j \sum_{k=1}^{5} c_{jk} x^k\right)}_{\text{jet systematics}} \quad \text{with } x = \frac{m}{\sqrt{s}}$$

$$f(x) = \left[\text{dijet}\right] \times \left(1 + \theta_1 \times \left[\text{syst 1}\right] + \theta_2 \times \left[\text{syst 2}\right] + \cdots\right)$$

F. Bartels

→ Tests following ATLAS' "Recommendations for the Modeling of Smooth Backgrounds"

Determining N

F-test

- Used to determine number of parameters N in fit function
- Choose N for which $N+1$ does not significantly improve goodness-of-fit p-value by > 0.05
- Resulting choice:

  $\rightarrow$ $N = 6$ both in J50 and J100

Additional tests (backup)

- Spurious signal
- Signal injection
- Coverage

J50

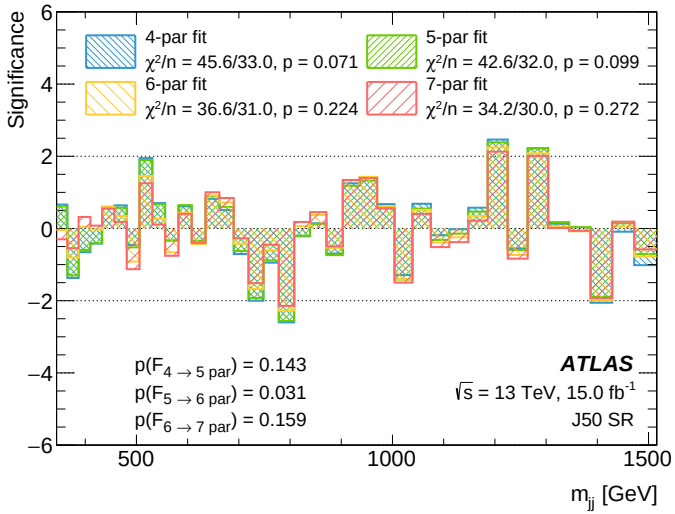

J100

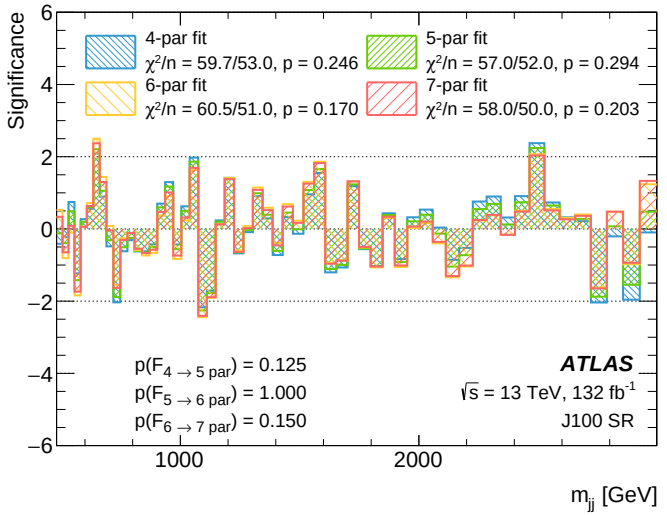

Phys. Rev. D 112, 092015

Phys. Rev. D 112, 092015

Results and Exclusion Limits

Gaussian

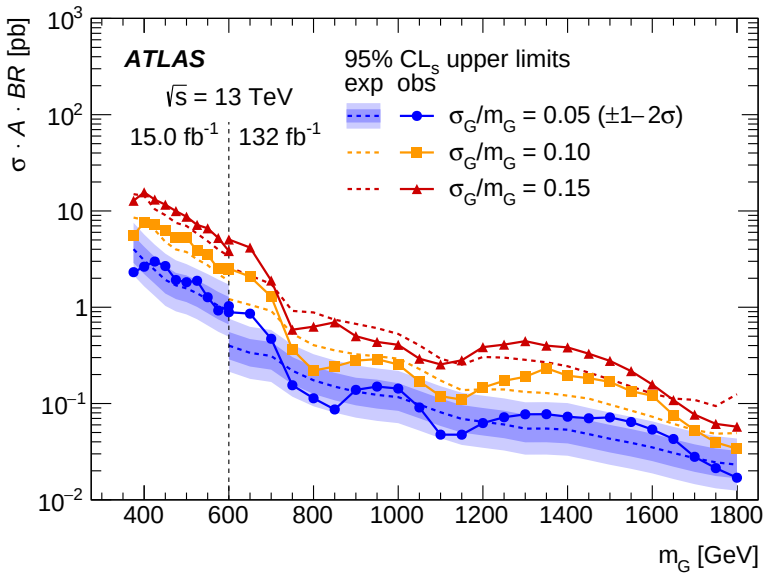

Phys. Rev. D 112, 092015

Z'

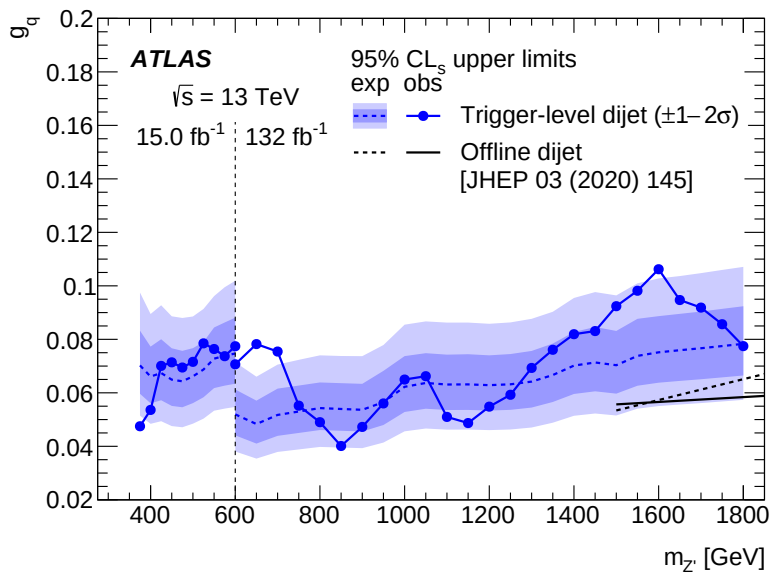

Phys. Rev. D 112, 092015

- Limits on Z' and Gaussian resonances (5%, 10%, 15% width)
- Starting at 375 GeV
- Most significant excess at 650 GeV for Z' (3.4 σ local, 2.2 σ global)

CMS: Data Scouting

CMS recently presented their full Run 2 dijet scouting analysis

- arxiv:2510.21641
- ATLAS TLA ≈ CMS Scouting
- Limits compatible with us at > 600 GeV
- Do not set limits below 600 GeV

  where ours uses J50 dataset
- CMS published multiple data scouting analyses before

CMS

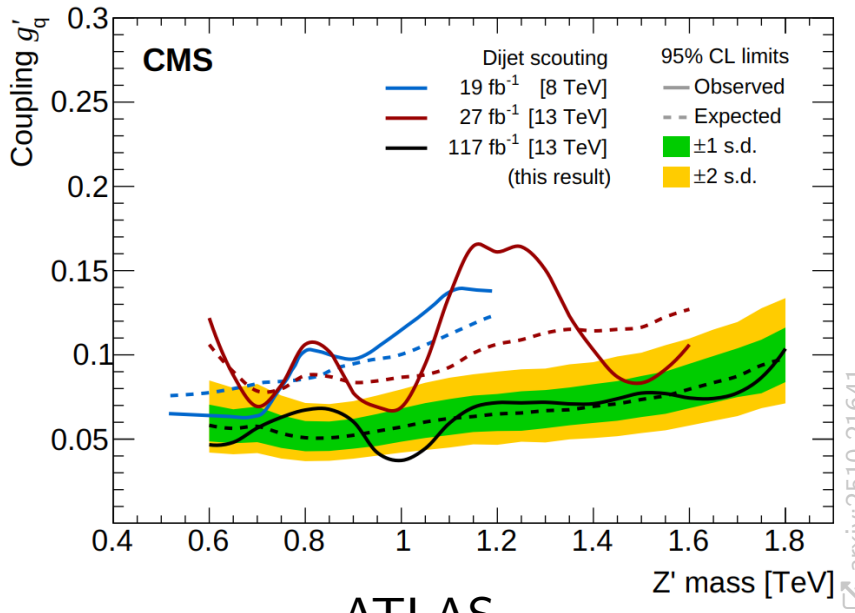

arxiv:2510.21641

ATLAS

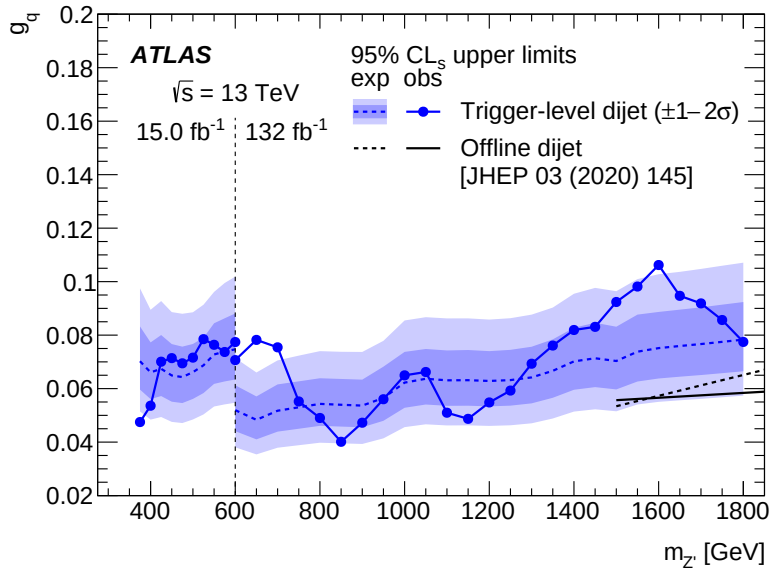

Phys. Rev. D 112, 092015

TLA / Data Scouting publications

experiment	signature	mass range [GeV]	publication
ATLAS	dijet	450-1800	PRL 121 (2018) 081801
	dijet	**375-1800**	Phys. Rev. D 112, 092015 (2025)
CMS	dijet	600-1800	arxiv:2510.21641
	dijet	500-900	CMS-PAS-EXO-11-094
	dijet	500-800	PRL 117 (2016) 031802
	dijet	600-1600	PLB 769 (2017) 520
	dijet	600-1600	JHEP 08 (2018) 130
	pair of 3j	200-700	Phys. Rev. D 99, 012010
	dijet + ISR jet	350-700	PLB 805 (2020) 135448
	LLP$\rightarrow$di-μ	10-50	Phys. Rev. 124, 131802
	LLP$\rightarrow$di-μ	0.6-50	JHEP 04 (2022) 062
	multi-μ ($\eta \rightarrow 4\mu$)	0.45-40	CMS-PAS-BPH-22-003

CMS multi-μ, 13 TeV (2022)

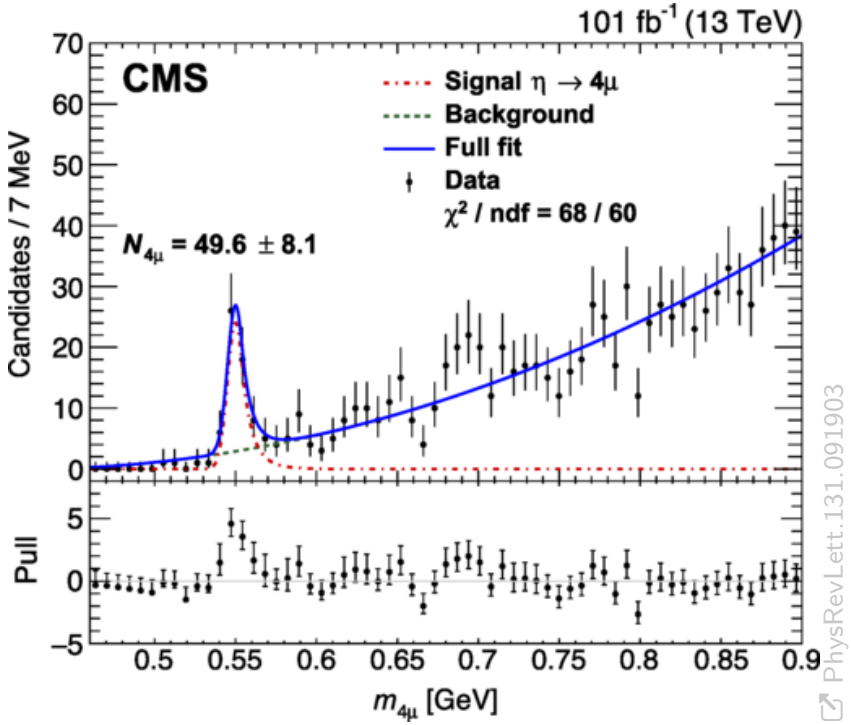

- 101 fb^{-1} (2017 & 2018)
- Scouting used in $<$ 40 GeV range
- First $\eta \to 4\mu$ observation!

Overcoming Trigger Limitations: Other Techniques

Initial State Radiation (ISR)

Trigger on ISR (γ or jet) instead

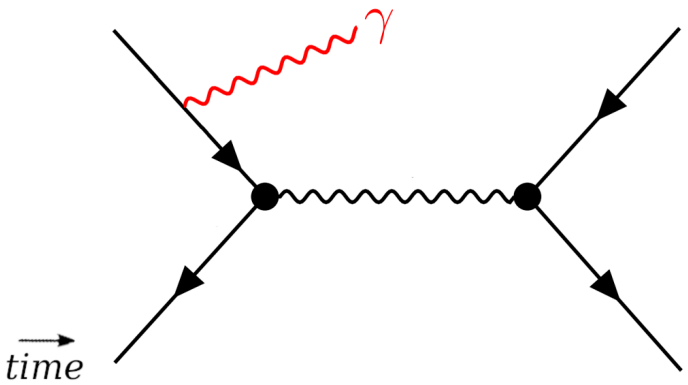

adapted: arXiv:2308.03680

Boosted large-R jets

Reconstruct highly collimated dijets in single jet

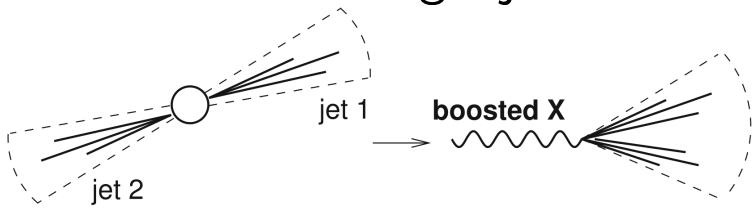

adapted: EPJC V75, 415 (2015)

b-tagging

b-initiated jets are much less abundant

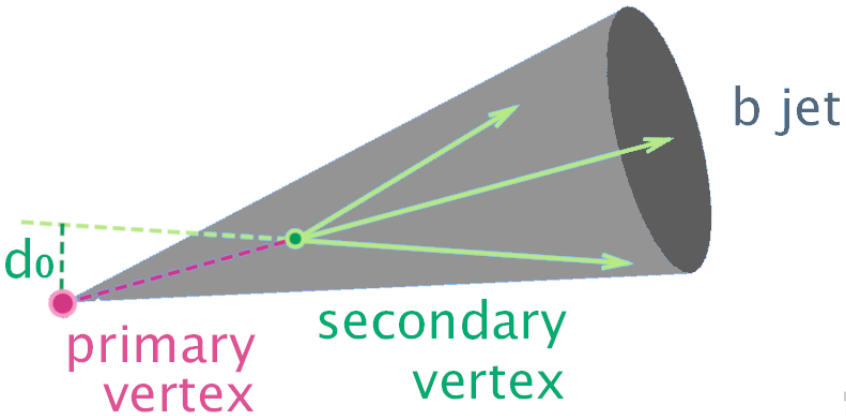

adapted: particlebites

Partial Event Building (PEB)

Save full data but only in region of interest

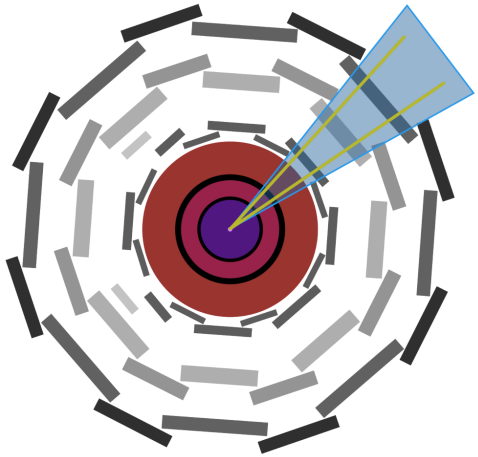

H. Russel

Dijet Resonance Searches

Expt.	Year	$\sqrt{s}$ [TeV]	$\int Ldt$ [pb^{-1}]	m_{jj} range [TeV]	Ref.	technique
UA1	1986	0.63	0.26	0.07 - 0.3	1	
UA1	1988	0.63	0.49	0.11 - 0.3	2	
CDF	1990	1.8	0.026	0.06 - 0.5	3	
UA2	1990	0.63	4.7	0.05 - 0.3	4	
CDF	1993	1.8	4.2	0.14 - 1.0	5	
UA2	1993	0.63	11	0.05 - 0.3	6	
CDF	1995	1.8	19	0.15 - 0.9	7	
CDF	1997	1.8	106	0.18 - 1.0	8	
D0	2004	1.8	109	0.18 - 1.2	9	
CDF	2009	1.96	1130	0.18 - 1.3	10	
ATLAS	2010	7	0.32	0.20 - 1.7	11	
CMS	2010	7	2.9	0.22 - 2.1	12	
ATLAS	2011	7	36	0.50 - 2.8	13	
CMS	2011	7	1000	0.84 - 3.7	14	
ATLAS	2011	7	1000	0.72 - 4.1	15	
ATLAS	2012	7	1000	0.8 - 4.0	16	
ATLAS	2012	7	4800	1.0 - 8.0	17	
CMS	2013	7	5000	1.0 - 4.0	18	b-tagged
CMS	2013	8	4000	1.0 - 4.8	18	
CMS	2015	8	19700	1.2 - 6.5	19	
ATLAS	2015	8	20300	0.8 - 4.5	20	
CMS	2016	8	18800	0.5 - 0.8	21	scouting
CMS	2016	13	2400	1.5 - 0.7	22	
ATLAS	2016	13	3200	1.1 - 5.0	23	b-tagged
ATLAS	2016	13	3600	1.5 - 6.5	24	
CMS	2017	13	12900	0.6 - 1.5	25	scouting
CMS	2017	13	12900	1.5 - 7.5	25	
ATLAS	2017	13	37000	1.5 - 3.5	26	
ATLAS	2018	13	29300	0.45 - 1.8	27	TLA
ATLAS	2018	13	36100	0.57 - 7.0	28	b-tagged
CMS	2018	13	36000	1.6 - 8.1	29	
CMS	2018	13	27000	0.6 - 1.6	30	scouting
CMS	2018	13	19700	0.325 - 1.2	31	b-tagged
ATLAS	2019	13	36100	0.1 - .22	32	boosted + ISR (γ, j)
ATLAS	2020	13	139000	1.5 - 5.0	33	
CMS	2020	13	77800	1.8 - 8.0	34	
CMS	2020	13	18300	0.35 - 0.7	35	ISR j
CMS	2023	13	138000	1.8 - 2.4	36	b-tagged
ATLAS	2025	13	140000	0.2 - 0.65	37	ISR (γ, j)
ATLAS†	2025	13	132000	0.375 - 1.8	38	TLA
CMS*	2025	13	117100	0.6 - 1.8	39	scouting

*:preliminary, †: this publication

Multiple techniques (and combinations) are needed to span the full mass range

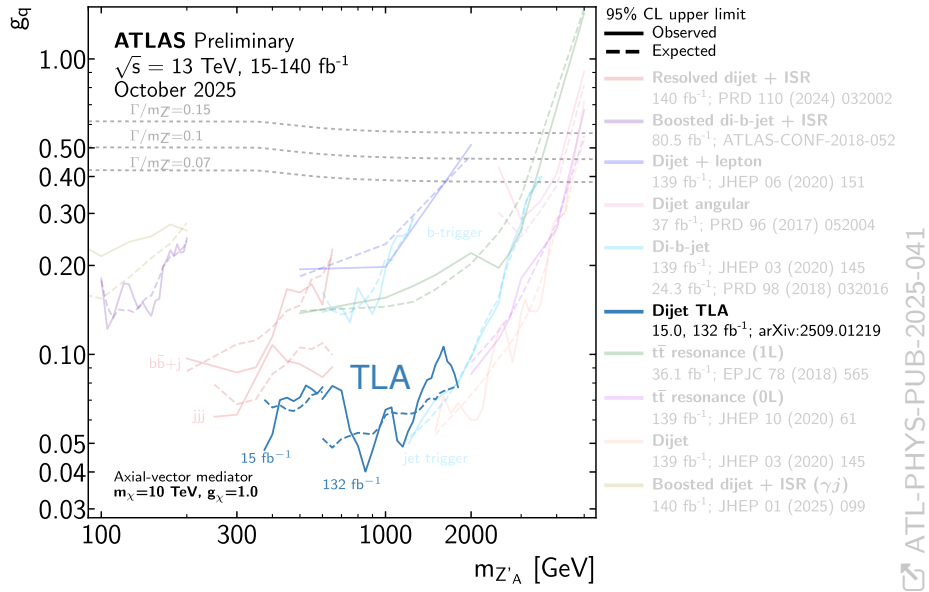

ATL-PHYS-PUB-2025-041

Dijet Resonance Searches

Expt.	Year	$\sqrt{s}$ [TeV]	$\int Ldt$ [pb^{-1}]	m_{jj} range [TeV]	Ref.	technique
UA1	1986	0.63	0.26	0.07 - 0.3	1	
UA1	1988	0.63	0.49	0.11 - 0.3	2	
CDF	1990	1.8	0.026	0.06 - 0.5	3	
UA2	1990	0.63	4.7	0.05 - 0.3	4	
CDF	1993	1.8	4.2	0.14 - 1.0	5	
UA2	1993	0.63	11	0.05 - 0.3	6	
CDF	1995	1.8	19	0.15 - 0.9	7	
CDF	1997	1.8	106	0.18 - 1.0	8	
D0	2004	1.8	109	0.18 - 1.2	9	
CDF	2009	1.96	1130	0.18 - 1.3	10	
ATLAS	2010	7	0.32	0.20 - 1.7	11	
CMS	2010	7	2.9	0.22 - 2.1	12	
ATLAS	2011	7	36	0.50 - 2.8	13	
CMS	2011	7	1000	0.84 - 3.7	14	
ATLAS	2011	7	1000	0.72 - 4.1	15	
ATLAS	2012	7	1000	0.8 - 4.0	16	
ATLAS	2012	7	4800	1.0 - 8.0	17	
CMS	2013	7	5000	1.0 - 4.0	18	b-tagged
CMS	2013	8	4000	1.0 - 4.8	18	
CMS	2015	8	19700	1.2 - 6.5	19	
ATLAS	2015	8	20300	0.8 - 4.5	20	
CMS	2016	8	18800	0.5 - 0.8	21	scouting
CMS	2016	13	2400	1.5 - 0.7	22	
ATLAS	2016	13	3200	1.1 - 5.0	23	b-tagged
ATLAS	2016	13	3600	1.5 - 6.5	24	
CMS	2017	13	12900	0.6 - 1.5	25	scouting
CMS	2017	13	12900	1.5 - 7.5	25	
ATLAS	2017	13	37000	1.5 - 3.5	26	
ATLAS	2018	13	29300	0.45 - 1.8	27	TLA
ATLAS	2018	13	36100	0.57 - 7.0	28	b-tagged
CMS	2018	13	36000	1.6 - 8.1	29	
CMS	2018	13	27000	0.6 - 1.6	30	scouting
CMS	2018	13	19700	0.325 - 1.2	31	b-tagged
ATLAS	2019	13	36100	0.1 - .22	32	boosted + ISR (γ, j)
ATLAS	2020	13	139000	1.5 - 5.0	33	
CMS	2020	13	77800	1.8 - 8.0	34	
CMS	2020	13	18300	0.35 - 0.7	35	ISR j
CMS	2023	13	138000	1.8 - 2.4	36	b-tagged
ATLAS	2025	13	140000	0.2 - 0.65	37	ISR (γ, j)
ATLAS†	2025	13	132000	0.375 - 1.8	38	TLA
CMS*	2025	13	117100	0.6 - 1.8	39	scouting

*:preliminary, †: this publication

Multiple techniques (and combinations) are needed to span the full mass range

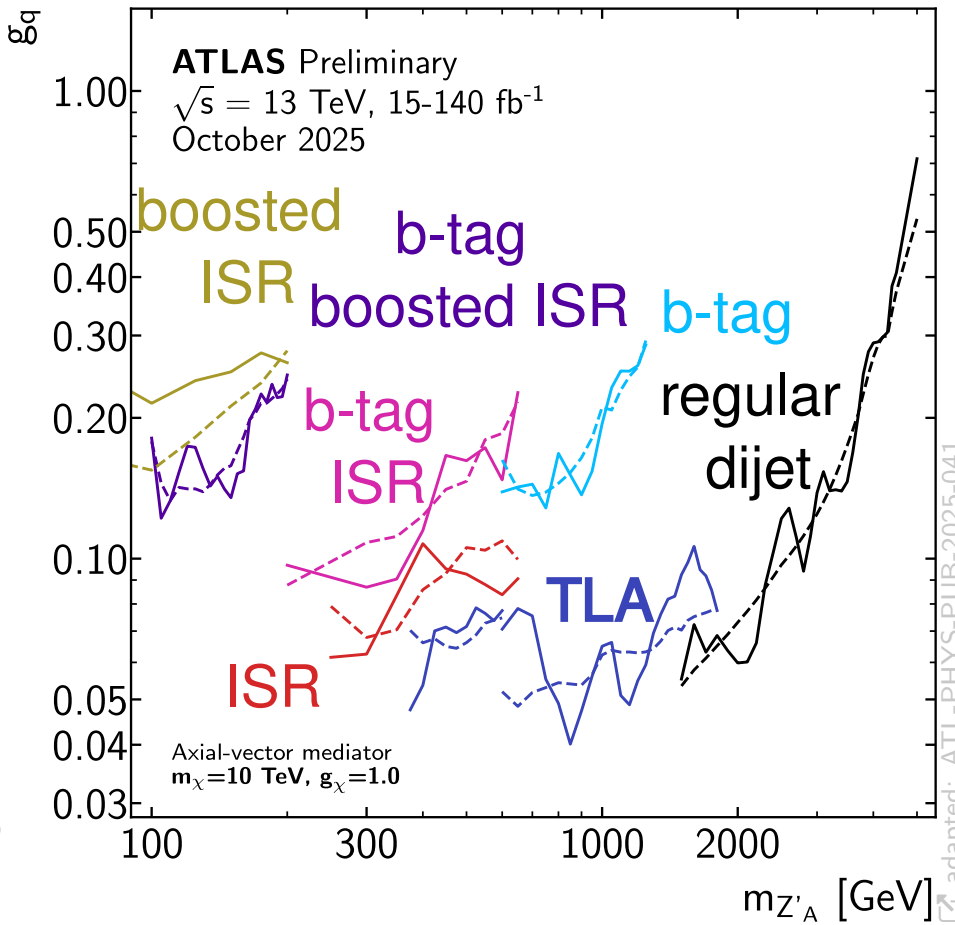

Dijet Resonance Searches

Expt.	Year	$\sqrt{s}$ [TeV]	$\int Ldt$ [pb^{-1}]	m_{jj} range [TeV]	Ref.	technique
UA1	1986	0.63	0.26	0.07 - 0.3	1	
UA1	1988	0.63	0.49	0.11 - 0.3	2	
CDF	1990	1.8	0.026	0.06 - 0.5	3	
UA2	1990	0.63	4.7	0.05 - 0.3	4	
CDF	1993	1.8	4.2	0.14 - 1.0	5	
UA2	1993	0.63	11	0.05 - 0.3	6	
CDF	1995	1.8	19	0.15 - 0.9	7	
CDF	1997	1.8	106	0.18 - 1.0	8	
D0	2004	1.8	109	0.18 - 1.2	9	
CDF	2009	1.96	1130	0.18 - 1.3	10	
ATLAS	2010	7	0.32	0.20 - 1.7	11	
CMS	2010	7	2.9	0.22 - 2.1	12	
ATLAS	2011	7	36	0.50 - 2.8	13	
CMS	2011	7	1000	0.84 - 3.7	14	
ATLAS	2011	7	1000	0.72 - 4.1	15	
ATLAS	2012	7	1000	0.8 - 4.0	16	
ATLAS	2012	7	4800	1.0 - 8.0	17	
CMS	2013	7	5000	1.0 - 4.0	18	b-tagged
CMS	2013	8	4000	1.0 - 4.8	18	
CMS	2015	8	19700	1.2 - 6.5	19	
ATLAS	2015	8	20300	0.8 - 4.5	20	
CMS	2016	8	18800	0.5 - 0.8	21	scouting
CMS	2016	13	2400	1.5 - 0.7	22	
ATLAS	2016	13	3200	1.1 - 5.0	23	b-tagged
ATLAS	2016	13	3600	1.5 - 6.5	24	
CMS	2017	13	12900	0.6 - 1.5	25	scouting
CMS	2017	13	12900	1.5 - 7.5	25	
ATLAS	2017	13	37000	1.5 - 3.5	26	
ATLAS	2018	13	29300	0.45 - 1.8	27	TLA
ATLAS	2018	13	36100	0.57 - 7.0	28	b-tagged
CMS	2018	13	36000	1.6 - 8.1	29	
CMS	2018	13	27000	0.6 - 1.6	30	scouting
CMS	2018	13	19700	0.325 - 1.2	31	b-tagged
ATLAS	2019	13	36100	0.1 - .22	32	boosted + ISR (γ, j)
ATLAS	2020	13	139000	1.5 - 5.0	33	
CMS	2020	13	77800	1.8 - 8.0	34	
CMS	2020	13	18300	0.35 - 0.7	35	ISR j
CMS	2023	13	138000	1.8 - 2.4	36	b-tagged
ATLAS	2025	13	140000	0.2 - 0.65	37	ISR (γ, j)
ATLAS†	2025	13	132000	0.375 - 1.8	38	TLA
CMS*	2025	13	117100	0.6 - 1.8	39	scouting

*:preliminary, †: this publication

Multiple techniques (and combinations) are needed to span the full mass range

Run 3 ATLAS TLA

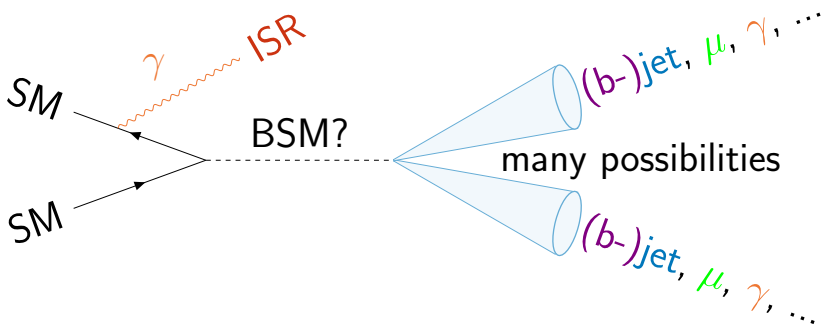

Summary

- **TLA is a great tool to increase physics reach**
- **With very limited cost on bandwidth**
- **Great potential in Run 3 and beyond**
- **Unconventional analyses expose you to many aspects of the experiment**

Appendix

Limits Before Run 2

Before the start of Run 2 (2015)

(simplified model: Z' coupling to baryon number)

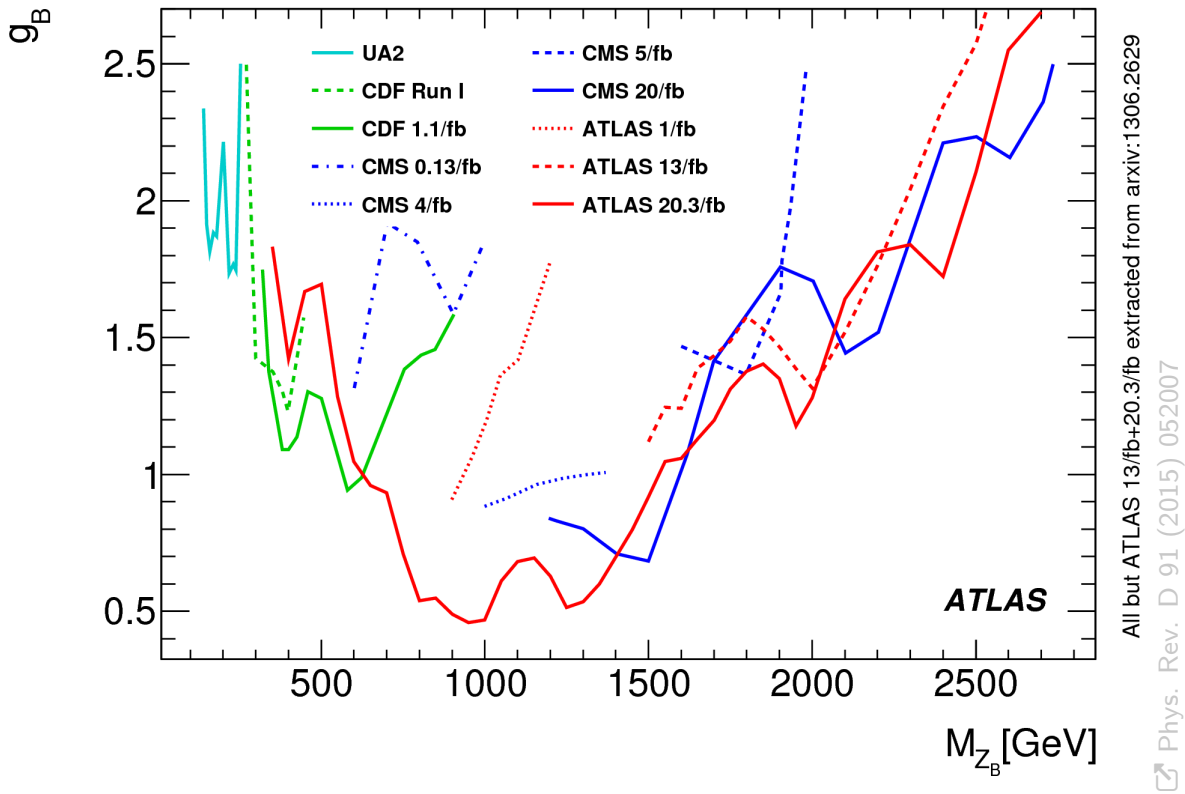

SpS̄pS (UA2) and Tevatron (CDF) probed up to 1 TeV

LHC (ATLAS, CMS) pushed towards high mass, but were not able to compete at low mass

TLA

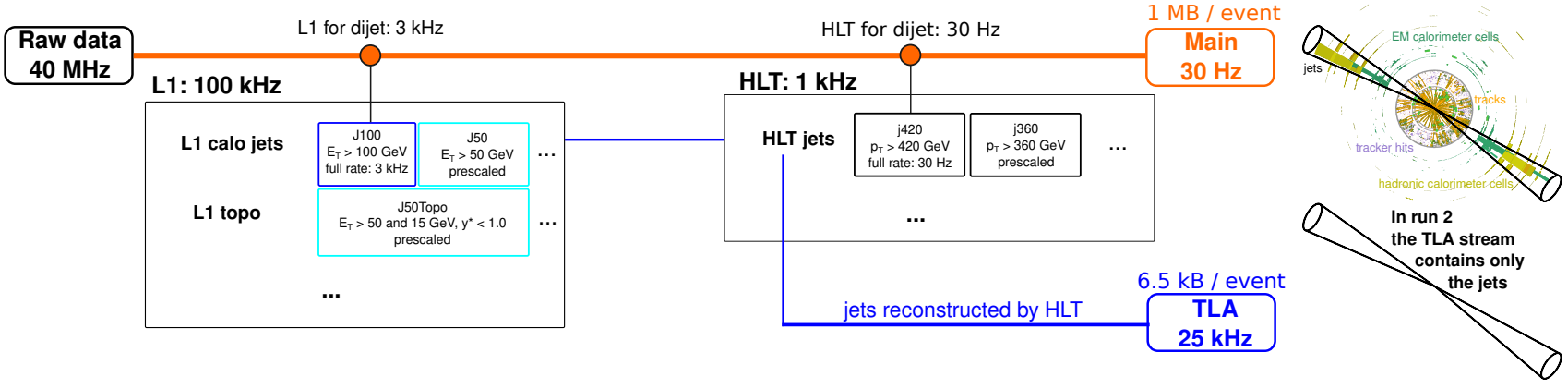
Raw data
40 MHz
L1 for dijet: 3 kHz
L1: 100 kHz
L1 calo jets
J100
E_T > 100 GeV
full rate: 3 kHz
J50
E_T > 50 GeV
prescaled
...
L1 topo
J50Topo
E_T > 50 and 15 GeV, y* < 1.0
prescaled
...
...
HLT for dijet: 30 Hz
HLT: 1 kHz
HLT jets
j420
p_T > 420 GeV
full rate: 30 Hz
j360
p_T > 360 GeV
prescaled
...
...
1 MB / event
Main
30 Hz
6.5 kB / event
jets reconstructed by HLT
TLA
25 kHz
EM calorimeter cells
jets
tracks
tracker hits
hadronic calorimeter cells
In run 2
the TLA stream
contains only
the jets

Limit Comparison

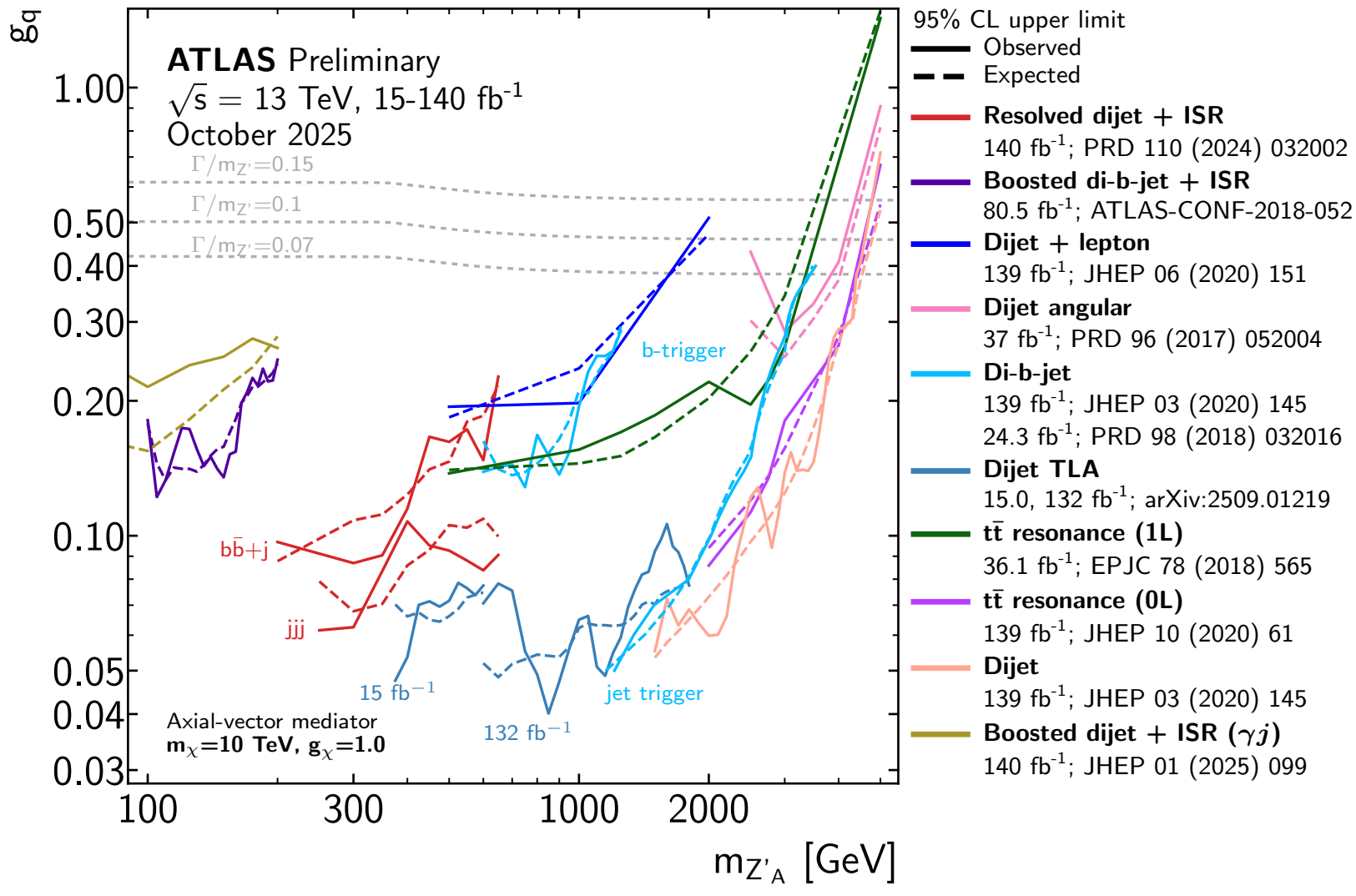

Limit Comparison

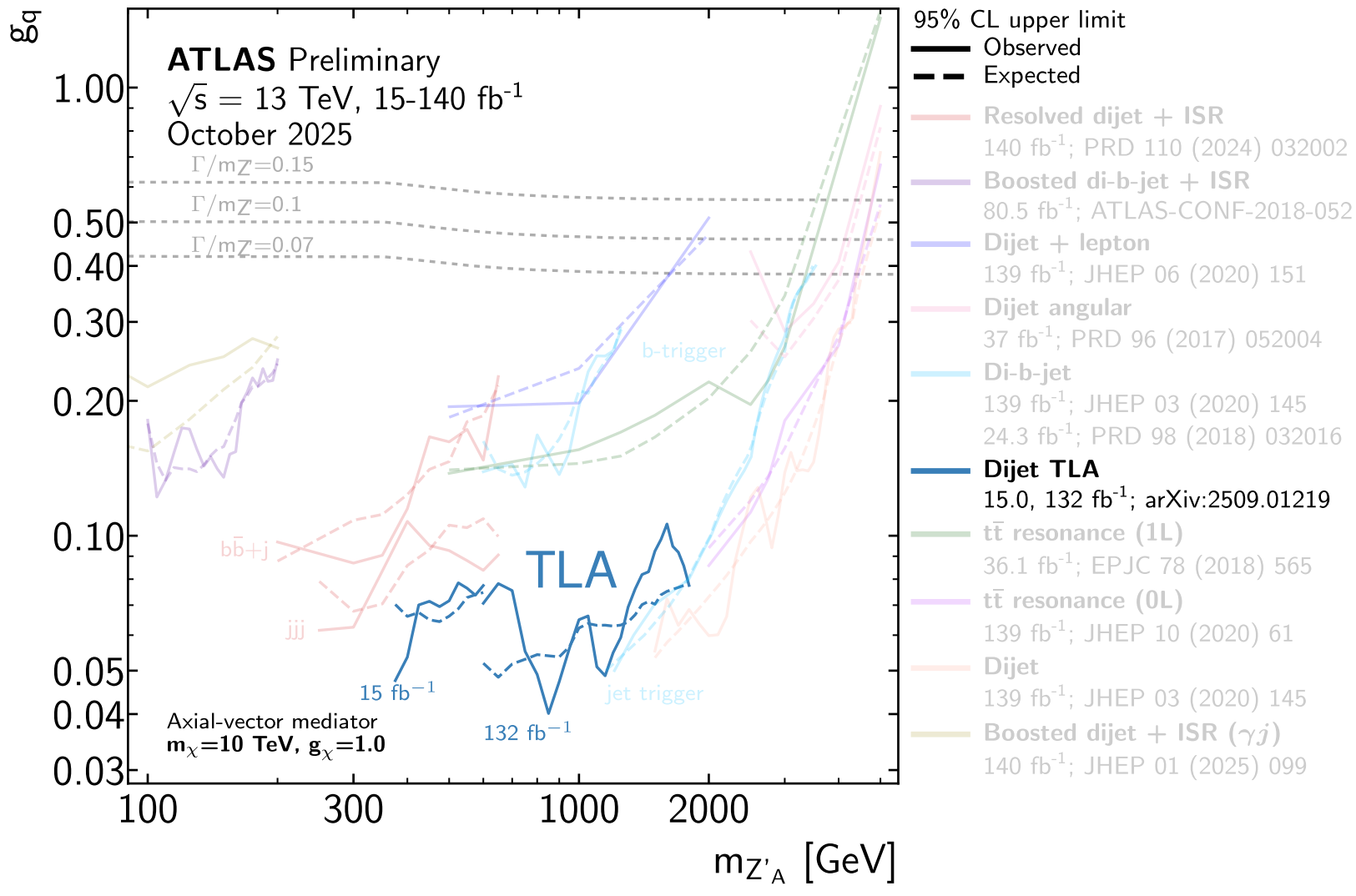

ATL-PHYS-PUB-2025-041

Limit Comparison

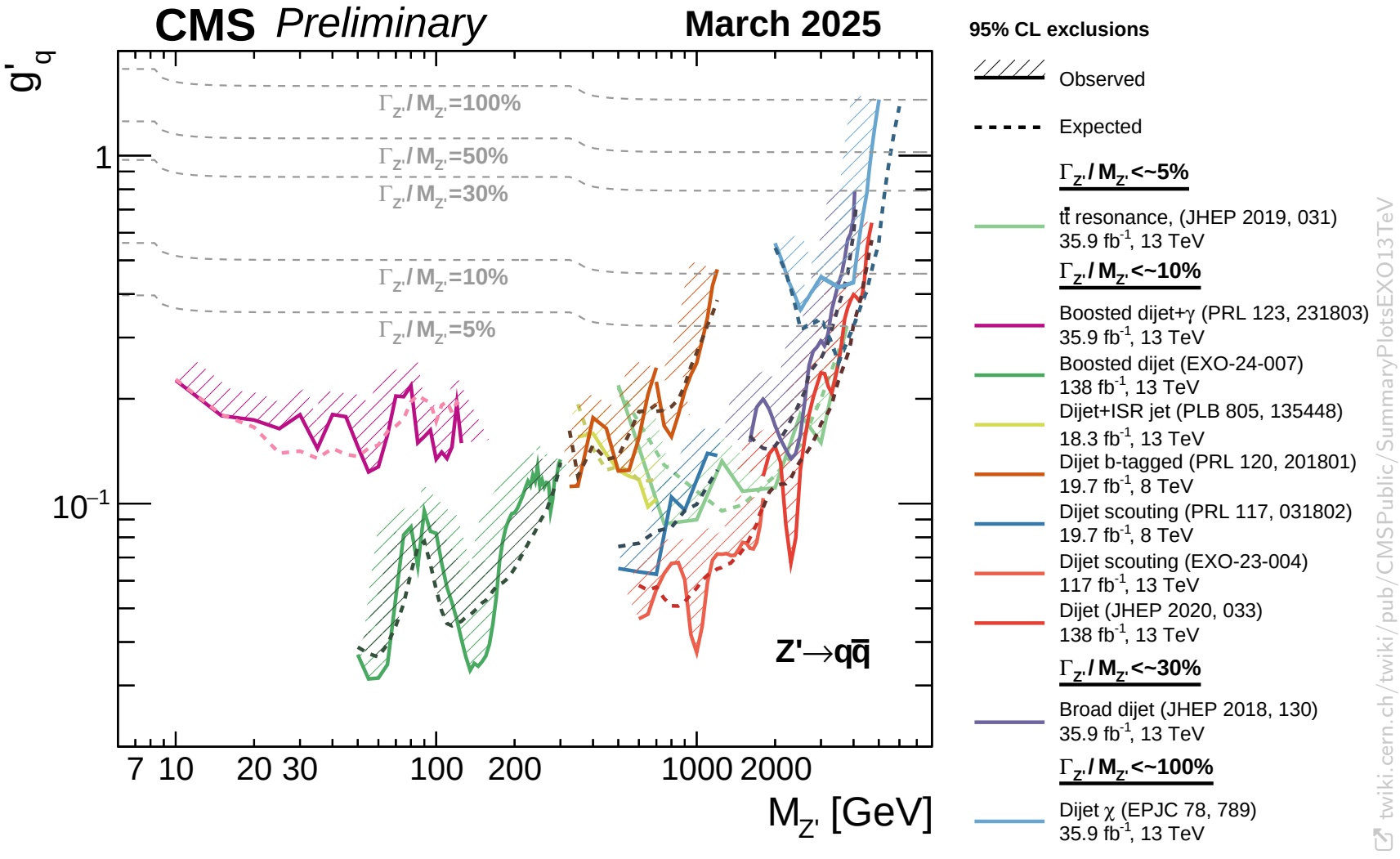

Event Display

Event with 356 GeV dijet mass (Physics Main), recorded on 22 May 2018

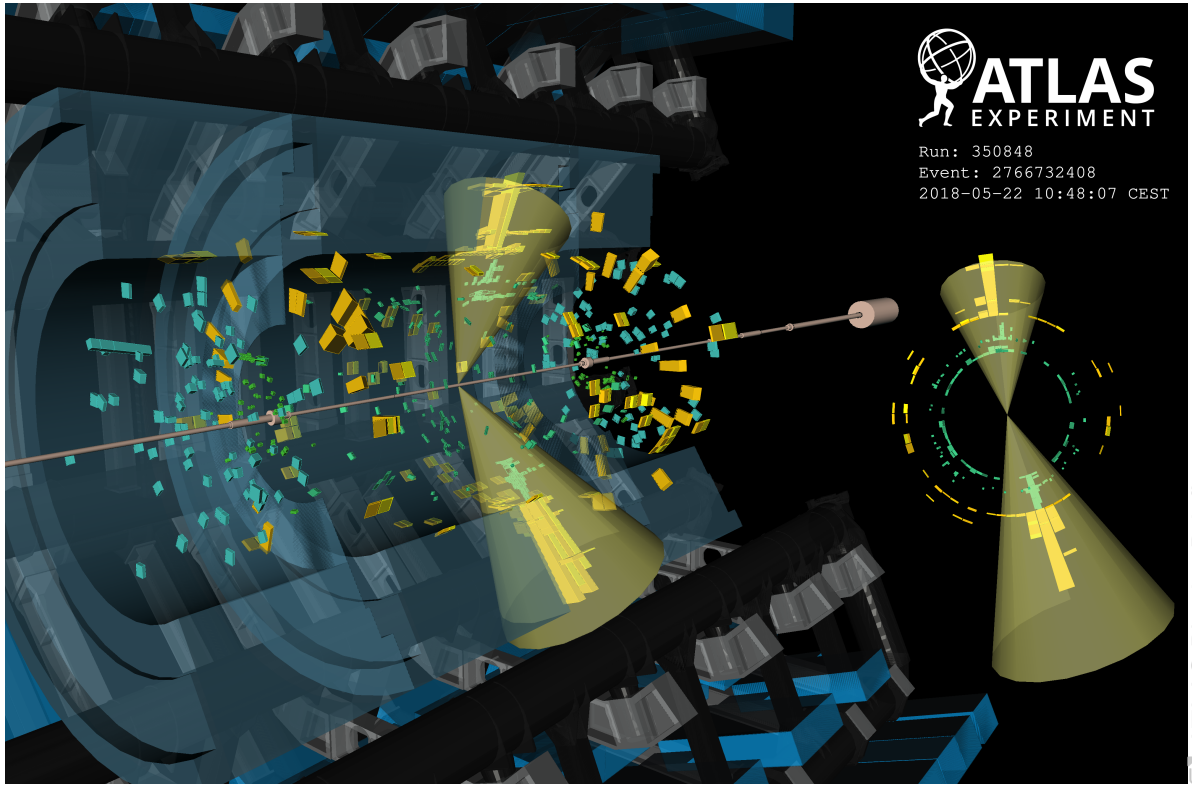

- Physics Main event contains many objects:

  Energy deposits in the calorimeter, tracks, ...
- The correponding TLA event only has the jets (yellow cones)
- It is rare to retain such a low mass dijet event in Physics Main
- In the TLA Dataset these events are abundant

Z' Signal Model

Z' signal distributions for various $m_{Z'}$ described by double sided Crystal Ball functions

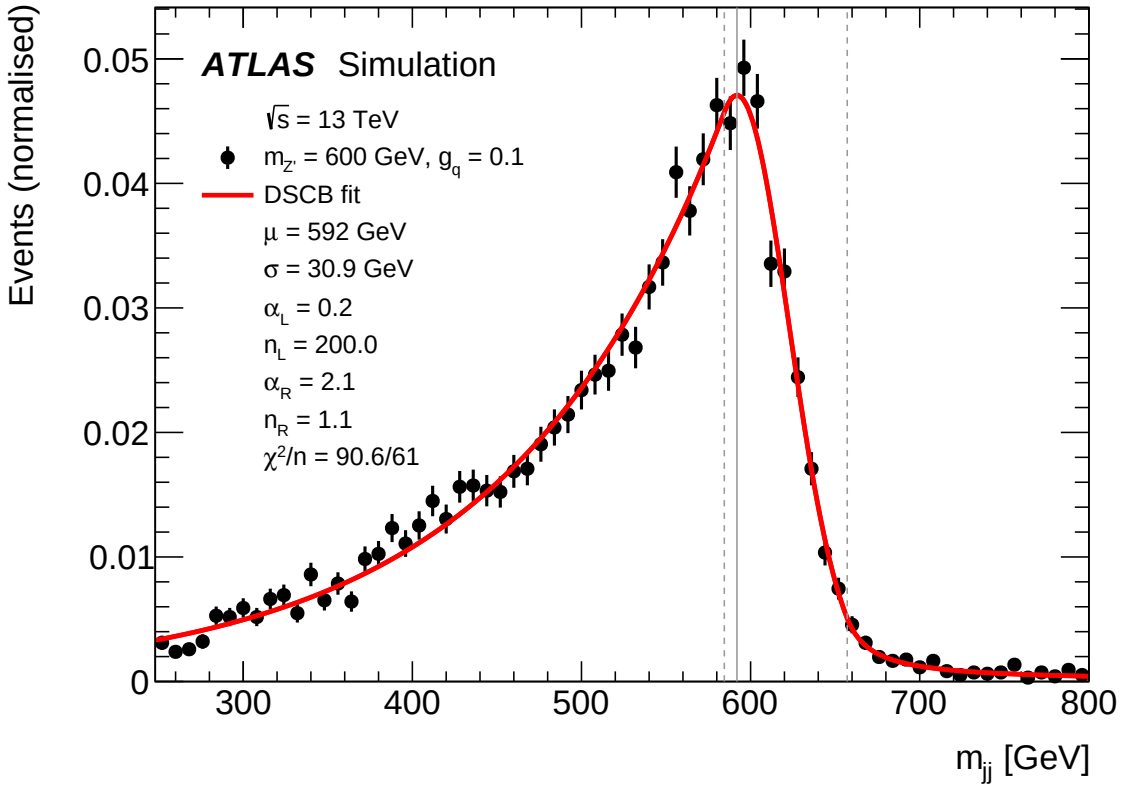

Phys. Rev. D 112, 092015

Direct decay to DM

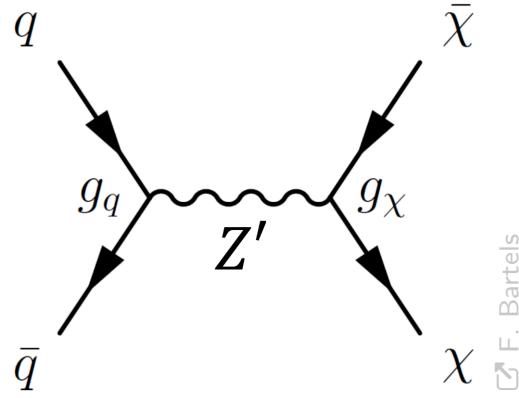

F. Bartels

Dijet production

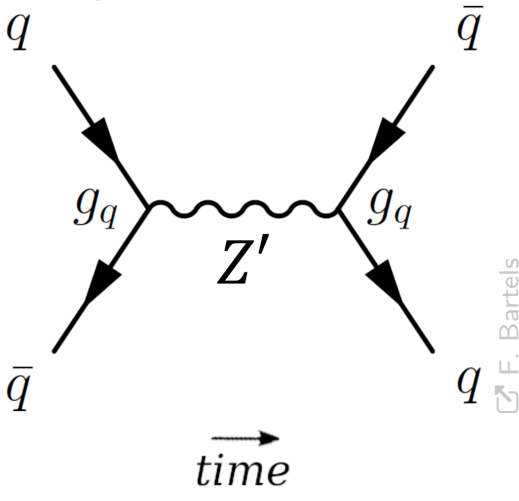

F. Bartels

Additionally performed all fits with generic gaussian signal models of various masses and width

Various trigger chains for different physics categories

Jet triggers are only a small fraction of the 1 kHz HLT rate

2015 L1 rate

Category	Rate [kHz]
Single MU	10.2
Multi MU	19.8
Single EM	13.8
Multi EM	15.3
Single JET	5.6
Multi JET	3.9
$E_{\mathrm{T}}^{\mathrm{miss}}$	0.5
TAU	12.0
Combined (inclusive)	6.5

TRIG-2016-01

2015 HLT rate

Category	Rate [Hz]
Single Muon	132
Single Electron	194
Multi Lepton	79
Single Jet	76
Multi Jet	62
b-jet	146
$E_{\mathrm{T}}^{\mathrm{miss}}$	210
Tau	72
Photon	68
B-physics	144
Combined (inclusive)	107
Combined Lepton	*21*
Combined $E_{\mathrm{T}}^{\mathrm{miss}}$	*31*
Combined Jet	*93*
Main Physics Stream	1163

TRIG-2016-01

Trigger monitoring for one run in 2018:

bandwidth

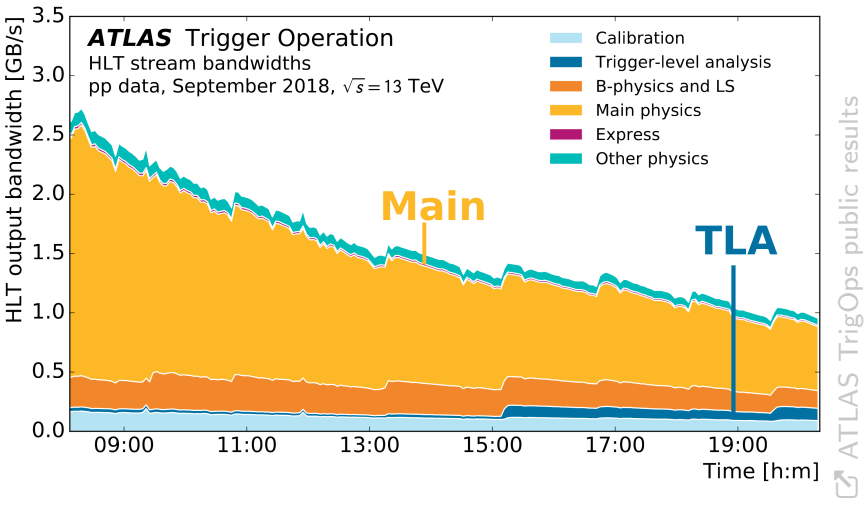

rate

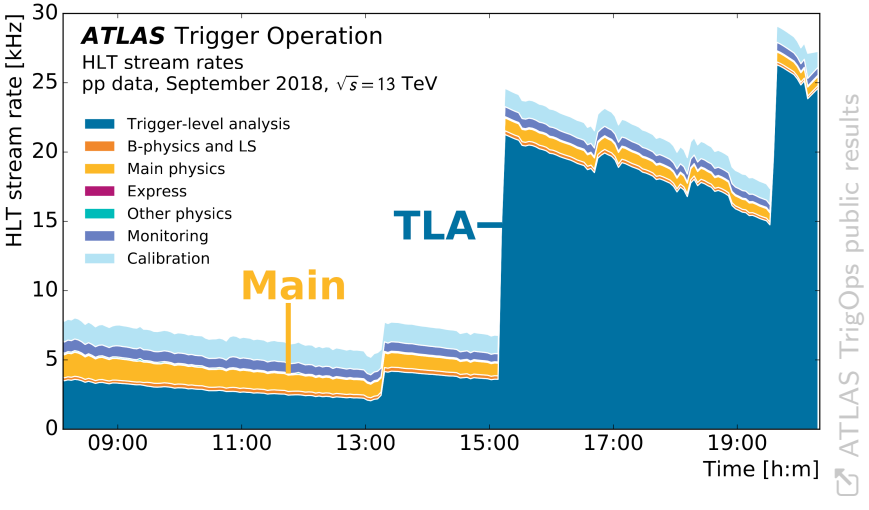

- Main: 1kHz event rate
- TLA: Up to 25 kHz

Jet Calibration: Summary

Differences in Offline and Trigger-Level jet calibration

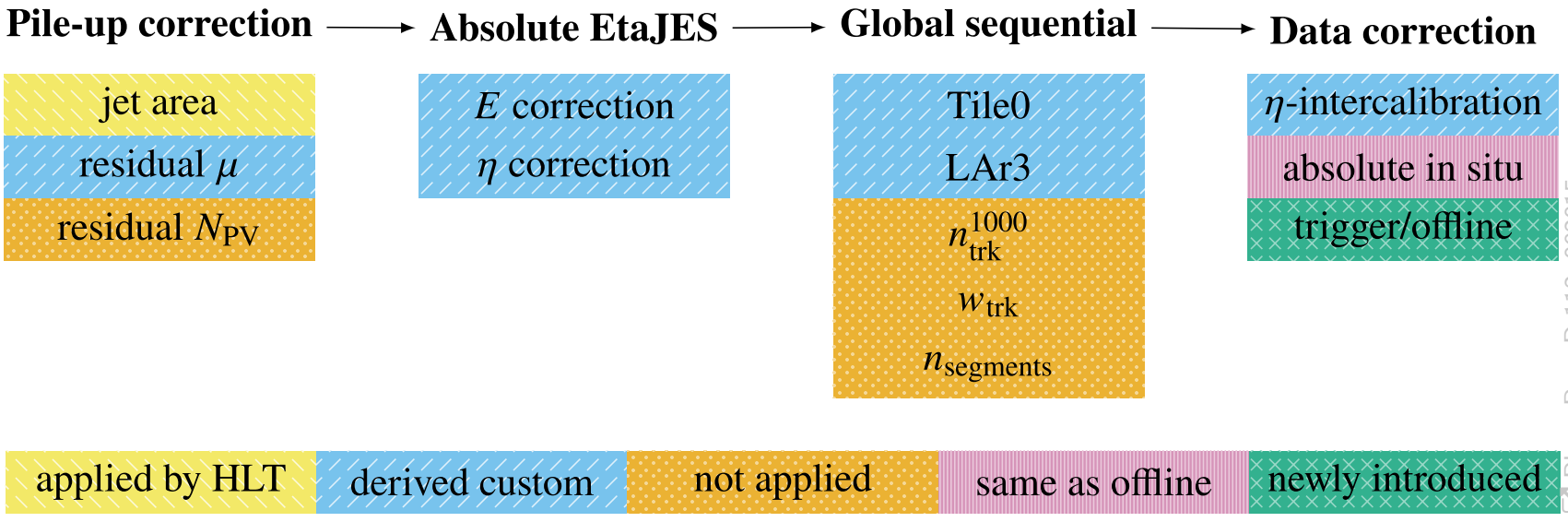

Phys. Rev. D 112, 092015

Jet Calibration

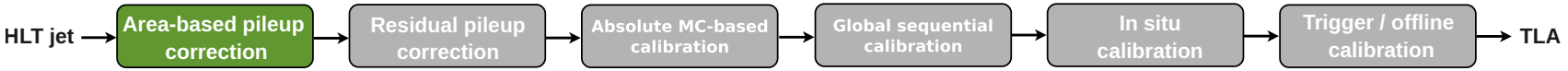

Area-based pileup correction

- Removes bulk of the pileup
- Pileup density ρ: Per-event measure for amount of pileup
- Jet area A: Estimator for jet's catchement area
- Combination gives estimate for how much of a jet's p_T is from pileup

$$p_\mathrm{T}^\mathrm{area} = p_\mathrm{T}^\mathrm{init} - \rho A$$

- Already applied within the HLT itself

ρ distributions for various number of vertices N_PV

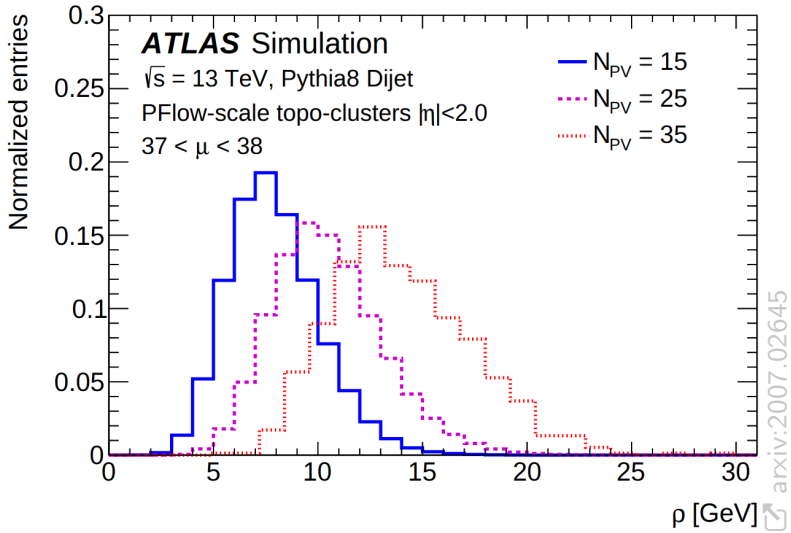

Jet area of anti-kT jets

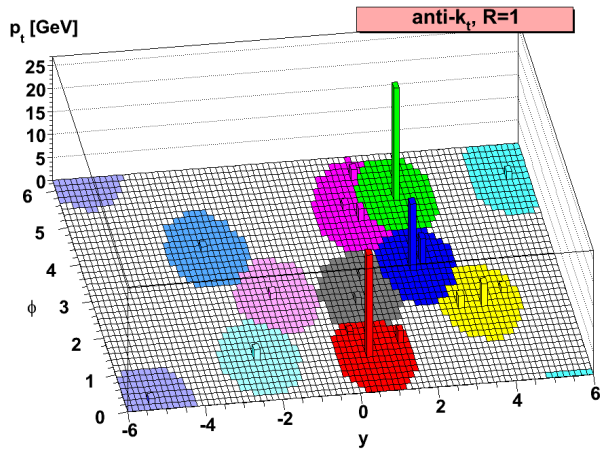

Statistical Tests

F-Test → Spurious Signal Test → Signal Injection Test → Coverage Test

Spurious signal test

- Add signal with Gaussian-constrained amplitude to the signal+background fits
- Spurious signal = difference between fitted and expectd signal yield
- Determined for each mass point and used as uncertainty
- On order of half the stats uncertainty for most singals considered

J50

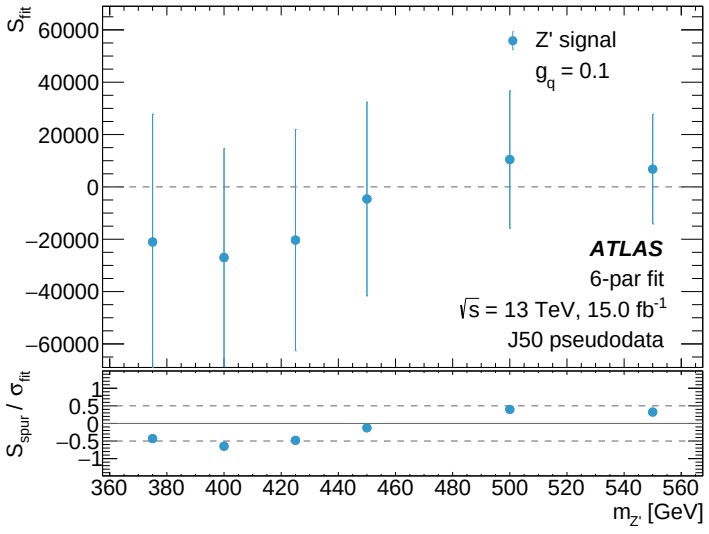

Phys. Rev. D 112, 092015

J100

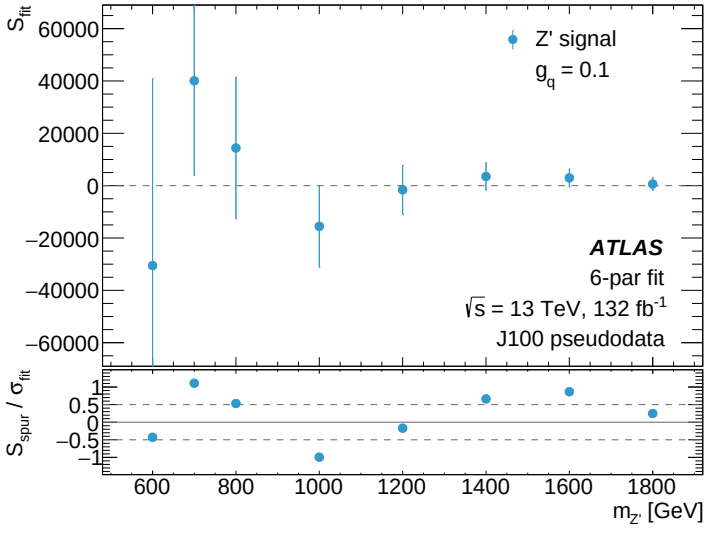

Phys. Rev. D 112, 092015

Statistical Tests

F-Test → Spurious Signal Test → **Signal Injection Test** → Coverage Test

Signal injection test

- Similar to spurious signal test
- Difference: Inject $\sqrt{B}$ events
- B: Integral of background-only fit within full-width-half-maximum of signal mass
- 100 toy experiments per signal hypothesis
- Goal: linear trend in $S_{\text{fit}}/\sqrt{B}$ vs $S_{\text{inj}}/\sqrt{B}$

J50

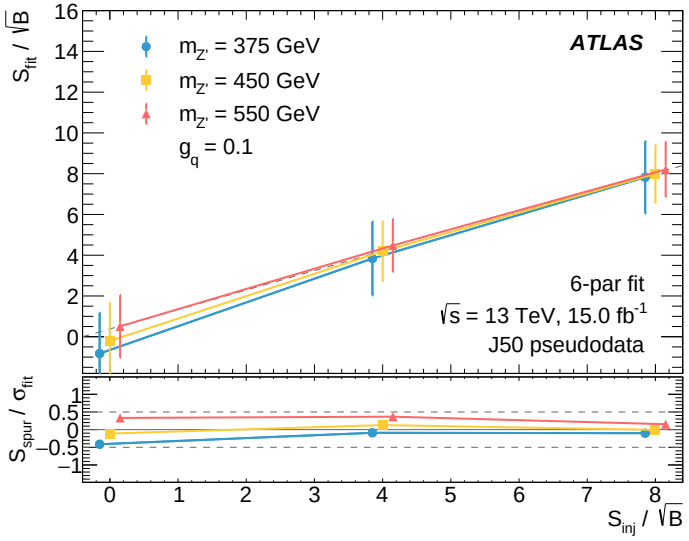

Phys. Rev. D 112, 092015

J100

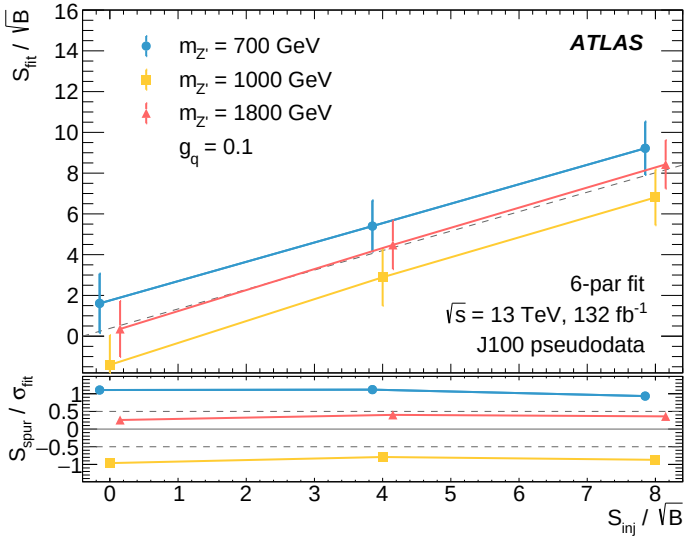

Phys. Rev. D 112, 092015

Statistical Tests

F-Test → Spurious Signal Test → Signal Injection Test → Coverage Test

Coverage test

- Final results are 95 % C_{LS} upper limits
- In at most 5% of toy datasets a limit stronger than the number of injected signal events should be derived
  - Else: undercoverage
- Even with largest spurious signals proper coverage was found
- Systematic uncertainty properly covers fit bias

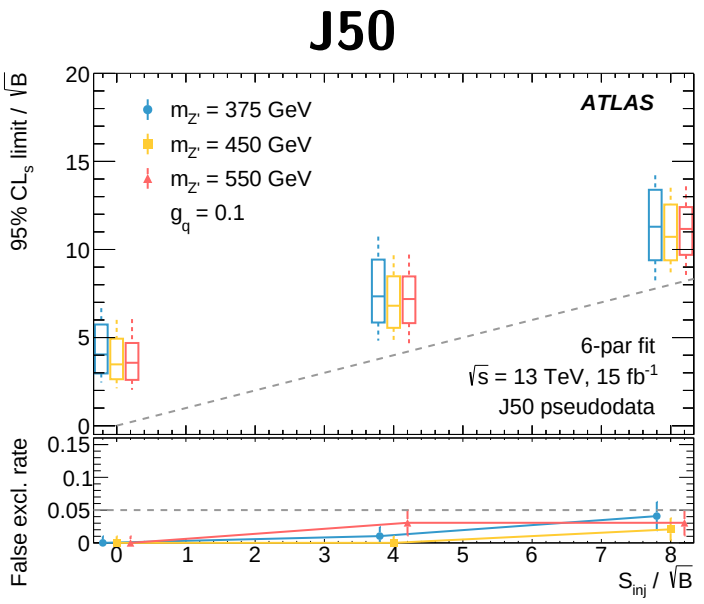

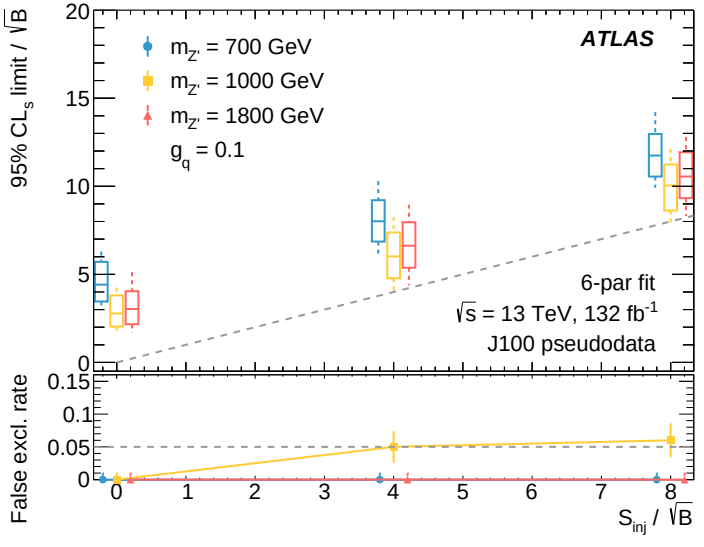

Trigger Efficiencies

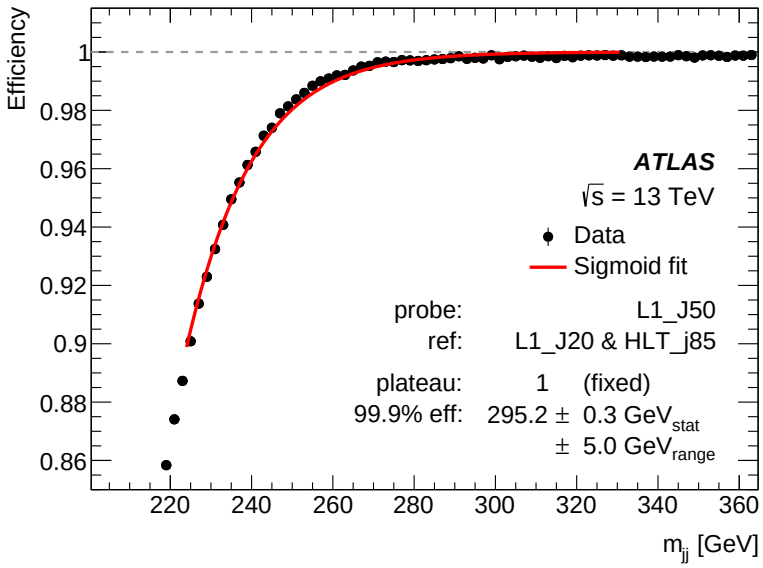

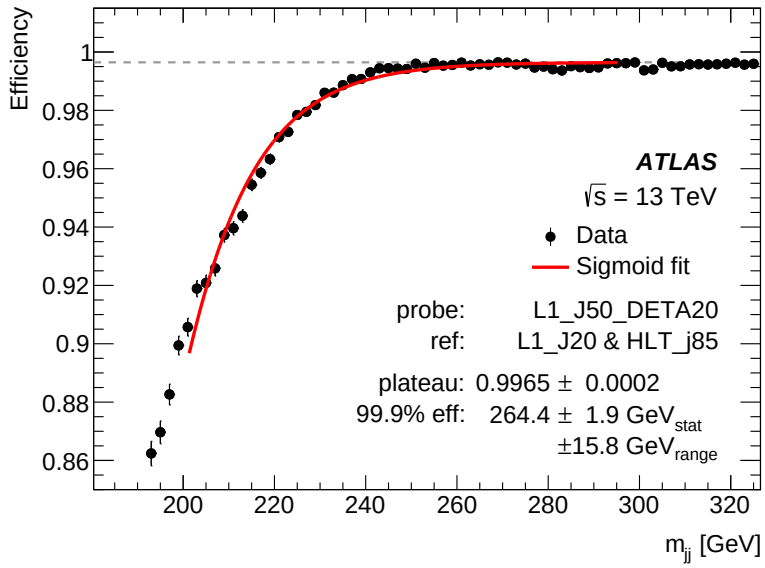

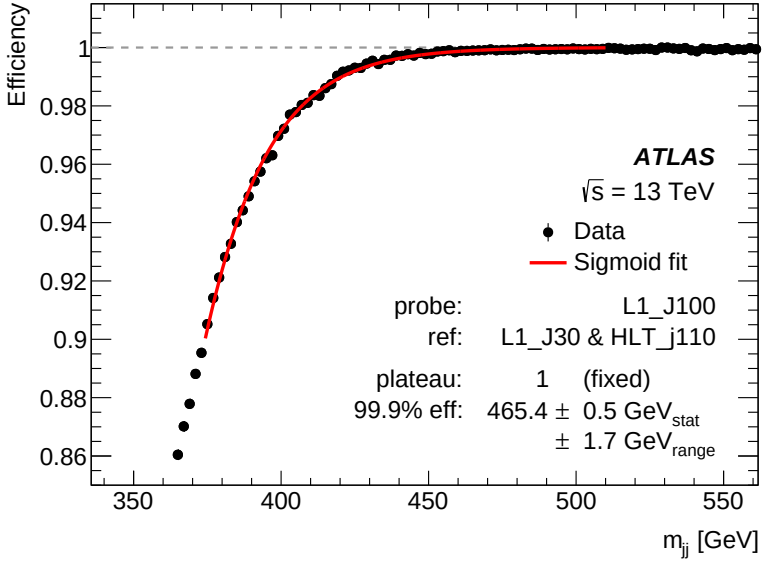

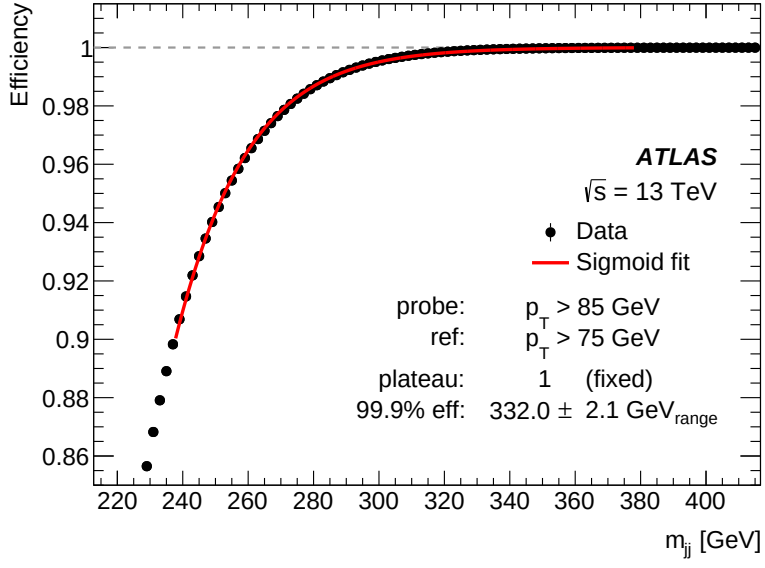

Phys. Rev. D 112, 092015

Z' Signal Shapes

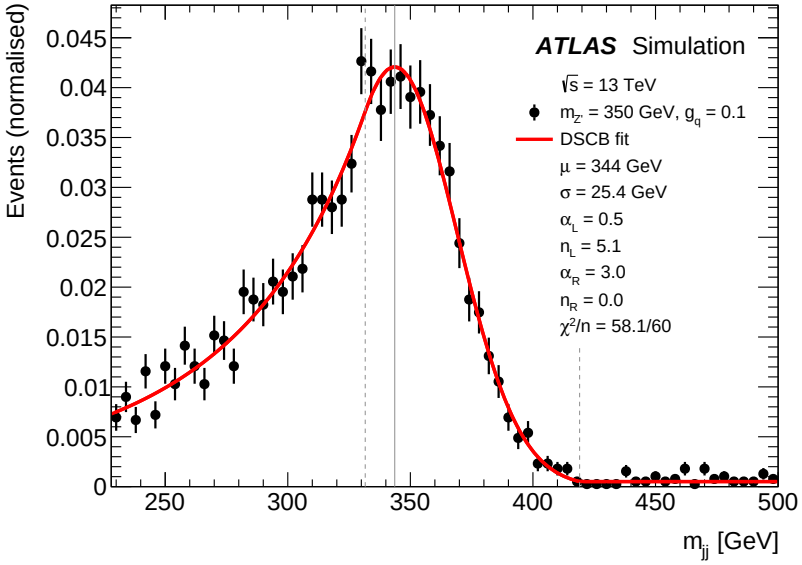

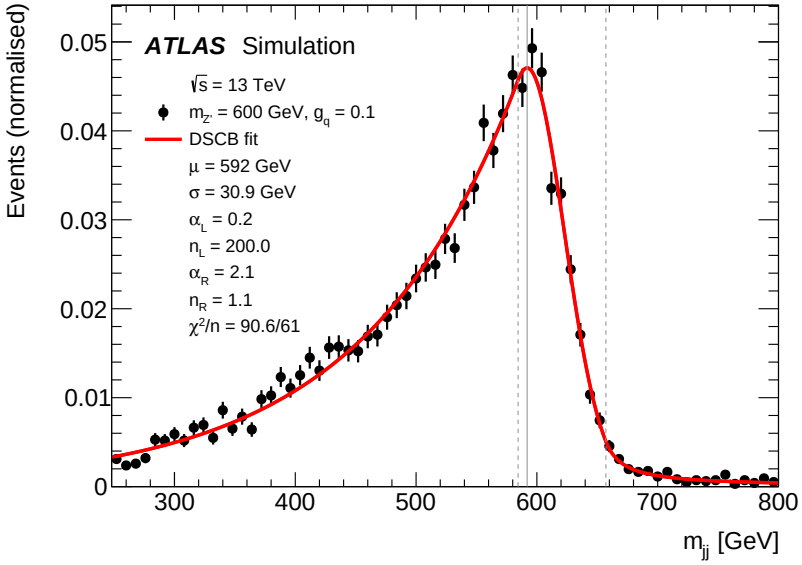

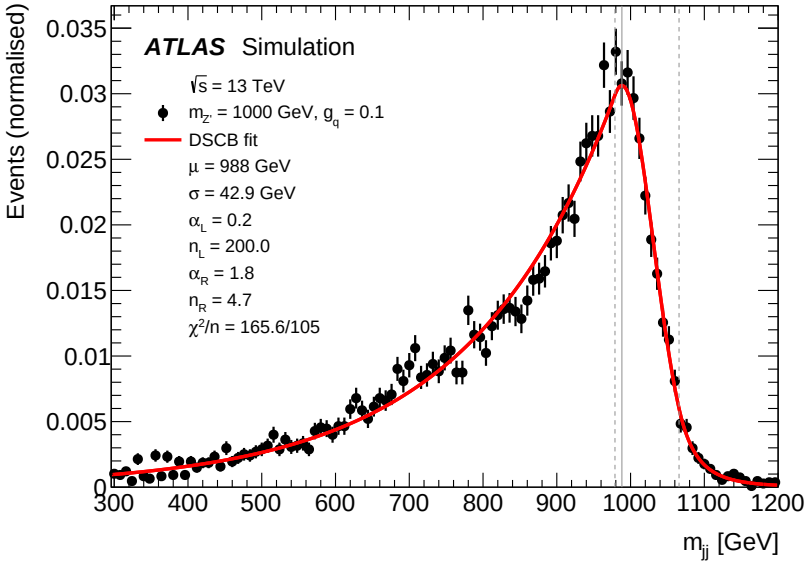

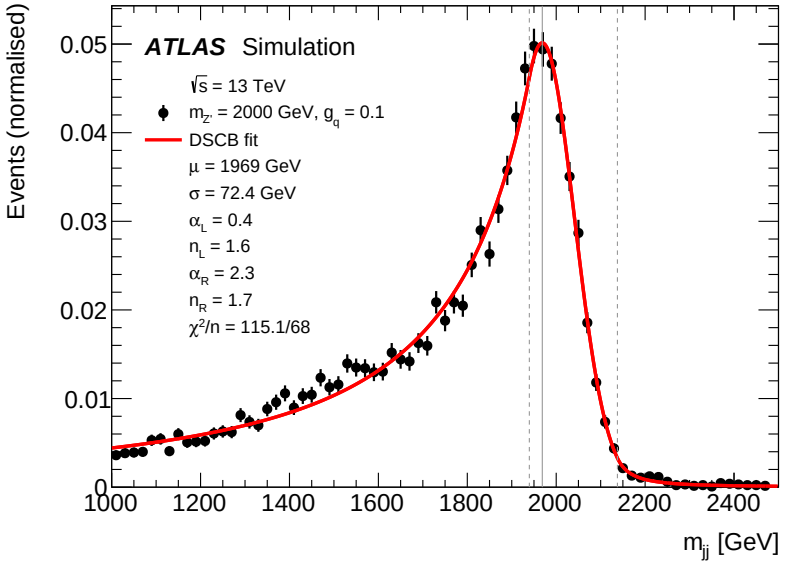

Signal Acceptance

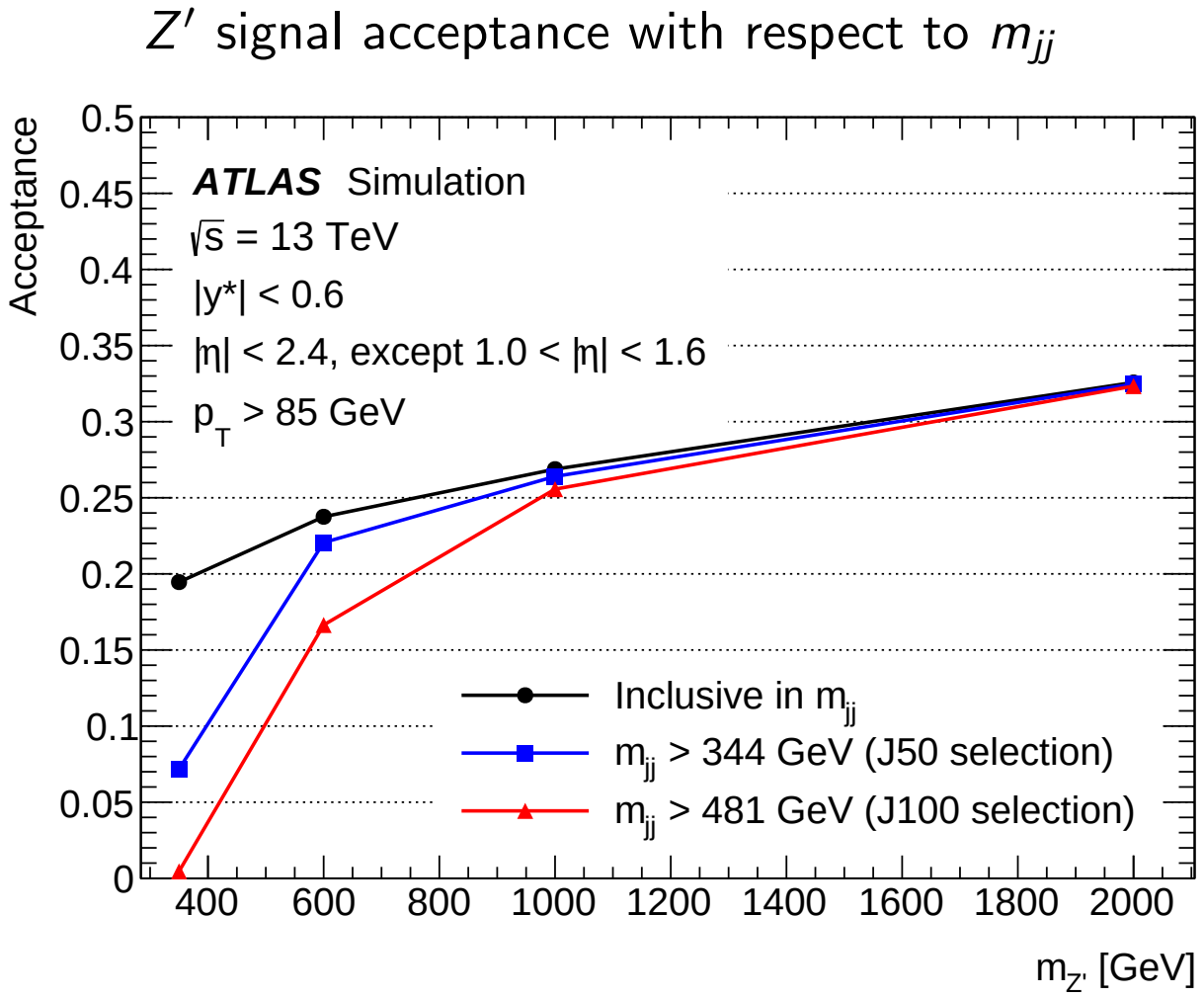

Phys. Rev. D 112, 092015

Flavour Uncertainties

The flavour uncertainties were re-derived as in Ref. [50],

$$\sigma^{\text{flavour}}_{\text{response}} = f_g \sigma_{R_g}, \tag{6}$$

$$\sigma^{\text{flavour}}_{\text{composition}} = \frac{\sigma_{f_g} |R_q - R_g|}{f_g R_g + (1 - f_g) R_q}, \tag{7}$$

where R_q dn R_g are the fraction of light quarks and gluons which were measured in PYTHIA 8 dijet simulated events. The gluon response modelling uncertainty σ_{R_g} was obtained as the maximum difference of the gluon response using PYTHIA 8, HERWIG [63, 64], or SHERPA [65, 66] simulated events. The gluon fraction f_g was set to a constant value of 50% with a conservative estimate on its uncertainty of $\sigma_{f_g} = 100\% f_g$. All other components were derived in bins of jet p_{T} and η. The flavour uncertainties are the dominant jet uncertainties and mainly arise due to the lack of tracking information which, for the offline jet calibration, is key to aligning the response of quark- and gluon-initiated jets [50].

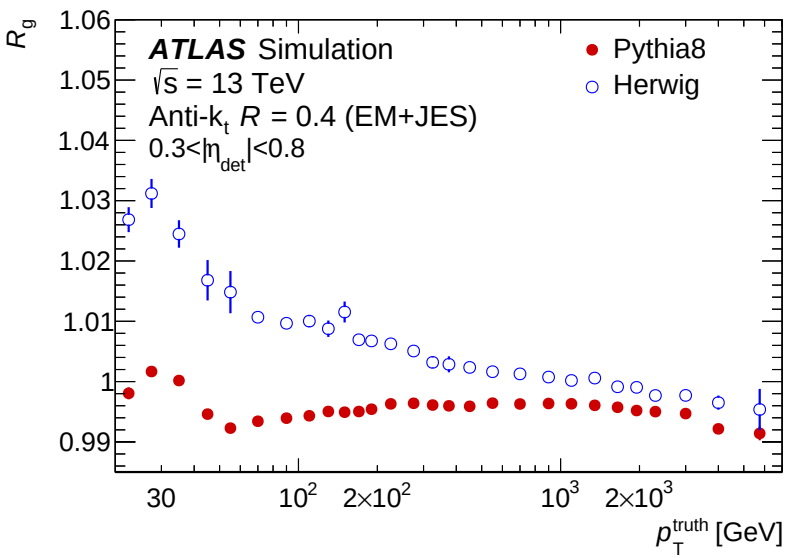

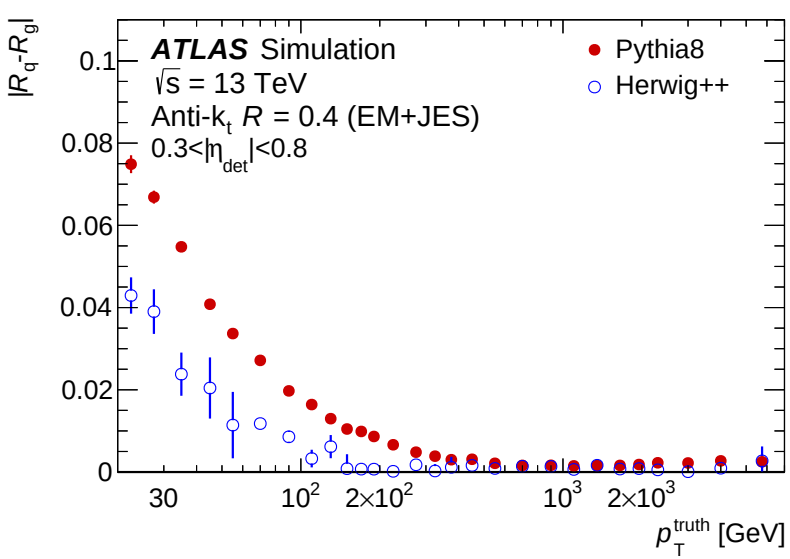

Systematics

- All offline jet systematics applied to trigger jets
- Plus uncertainty from spurious signal test
- Re-derived flavour systematics have highest impact on signal mean μ ($8 - 20$ GeV)
- Pulls on signal widht σ negligible (< 1 GeV)

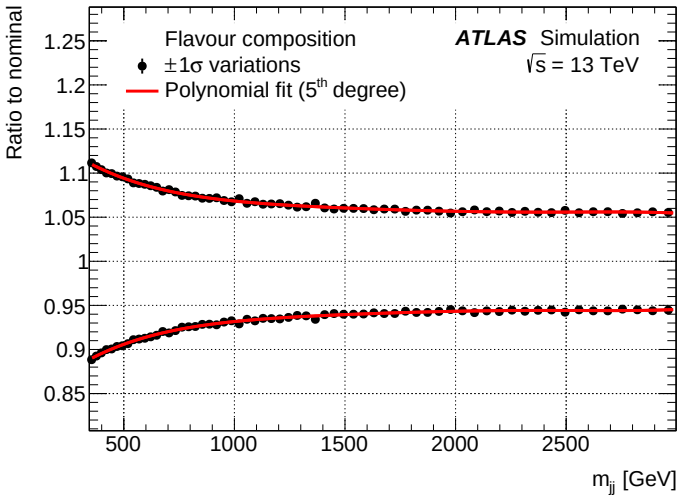

Phys. Rev. D 112, 092015

Impact on signal mean μ

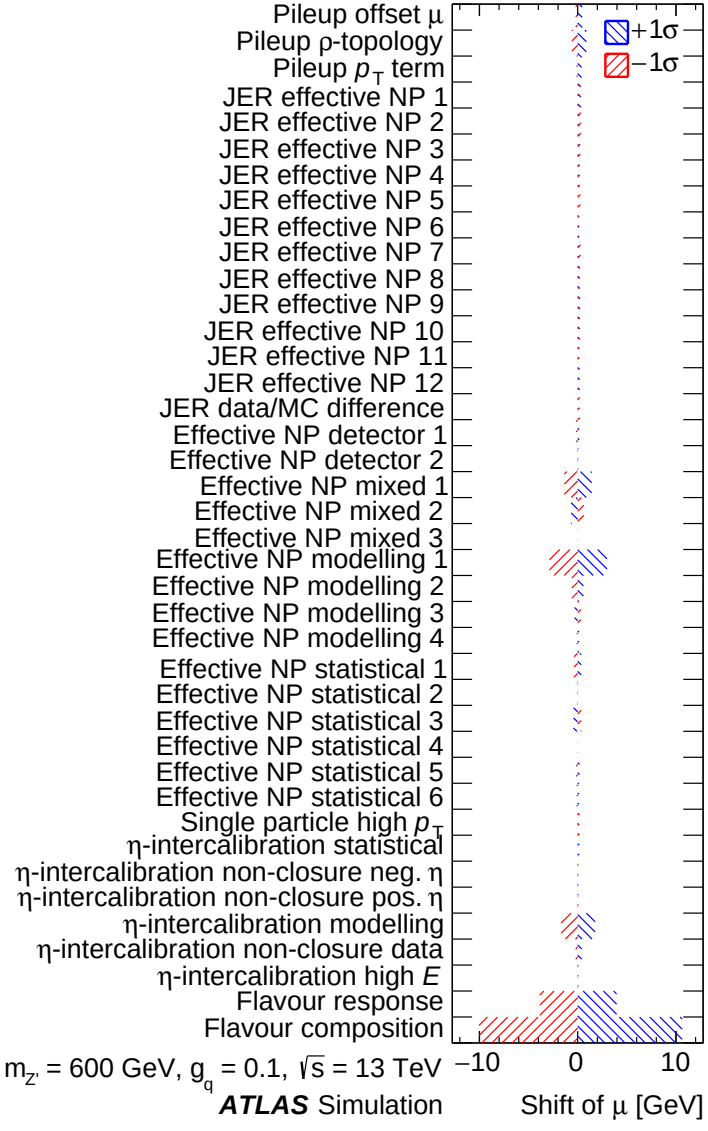

Phys. Rev. D 112, 092015

Turnons

- Turnon: Efficiency of trigger when compared to other trigger with lower threshold
- Used here to determine starting points of m_{jj}
- To avoid kinematic sculpting of m_{jj} spectrum by inefficiencies

J50

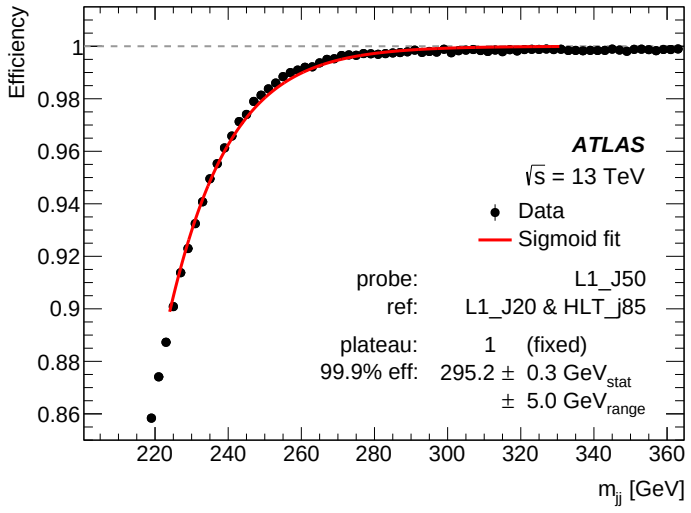

Phys. Rev. D 112, 092015

J100

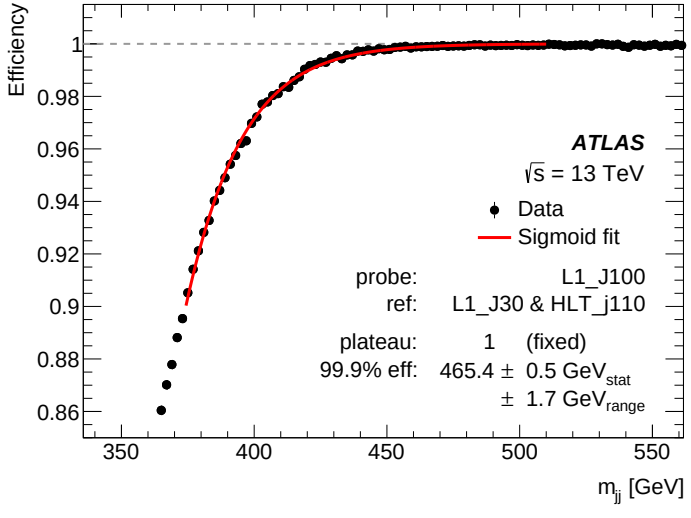

Phys. Rev. D 112, 092015

J50Topo

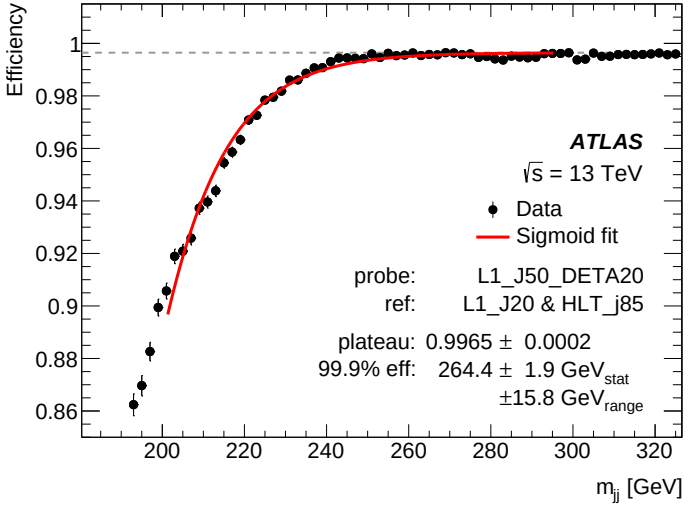

Phys. Rev. D 112, 092015

Tile Gap Veto

Tile gap veto: exclude event if any of $1.0 < |\eta^{0,1}| < 1.6$

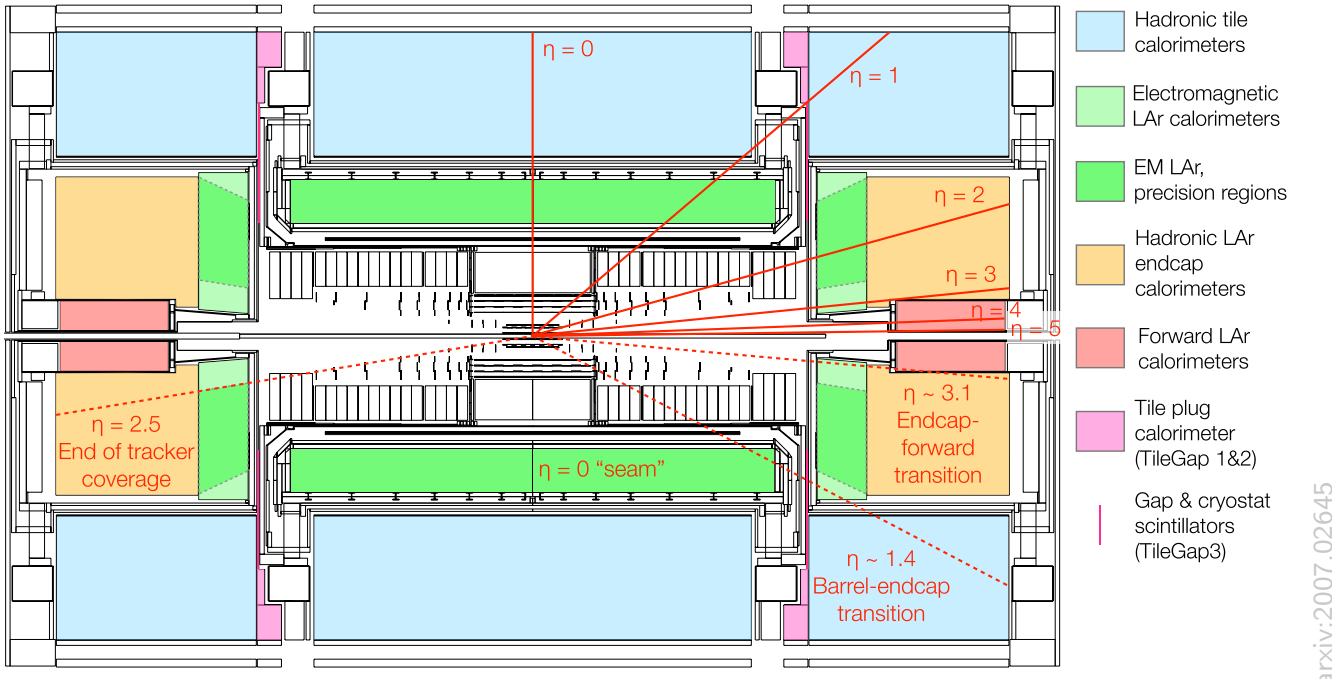

- Narrow region between hadronic calorimeters instrumented only by a thin set of gap and cryostat scintillators
- Due to lack of tracking in Run 2 TLA stream, unable to perform stable calibration here
- Excluded after discussion with JetEtMiss and Exotics conveners

Tile Gap Veto

Tile gap veto: exclude event if any of $1.0 < |\eta^{0,1}| < 1.6$

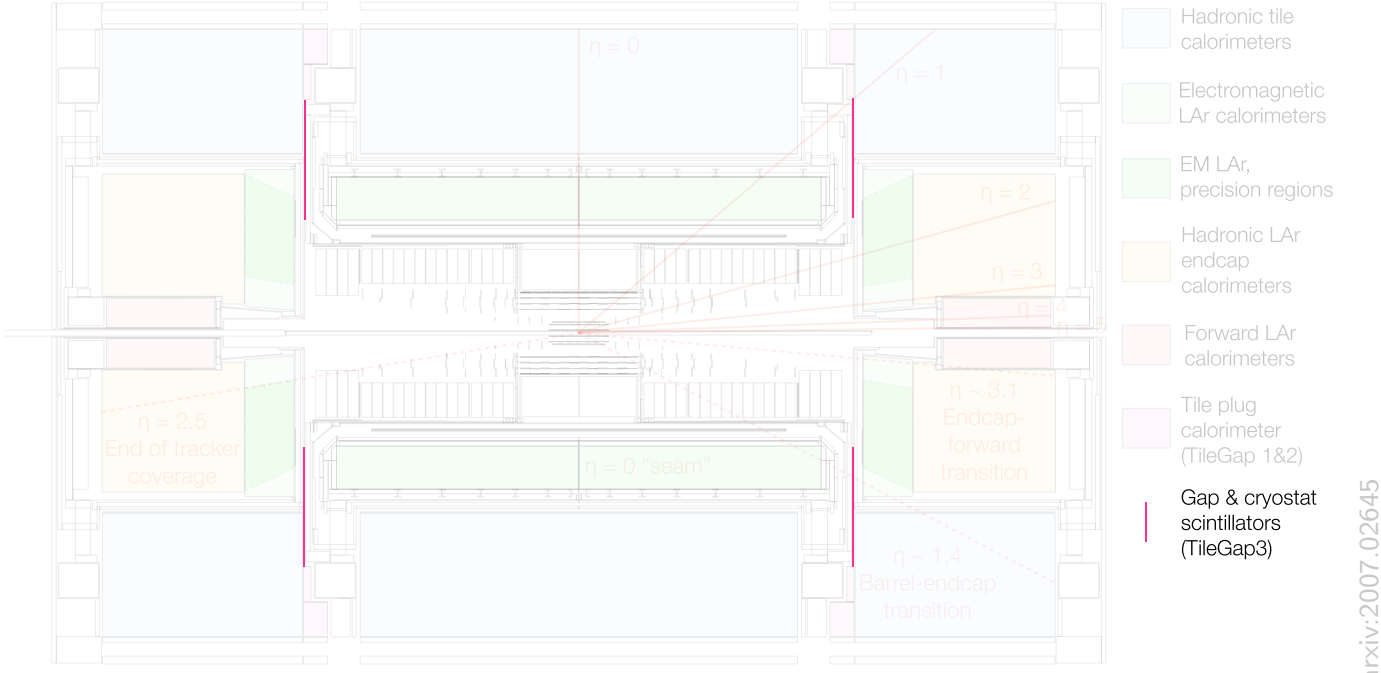

- Narrow region between hadronic calorimeters instrumented only by a thin set of gap and cryostat scintillators
- Due to lack of tracking in Run 2 TLA stream, unable to perform stable calibration here
- Excluded after discussion with JetEtMiss and Exotics conveners

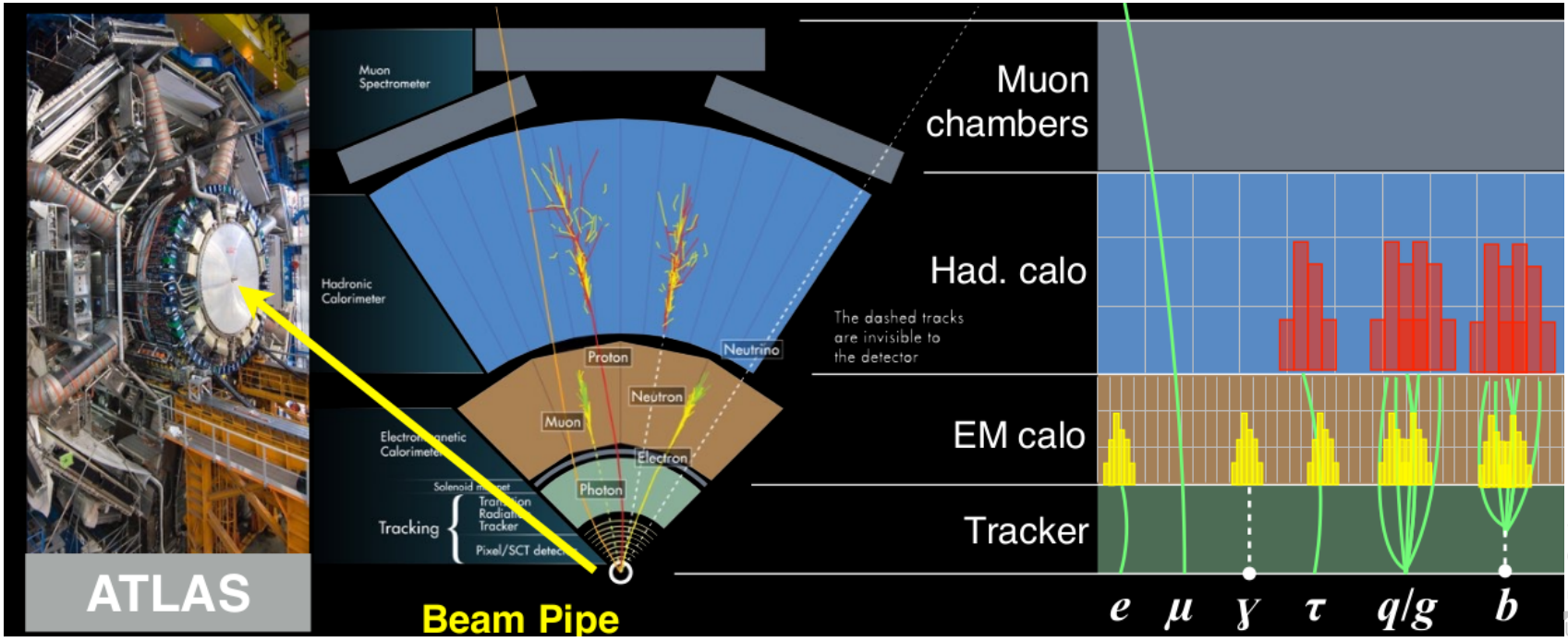
Muon Spectrometer
Hadronic Calorimeter
Tracking
Proton
Neutrino
Neutron
Muon
Electron
Photon
ATLAS
Beam Pipe
Muon chambers
Had. calo
The dashed tracks are invisible to the detector
EM calo
Tracker
e
μ
γ
τ
q/g
b
B. Carlson

Run 3 TLA: Adding Tracker Information

At low p_T the tracker p_T resolution

$$\sigma\left(\frac{1}{p_T}\right) = 0.036\% \cdot p_T \oplus 1.3\%$$

is better than the calorimeter E resolution

$$\frac{\sigma(E)}{E} = \frac{50\%}{\sqrt{E}} \oplus 3.4\% \oplus \frac{1\%}{E}$$

source

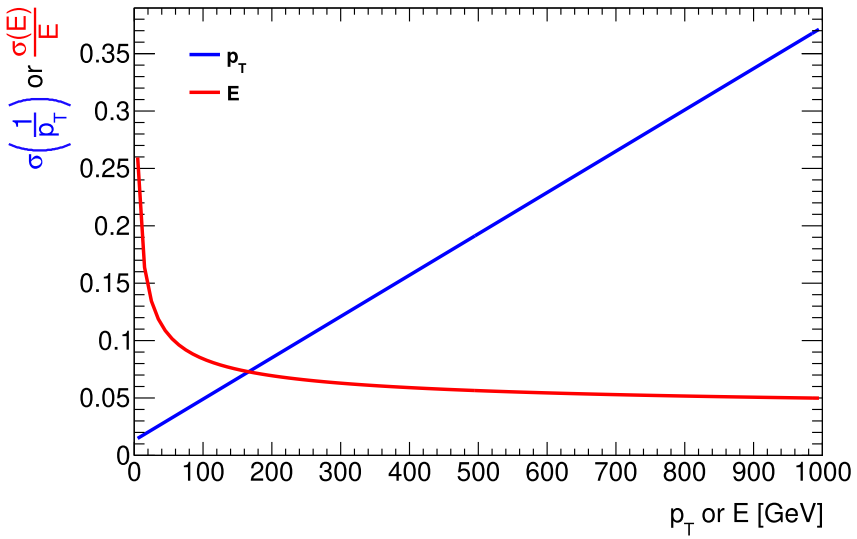

- Run 2: Only EMTopo (calo only) jets in TLA stream
- Run 3: Full-scan tracking $\rightarrow$ ParticleFlow jets

Jet definitions used in Run 3 rely on calo+track information

Run 3 TLA Contributions to the Collaboration

Run 3 HLT jet calibration performance derived within dijet+ISR TLA

TLA work benefits the wider collaboration

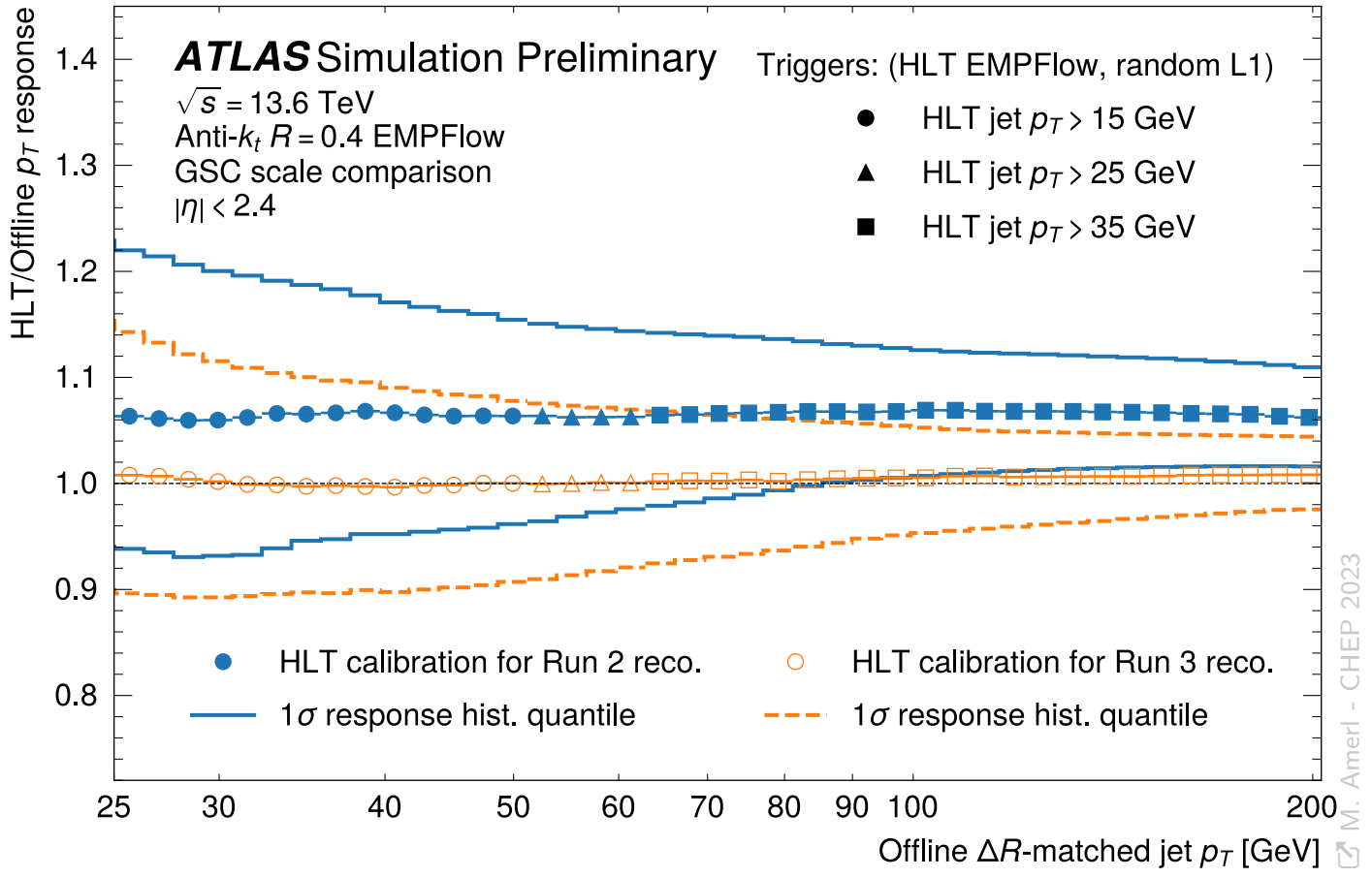

Strong Coupling Constant α_s

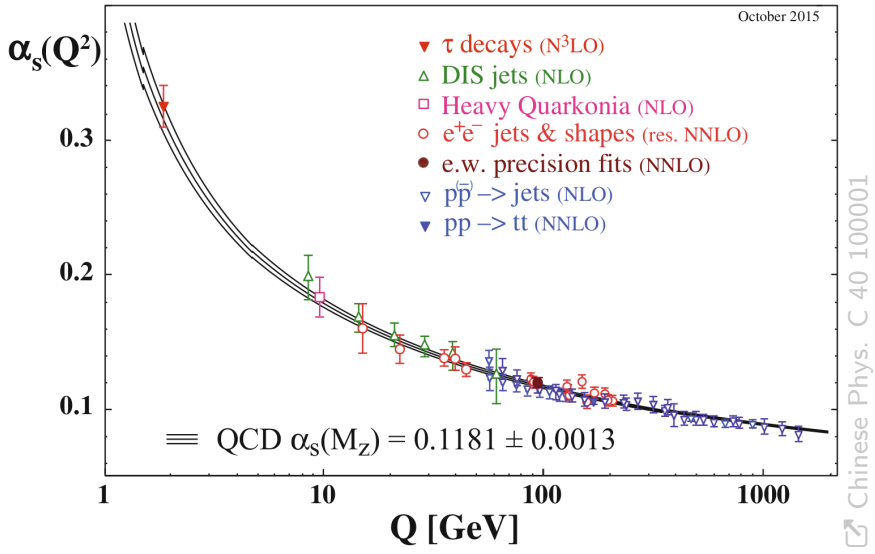

Partonic cross section further contributes to falling: $\propto \frac{d\hat{\sigma}}{d\hat{t}} \propto \frac{\alpha_s^2}{\hat{s}^2}$

High M $\rightarrow$ high Q^2 $\rightarrow$ low α_s

p_T falls too but not quite as steeply:

$$M = \hat{s} = 4p_T^2 \cosh^2 y^*$$

$$\Rightarrow p_T \propto \sqrt{M}$$

Result: M distribution is steeply falling (up to $\propto M^{-10}$) with non-trivial but smooth shape

Simplified DM Models

Mediator	Spin	Parity	Coupling
Scalar (S)	0	even	$g_S\, S\, \bar{\psi}\psi$
Pseudo-scalar (P)	0	odd	$g_P\, P\, \bar{\psi} i\gamma_5 \psi$
Vector (V)	1	odd	$g_V\, V_\mu\, \bar{\psi}\gamma^\mu \psi$
Axial-vector (A)	1	even	$g_A\, A_\mu\, \bar{\psi}\gamma^\mu\gamma_5 \psi$

Scalar

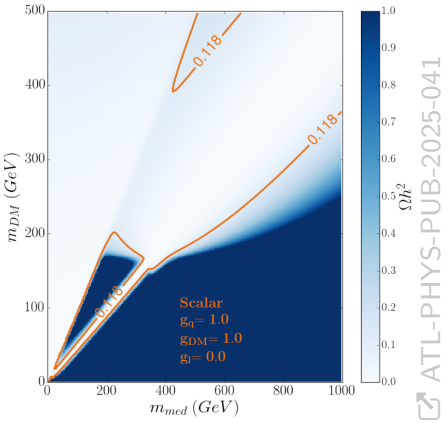

ATL-PHYS-PUB-2025-041

Pseudo-scalar

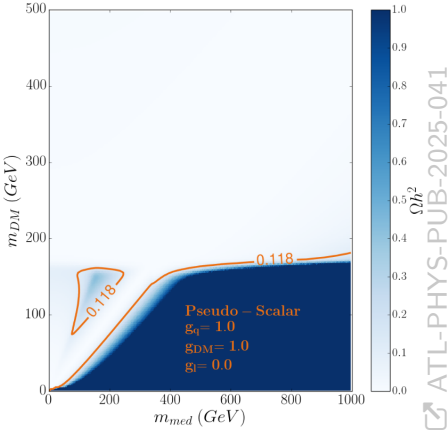

ATL-PHYS-PUB-2025-041

Vector

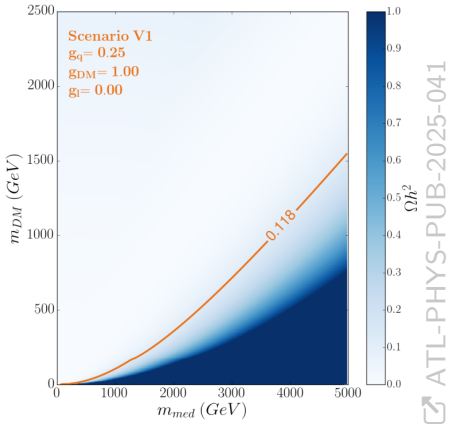

ATL-PHYS-PUB-2025-041

Axial-vector

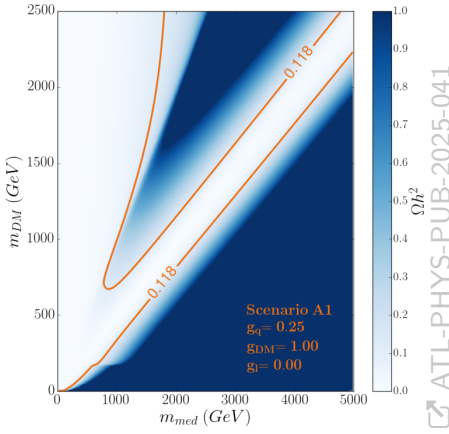

ATL-PHYS-PUB-2025-041

Simplified DM Models

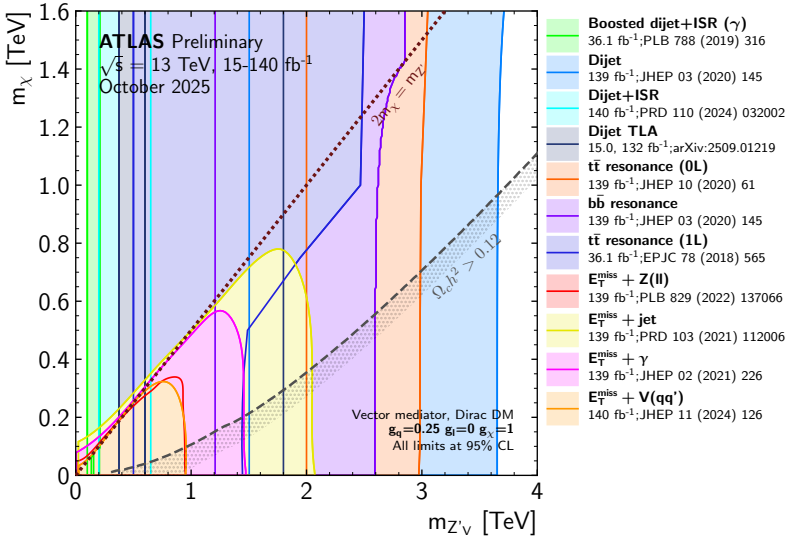

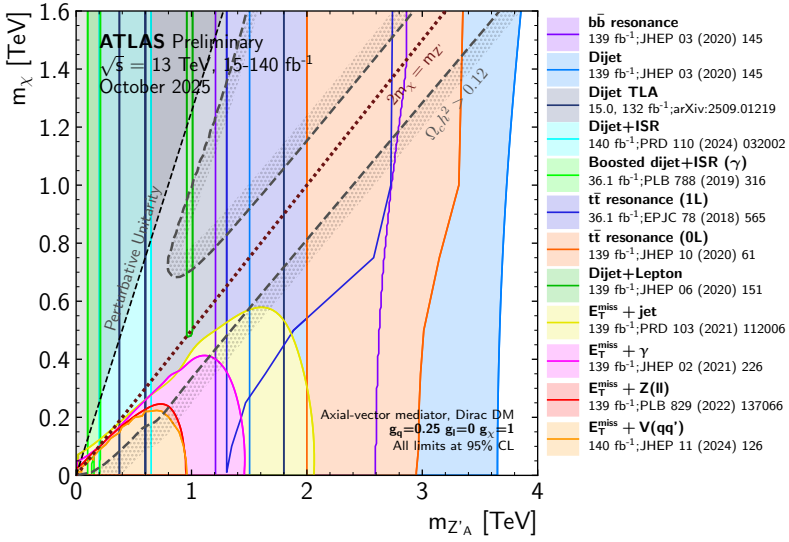

Simplified DM Models

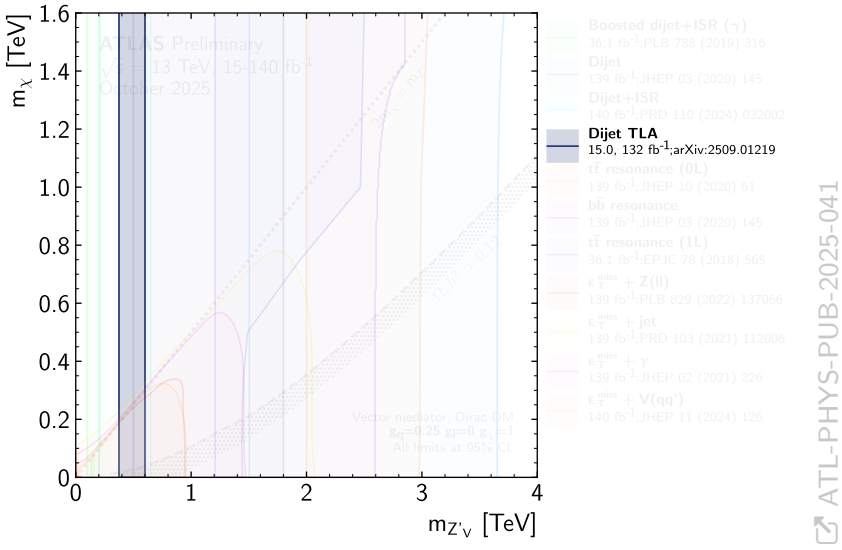

ATL-PHYS-PUB-2025-041

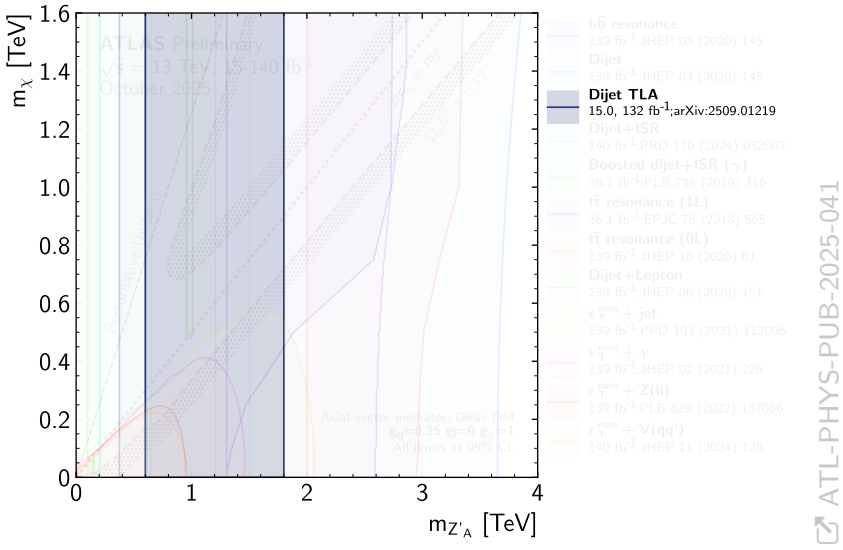

ATL-PHYS-PUB-2025-041

DM Landscape

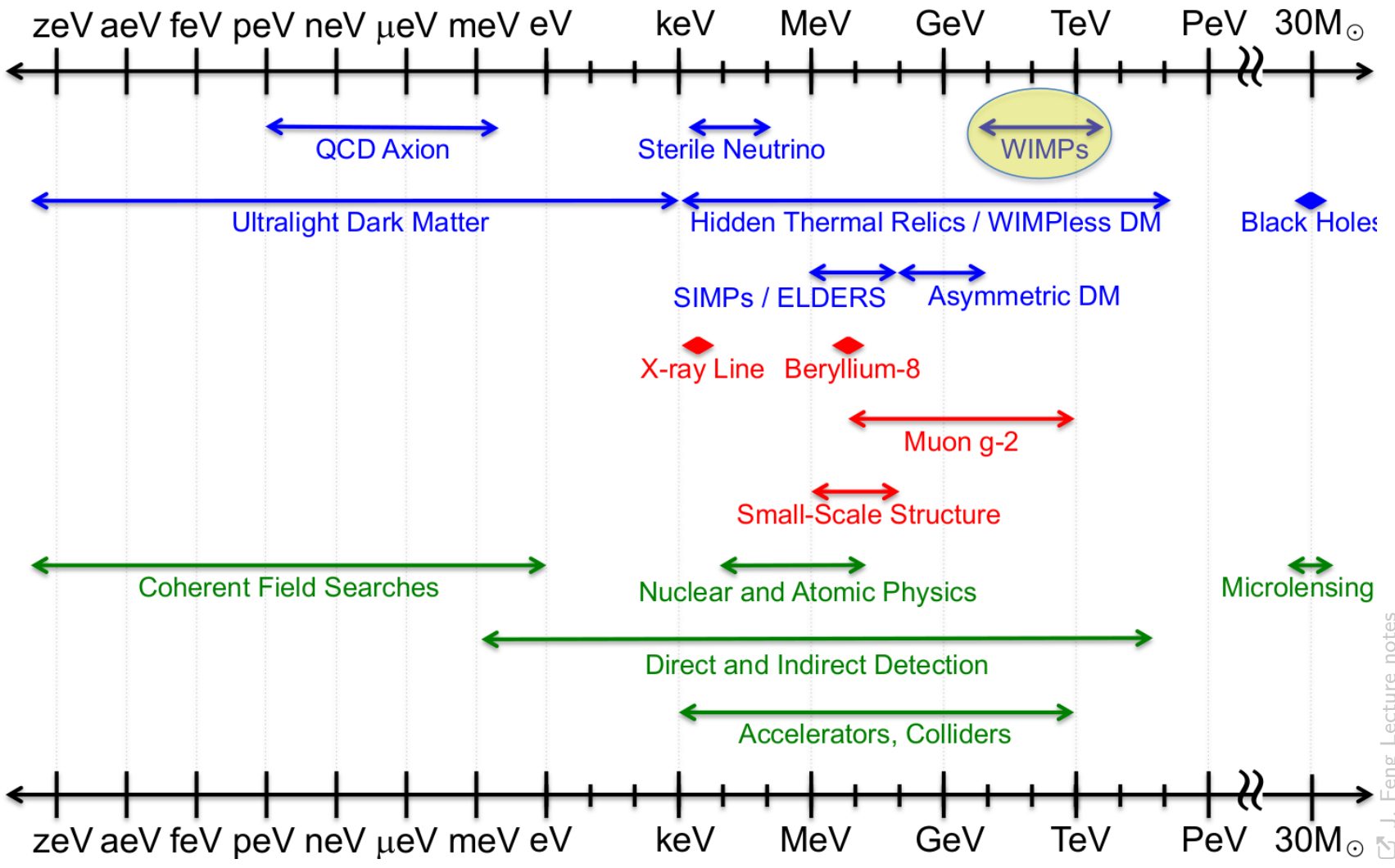

DØ: NLO QCD Backround Estimate

DØ dijet mass search in 2004:

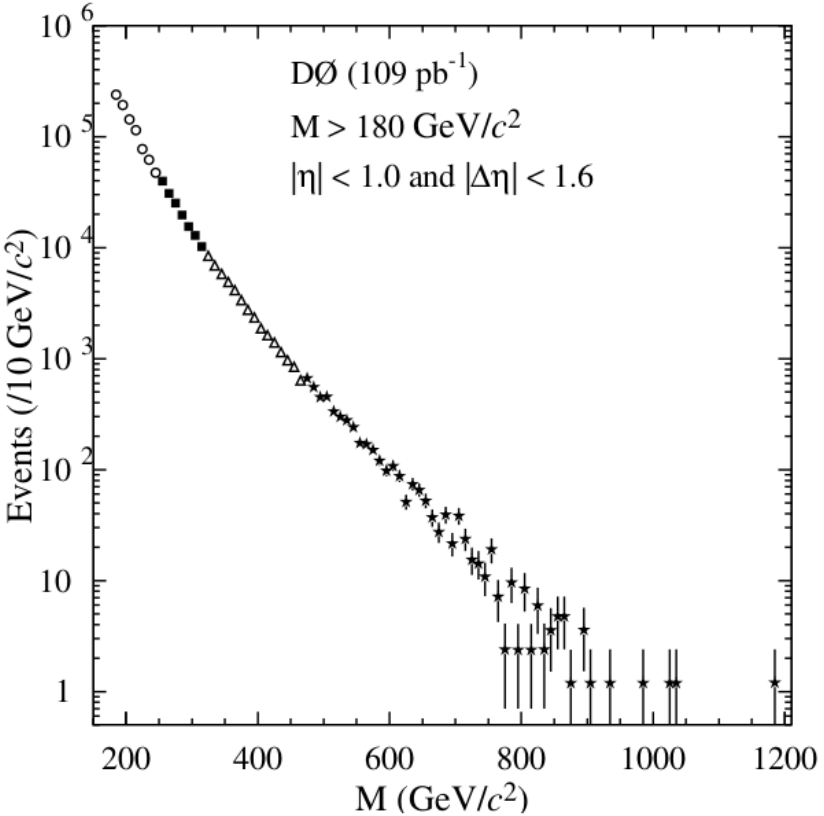

arxiv:hep-ex/0308033

Agrees well with NLO QCD calculation

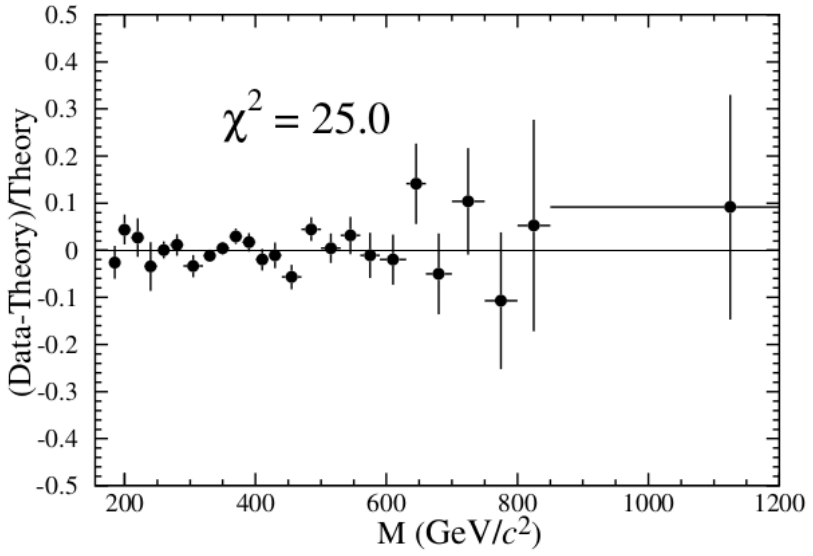

arxiv:hep-ex/0308033

Appendix
TLA Publications

experiment	signature	mass range [GeV]	publication
ATLAS	dijet	450-1800	PRL 121 (2018) 081801
	dijet	375-1800	Phys. Rev. D 112, 092015 (2025)
CMS	dijet	600-1800	arxiv:2510.21641
	dijet	500-900	CMS-PAS-EXO-11-094
	dijet	500-800	PRL 117 (2016) 031802
	dijet	600-1600	PLB 769 (2017) 520
	dijet	600-1600	JHEP 08 (2018) 130
	pair of 3j	200-700	Phys. Rev. D 99, 012010
	dijet + ISR jet	350-700	PLB 805 (2020) 135448
	LLP$\rightarrow$di-μ	10-50	Phys. Rev. 124, 131802
	LLP$\rightarrow$di-μ	0.6-50	JHEP 04 (2022) 062
	multi-μ ($\eta \rightarrow 4\mu$)	0.45-40	CMS-PAS-BPH-22-003

TLA @ ATLAS: Early Run 2 dijet

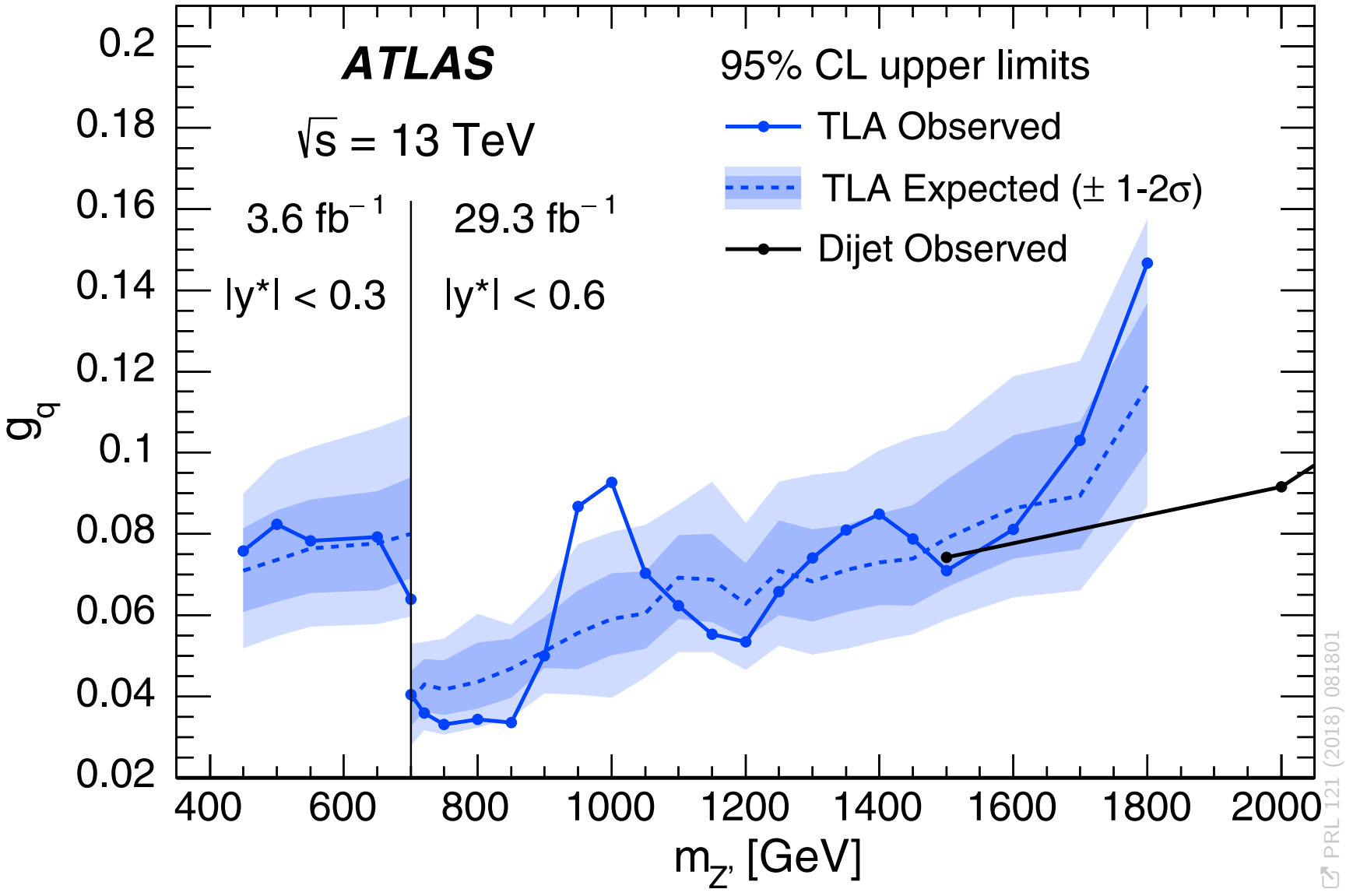

PRL 121 (2018) 081801

TLA @ CMS: Data Scouting (DS)

CMS equivalent to TLA: Data Scouting

First use: dijets @ 7 TeV (2013)

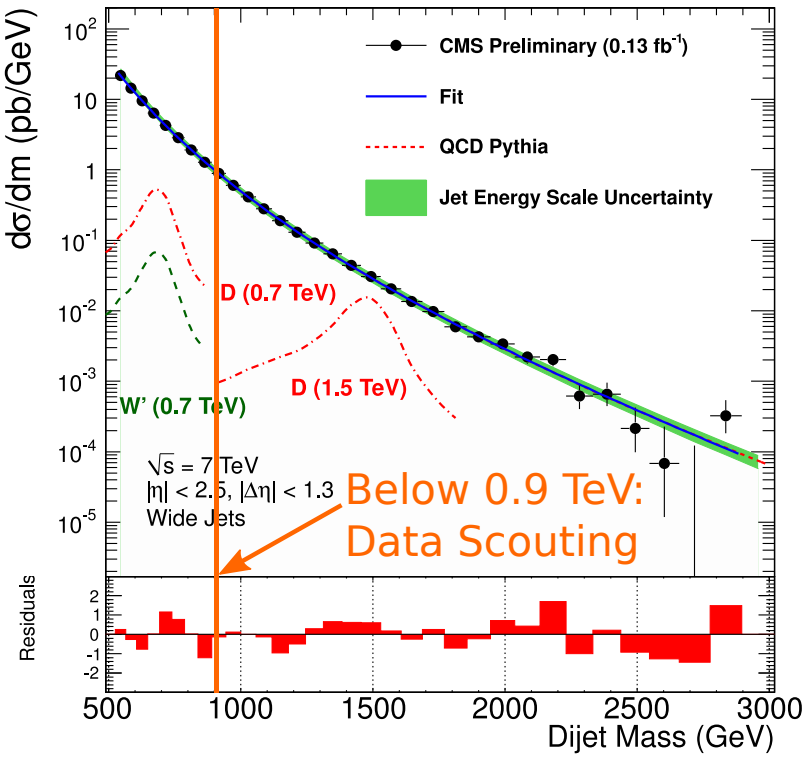

CMS-PAS-EXO-11-094

- TLA used to extend limits from 0.9 down to 0.5 TeV

dijets @ 8 TeV (2016)

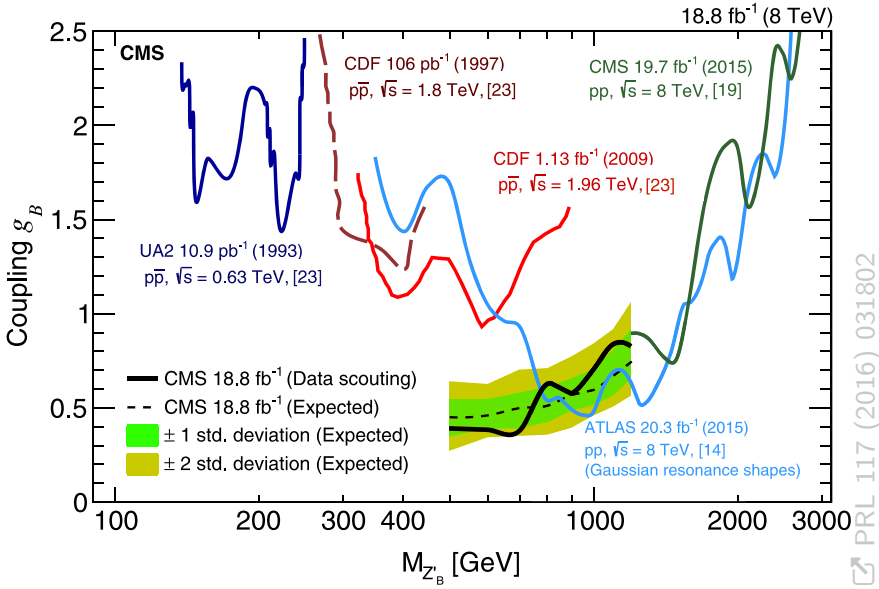

PRL 117 (2016) 031802

- Best limits in 0.5-0.8 TeV range

TLA @ CMS: Data Scouting (DS)

dijets @ 13 TeV (2017)

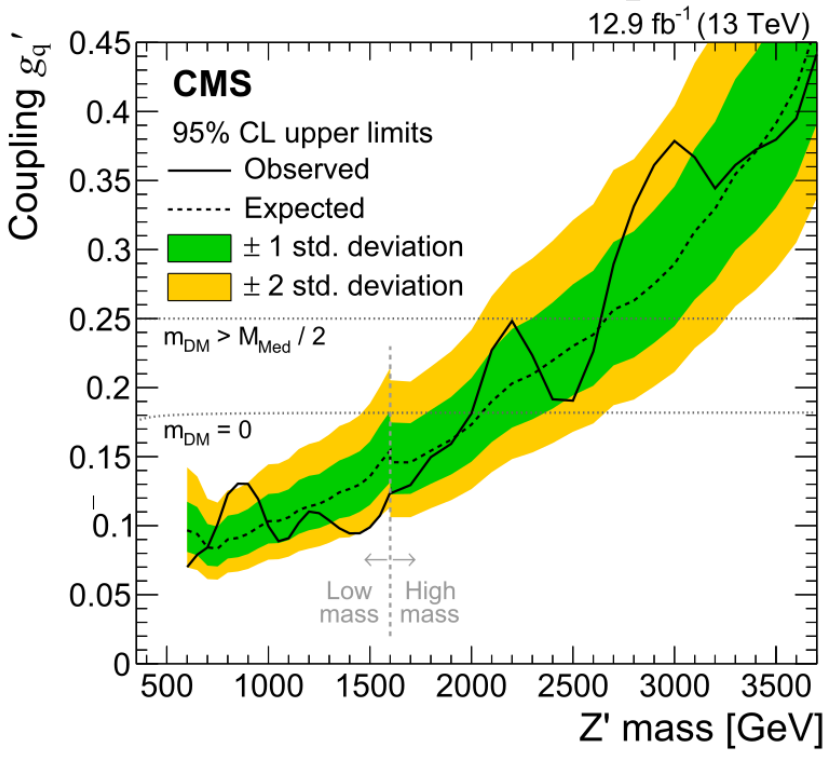

PLB 769 (2017) 520

- 12.9 fb^{-1}
- 0.6-1.6 TeV

dijet @ 13 TeV (2018)

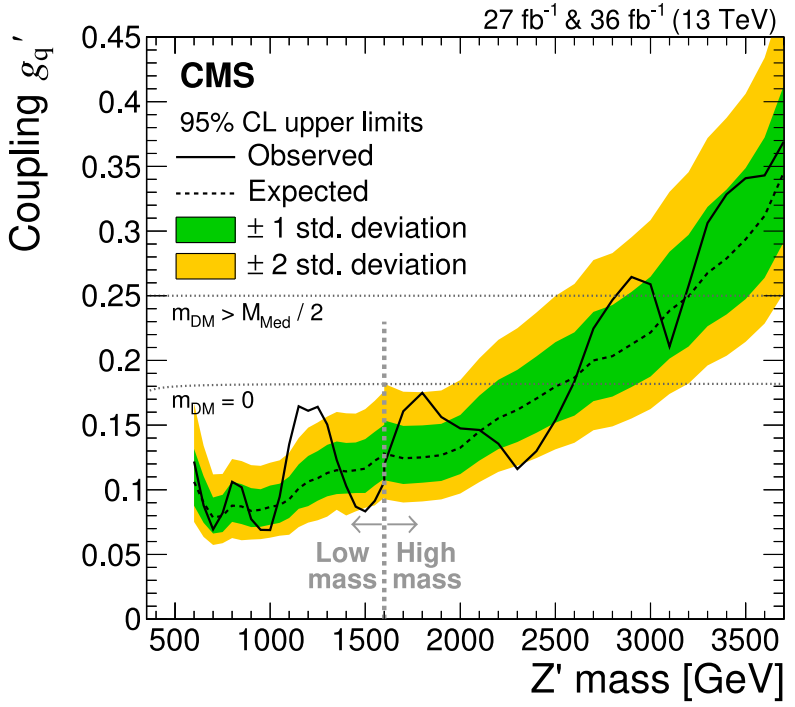

JHEP 08 (2018) 130

- 27 fb^{-1}
- 0.6-1.6 TeV

TLA @ CMS: Data Scouting (DS)

pair of 3j resonances @ 13 TeV (2019)

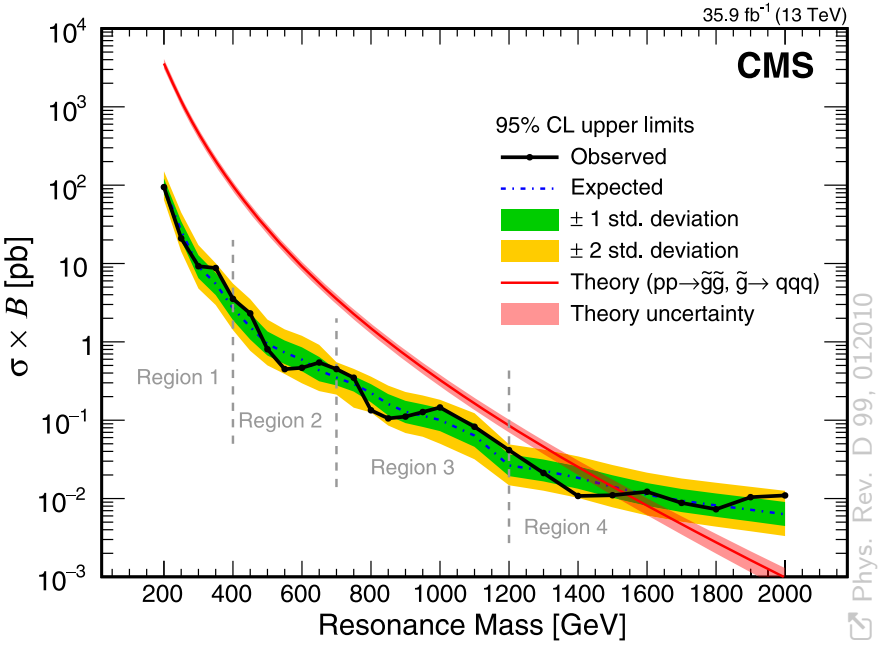

- $H_T > 410$ GeV from $p_T > 20$ GeV jets
- DS: 0.2-0.7 TeV

dijets + ISR jet @ 13 TeV (2020)

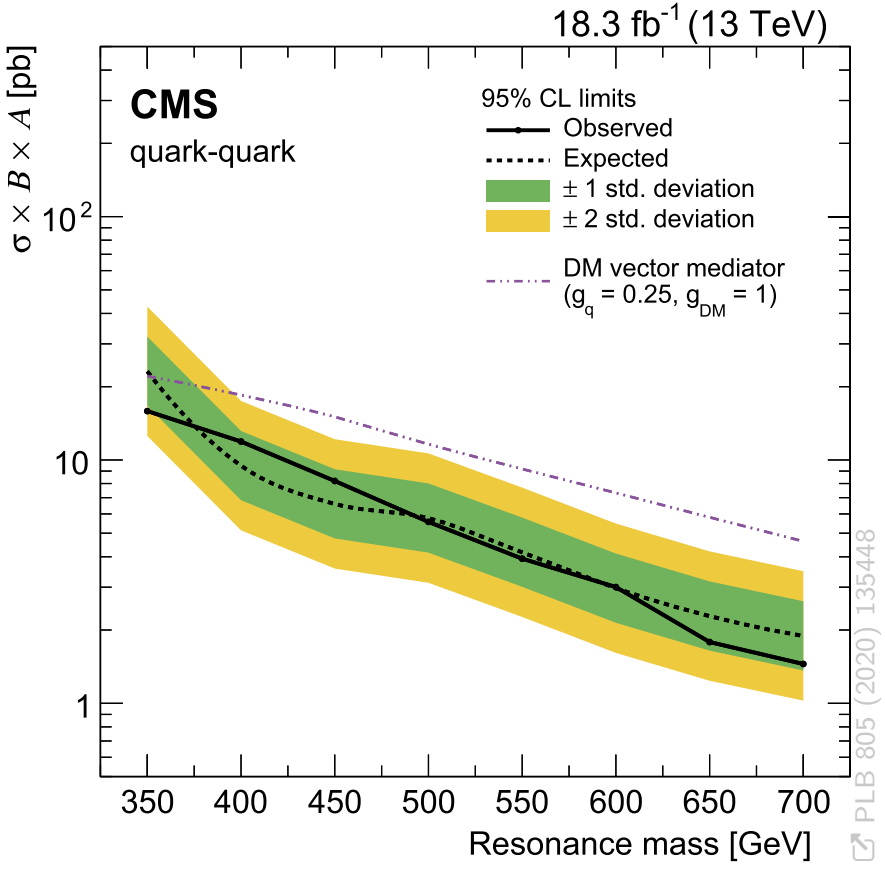

- 18.3 fb^{-1}
- 350-700 GeV

TLA @ CMS: Data Scouting (DS)

LLP $\rightarrow$ di-μ @ 13 TeV (2020)

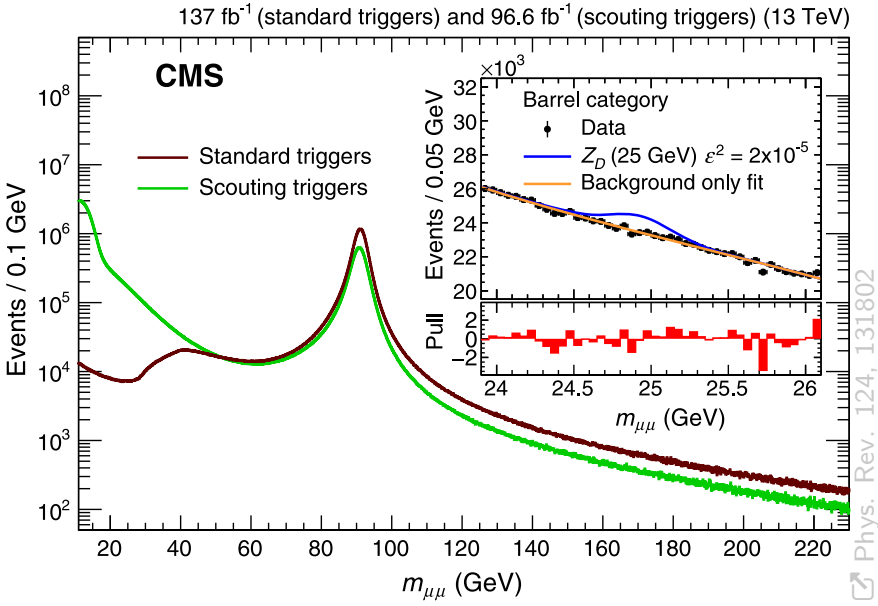

Phys. Rev. 124, 131802

- 96.6 fb^{-1} (2017 & 2018)
- DS advantage kicks in <50 GeV

LLP $\rightarrow$ di-μ @ 13 TeV (2022)

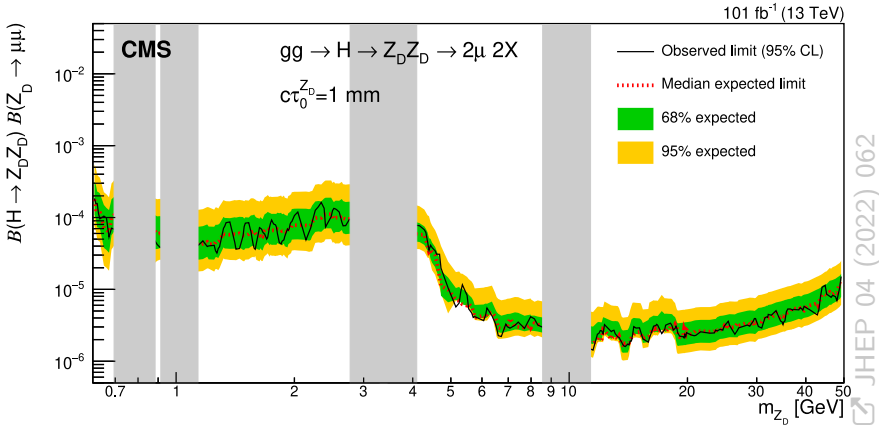

JHEP 04 (2022) 062

- 101 fb^{-1} (2017 & 2018)
- E.g. Dark photon Z_D down to sub-GeV range

TLA @ CMS: Data Scouting (DS)

multi-μ @ 13 TeV (2022)

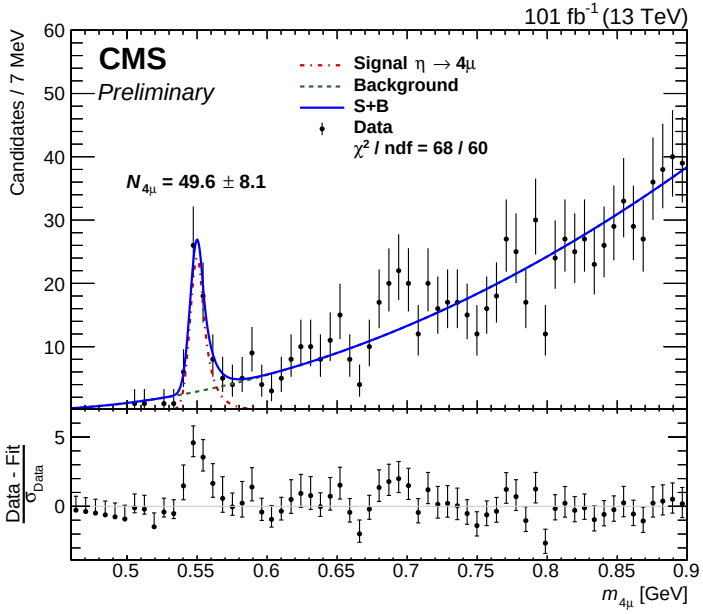

CMS-PAS-BPH-22-003

- 101 fb^{-1} (2017 & 2018)
- DS in $<$ 40 GeV range
- First $\eta \to 4\mu$ observation